REPORT DOCUMENTATION PAGE

Form Approved OMB No. 074-0188

1. REPORT DATE *(DD-MM-YYYY)*	2. REPORT TYPE	3. DATES COVERED *(From – To)*
12-1986	**PhD Dissertation**	

4. TITLE AND SUBTITLE

Crack Growth in Alloy 718 Under Thermal-Mechanical Cycling

5a. CONTRACT NUMBER

5b. GRANT NUMBER

5c. PROGRAM ELEMENT NUMBER

6. AUTHOR(S)

Heil, Michael L., Maj, USAF

5d. PROJECT NUMBER

5e. TASK NUMBER

5f. WORK UNIT NUMBER

7. PERFORMING ORGANIZATION NAMES(S) AND ADDRESS(S)

Air Force Institute of Technology
School of Engineering (AFIT/ENY)
2950 P Street, Building 640
WPAFB OH 45433

8. PERFORMING ORGANIZATION REPORT NUMBER

AFIT/DS/AA/86-1

9. SPONSORING/MONITORING AGENCY NAME(S) AND ADDRESS(ES)

Air Force Wright Aeronautical Laboratories
Materials Laboratory (AFWAL/MLLN)
WPAFB OH 45433

10. SPONSOR/MONITOR'S ACRONYM(S)

AFWAL/MLLN

11. SPONSOR/MONITOR'S REPORT

12. DISTRIBUTION/AVAILABILITY STATEMENT

APPROVED FOR PUBLIC RELEASE; DISTRIBUTION UNLIMITED.

13. SUPPLEMENTARY NOTES

14. ABSTRACT

An investigation was conducted to evaluate and model the crack growth rates in a nickel-base superalloy under load controlled thermal-mechanical cycling. Experiments were conducted on center-cracked panel specimens of Inconel 718 with temperature limits of 427° to 649°C. Closed-loop temperature control in the cracked region of the specimen was maintained by a microcomputer and four quartz heating lamps. A D.C. electric factor, K, was used to correlate all crack growth data.

A linear cumulative damage model was developed which sums cycle-dependent, mixed-mode, and time-dependent damage terms to predict thermal-mechanical fatigue crack growth rates. The model was developed entirely from isothermal fatigue and sustained load test data.

All thermal and mechanical cycles used during the thermal-mechanical fatigue (TMF) testing were symmetric, triangular, and 96 seconds long. Crack growth rates were determined over a range of K using a stress ratio, R of 0.1. Tests were conducted with the maximum load leading the maximum temperature by phase angles of 0°, 90°, 180°, 225°, 270°, and 215°. The in-phase test (0°) produced the highest crack growth rates, with the 315°, 270°, 225°, 180°, and 90° tests following in order. The 0° and 90° crack growth rates were bracketed by the isothermal growth rates at 427°C and 649°C.

The mixed-mode damage term did not significantly contribute to the linear cumulative damage model crack growth rate predictions. The original model integrated sustained load crack growth over the entire loading portion of the thermal-mechanical cycle and overpredicted TMF crack growth rates by a factor of up to four (270° test). The modified model integrated sustained load crack growth over the loading portion of the cycle as the sustained load crack growth rate is increasing. Two proof tests were conducted to evaluate the applicability of the modified model. All modified model predictions were within a factor of two of the experimental results.

15. SUBJECT TERMS

Fracture, Fatigue, Thermal Cycling Tests, Nickel Alloy, Inconel, Superalloys

16. SECURITY CLASSIFICATION OF:			17. LIMITATION OF ABSTRACT	18. NUMBER OF PAGES	19a. NAME OF RESPONSIBLE PERSON
a. REPORT	b. ABSTRACT	c. THIS PAGE			George K. Haritos, Major, USAF (AFOSR/NA)
U	U	U	UU	185	19b. TELEPHONE NUMBER *(Include area code)* AV297-4935

Standard Form 298 (Rev. 8-98)
Prescribed by ANSI Std. Z39-18

AFIT/DS/AA/86-1

CRACK GROWTH IN ALLOY 718 UNDER THERMAL-MECHANICAL CYCLING

DISSERTATION

Presented to the Faculty of the School of Engineering

of the Air Force Institute of Technology

Air University

In Partial Fulfillment of the

Requirements for the Degree of

Doctor of Philosophy

Michael L. Heil, B.S., M.S.

Major, USAF

December 1986

AFIT/DS/AA/86-1

CRACK GROWTH IN ALLOY 718 UNDER THERMAL-MECHANICAL CYCLING

Michael L. Heil, B.S., M.S.

Major, USAF

Approved:

George K Haritos	24 NOV 86
	24 Nov 86
	5 Dec 86
	5 Dec 86
	5 Dec 86
	5 Dec 86

Accepted:

5 Dec 86

Dean, School of Engineering

Acknowledgments

I would like to express my gratitude to Major George K. Haritos for his invaluable overall guidance and support of my research efforts. His experience and advice helped make my research more productive and complete.

I would also like to thank the Materials Laboratory Metals Behavior Branch for sponsoring this work. The members of the branch often provided useful advice and suggestions. My most sincere gratitude goes to Dr. Theodore Nicholas, who always made time to help me when I had a problem. He provided encouragement and outstanding support through all stages of my research.

I am very grateful to Mr. George Hartman and Mr. David Johnson of the University of Dayton Research Institute for their help in the experimental program. They developed and maintained the testing apparatus, and assisted me in running tests.

Table of Contents

List of Figures

List of Figures (continued)

List of Figures (continued)

List of Tables

Abstract

An investigation was conducted to evaluate and model the crack growth rates in a nickel-base superalloy under load controlled thermal-mechanical cycling. Experiments were conducted on center-cracked panel specimens of Inconel 718 with temperature limits of 427°C to 649°C. Closed-loop temperature control in the cracked region of the specimen was maintained by a microcomputer and four quartz heating lamps. A D.C. electric potential drop method was used to monitor crack lengths. The elastic stress intensity factor, K, was used to correlate all crack growth data.

A linear cumulative damage model was developed which sums cycle-dependent, mixed-mode, and time-dependent damage terms to predict thermal-mechanical fatigue crack growth rates. The model was developed entirely from isothermal baseline test data. The cycle-dependent term was based on low temperature (427°C) high frequency (10 Hz) crack growth data. The mixed-mode term was developed from low frequency (0.01 Hz) fatigue crack growth tests at 538°C and 649°C. The time-dependent term was developed from sustained-load crack growth tests at 538°C, 593°C, and 649°C.

All thermal and mechanical cycles used during thermal-mechanical fatigue (TMF) testing were symmetric, triangular, and 96 seconds long. Crack growth rates were determined over a range of ΔK using a stress ratio, R, of 0.1. Tests were conducted with the maximum load leading the maximum temperature by phase angles of 0°, 90°, 180°, 225°, 270°, and 315°. The in-phase test (0°) produced the highest crack growth rates, with the 315°, 270°, 225°, 180°, and 90° tests following in order. The 0° and 90° crack growth rates were separated by over a factor of ten at all ΔK values tested. All TMF crack growth rates were bracketed by the isothermal growth rates at 427°C and 649°C.

The mixed-mode damage term did not significantly contribute to the linear cumulative damage model crack growth rate predictions. The original model integrated

sustained load crack growth over the entire loading portion of the thermal-mechanical cycle and overpredicted TMF crack growth rates by a factor of up to four (270° test). The modified model integrated sustained load crack growth over the loading portion of the cycle as the sustained load crack growth rate is increasing. Two proof tests were conducted to evaluate the applicability of the modified model. All modified model predictions were within a factor of two of the experimental results.

CRACK GROWTH IN ALLOY 718 UNDER THERMAL-MECHANICAL CYCLING

I. Introduction

Low cycle fatigue is the life limiting factor for turbine disks in most advanced Air Force gas turbine engines (1). Low cycle fatigue failures occur due to the application of a relatively low number of high stress cycles (2). To prevent in-service failures, disks are retired upon reaching a statistically determined low cycle fatigue design lifetime. Since the lifetime is based upon one in 1000 initially flaw-free disks developing a detectable fatigue crack, 999 of 1000 retired disks have useful life remaining (3). This extremely conservative approach is very expensive.

The Air Force is implementing a new life management philosophy entitled Retirement-for-Cause (RFC) on some existing engines to safely use a greater portion of the available structural life of turbine disks. The total fatigue life of a disk consists of a crack initiation phase followed by crack growth until failure at a critical crack length. Under RFC, disks are removed for periodic crack inspections and retired only if a crack larger than a specified detectable size is found. A fracture mechanics analysis is performed to determine the time required for a crack just below the specified detectable size to grow to critical length. This time is divided by a factor of safety (say two or three) to determine the inspection interval.

Future engines procured by the Air Force must meet the damage tolerance requirements of the Engine Structural Integrity Program (ENSIP) contained in MIL-STD-1783 (USAF) dated 30 November 1984 (4). Under ENSIP, initial flaws are assumed to exist in fracture critical components at the time of production. Fracture mechanics calculations and component testing must demonstrate that such flaws will not grow to

critical size within the lifetime of the engine. If this requirement incurs a prohibitive weight penalty, in-service inspections of the component will be allowed. Fracture mechanics calculations must show that the initial flaw will not grow to critical size in twice the inspection interval.

In order for RFC and ENSIP to conservatively assure safety of flight, cracks above the specified size must be reliably detected during each inspection. Also, engineers must be able to accurately predict crack growth under the engine thermal-mechanical cycling spectrum to show that cracks of the specified detectable size and smaller will not grow to critical size during the engine lifetime or an inspection interval. The spectrum includes variations in temperature, load magnitude, load frequency, mean load, and hold times at sustained loads. A typical mission spectrum for a critical turbine disk location is shown in Figure 1.1 (5). Note that the temperature and load are varied simultaneously, causing thermal-mechanical fatigue (TMF). At sufficiently high temperatures, the environment and creep become important factors affecting crack growth, and the question of whether linear elastic fracture mechanics (LEFM) is still applicable for crack-growth analysis arises (6). Virtually all fatigue crack-growth testing of turbine disk materials to date has been performed under isothermal conditions. In a TMF crack-growth test, load and temperature are simultaneously cycled. Very few such tests have been conducted, and to date, no model has been developed to successfully predict the crack-growth rates over a wide variety of cycles (7).

This dissertation examines factors influencing fatigue crack growth in Inconel 718 under thermal-mechanical cycling and develops a crack-growth predictive model using isothermal data. The mechanisms of elevated temperature crack growth in this material provide the basis of the model. Inconel 718 is a precipitation-hardenable nickel-base superalloy commonly used in compressor and turbine disks. Isothermal fatigue crack growth and sustained-load crack-growth tests were conducted to provide the baseline data

needed to develop a TMF crack-growth predictive model. The model was applied to several types of thermal-mechanical cycles and fatigue crack-growth tests were conducted for those cycles. The model predictions fit the experimental data quite successfully.

This dissertation presents the development of the thermal-mechanical fatigue crack growth model in successive stages. In Chapter II, previous research in the field of elevated temperature crack growth is discussed. The apparatus and procedure used to develop all experimental data are discussed in Chapter III. Chapter IV deals with the physical basis of the model and its development from baseline isothermal data. Thermal-mechanical fatigue crack growth test results and model predictions are discussed in Chapter V. In Chapter VI, conclusions are made about the model and its applicability to future research.

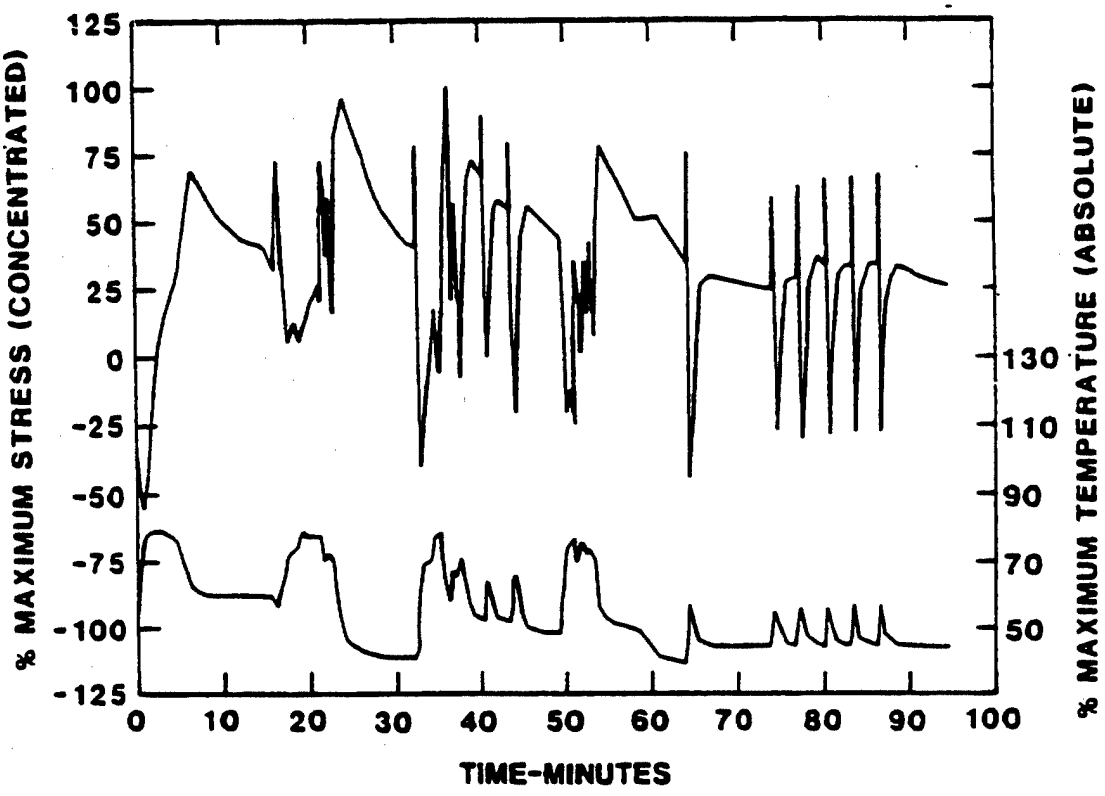

Figure 1.1: Thermal-Mechanical Spectrum

II. Elevated Temperature Crack Growth

In this chapter, pertinent literature related to elevated temperature crack growth in nickel-base alloys is reviewed. Previous studies of the mechanisms of elevated temperature crack growth and of factors affecting crack growth are discussed. The applicability of linear elastic fracture mechanics to elevated temperature crack growth is reviewed. Prior work in modeling of both isothermal and thermal-mechanical fatigue crack growth is summarized. In Chapter IV, the mechanisms of elevated temperature crack growth are applied to the development of a crack growth predictive model for thermal-mechanical fatigue.

Mechanisms of Fatigue Crack Growth at Elevated Temperatures

Mechanical fatigue, environmentally-enhanced crack growth, and creep crack growth can all contribute to elevated temperature fatigue crack growth in high-strength nickel-base alloys (8). Creep and environmental interaction depend on time, leading to time-dependent crack growth and crack growth under a sustained load. Sadananda and Shahinian (9, 10) found mechanical fatigue to be the main contributor to the fatigue crack-growth process in Inconel 718 for temperatures up to 538 °C. At such temperatures, crack-growth depends upon the number of loading cycles and not the cycle period. This type of damage is called cycle-dependent. They suggest that this damage occurs through a mechanism of reversed slip at the crack tip (11). Examinations of the fracture surface resulting from cycle-dependent damage show that the fracture mode is transgranular (9, 11).

The environment plays an important role in elevated temperature crack growth in Inconel 718. Floreen and Kane (12) examined crack growth in this alloy at 650 °C in 14 gaseous environments and found that oxygen and sulfur significantly increase crack growth

rates. In a later study, they noted that crack growth rates in an inert helium environment were an order of magnitude less than those in laboratory air (13). Pédron and Pineau (14) and Sadananda and Shahinian (15) found the crack-growth rates in Inconel 718 to be much slower in a vacuum than in laboratory air. Mills and James (16) noted a similar decrease in an inert liquid sodium environment versus laboratory air. Shahinian and Sadananda (9) examined the fracture surface resulting from environmentally-enhanced crack growth and found that fracture occurred along the grain boundaries. They found that environmentally-enhanced damage is time-dependent and apparently controls crack growth in Inconel 718 at 649°C (9, 10). It is thought that this environmentally-enhanced crack growth occurs in laboratory air when oxygen diffuses into the region ahead of the crack tip and the resulting oxidation embrittles the material. The stress field ahead of the crack tip may enhance oxidation and environmentally assisted crack growth by increasing the number of vacancy sources (17). The oxidation often occurs along the grain boundaries (18).

Sadananda and Shahinian also examined sustained-load crack growth in Inconel 718 at 760°C and found inhibited crack growth which they attributed to creep relaxation at the crack tip (19). They postulated that creep becomes appreciable in Inconel 718 at this temperature (9). They also presumed creep crack growth to result from two competing processes: grain boundary diffusion of point defects at the crack tip, leading to intergranular cavities and crack growth, and plastic deformation at the crack tip, which blunts the crack and retards growth (19).

Time-dependent damage and cycle-dependent damage can interact to produce additional damage in Inconel 718 at temperatures above 427°C.. This is called "mixed-mode damage" by a number of researchers (1, 20). Fractographic analysis of the fracture surface resulting from mixed-mode damage shows a mixture of transgranular and intergranular types of failure (9). The point defects generated during fatigue cycling may

enhance the diffusion and oxidation controlled time-dependent crack growth process, resulting in mixed-mode damage (19).

Applicability of Linear Elastic Fracture Mechanics

In a linear elastic material, the stress intensity factor K describes the stress field at the crack tip and governs fatigue crack growth. K is defined as the linear elastic fracture mechanics (LEFM) constant which governs the intensity of the square root singularity of stresses at the crack tip and has units stress$\times\sqrt{\text{length}}$. In order for K to be an adequate crack growth correlation parameter, LEFM requires the plastic zone at the crack tip to be small compared to the crack length (21). Paris, Gomez, and Anderson were the first to note that the crack growth rate per cycle, da/dN, can be accurately expressed as a function of the stress intensity range, ΔK, when LEFM applies (22). Under these conditions, K may be used to characterize the fatigue crack-growth rates for different crack lengths, loads, and geometries.

At high temperatures, creep may induce inelastic effects at the crack tip and reduce the validity of K as a crack-growth parameter. Ellison and Harper (17) argued that if the cyclic plastic zone is small at elevated temperatures, K remains a valid fatigue crack-growth correlation parameter. Numerous governing parameters other than K have been proposed to describe crack growth at elevated temperatures (23). Some examples include net section stress or some other reference stress state (6, 17, 19, 23, 24), energy rate line integral C* (17, 23, 25, 26), the J integral (17, 19, 23, 26, 27), and crack opening displacement (17, 23, 27).

It appears that the governing parameter of fatigue crack growth at elevated temperatures in high strength nickel-base alloys depends upon the relative roles of creep, environmentally-enhanced crack growth, and mechanical fatigue (8). Creep appears to dominate at temperatures much above 650°C in Inconel 718 and K becomes a less useful parameter (9). At lower temperatures, the oxidizing environment of the gas turbine engine

embrittles the crack-tip region and reduces large scale inelasticity. This embrittlement also discourages through-the-thickness strain, approximating plane strain conditions. Thus, LEFM applies (6). Test results confirm the validity of K in describing fatigue crack growth and sustained-load crack growth in Inconel 718 at temperatures up to about 650°C (14, 19, 28, 29). For this reason, all isothermal and thermal-mechanical tests for this study were conducted at temperatures below 650°C.

Factors Affecting Crack Growth

Many factors affect crack growth in Inconel 718. Elevated temperature crack growth in this alloy under low frequency loading is observed to be time-dependent with an intergranular fracture mode. Thus crack growth per cycle will be greater for a very low frequency (long period) cycle than for a higher frequency (shorter period) cycle. Numerous researchers have observed this frequency effect during tests (17, 20, 24, 29-32). Since time-dependent crack growth is environmentally enhanced (15), the frequency effect is much smaller in an inert environment (13, 14). At frequencies below a certain threshold, crack growth per cycle is dependent only upon the period of the cycle. Doubling the cycle period will double the crack-growth rate per cycle. This is the time-dependent region. In this region, fracture occurs along the grain boundaries due to environmental degradation. At high frequencies above a different threshold, however, crack growth per cycle ceases to be frequency-dependent. This region is called fully cycle-dependent. In this region, the fracture mode is transgranular. Between the two thresholds, mixed-mode behavior is observed and the fracture surface shows a mixture of transgranular and intergranular damage (20, 30, 33). Weerasooriya (20) noted that plots on log-log paper of crack-growth rate versus loading frequency at constant values of K_{max} are linear in the time-dependent, mixed-mode, and cycle-dependent regions. This behavior is depicted for a temperature of 649°C and a K_{max} of 40 MPa$\sqrt{m}$ in Figure 2.1.

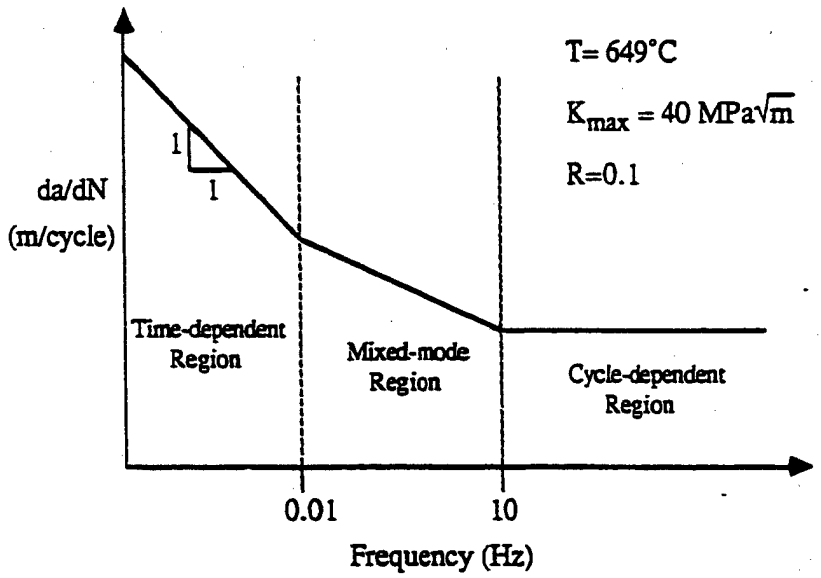

Figure 2.1: Frequency Dependence of Crack Growth Rate (20)

Fatigue crack growth is highly dependent upon temperature. In general, the total crack growth per cycle and the sustained-load crack-growth rate increase with increasing temperature. At 650°C, time-dependent crack growth is very important and dominates at low frequency cycling (30). The cycle-dependent damage at this temperature under high frequency cycling was found to be approximately the same as room temperature cycle-dependent damage (20). At temperatures below 538°C, cycle-dependent damage is found to dominate (9). Sadananda and Shahinian observed very low sustained-load crack growth rates at temperatures as low as 425°C (11).

Hold times at various load levels within fatigue cycles can have varying effects on crack growth in Inconel 718. Hold times at the maximum load tend to increase the crack growth per cycle and are the most damaging. Hold times at the minimum load seem to have no effect upon the growth rate when the K-level is below the threshold for sustained-load crack growth (31). In general, sustained loads appear to be significant only when applied at or near the maximum load of a fatigue spectrum (31).

The load ratio R is another parameter which affects fatigue crack growth rates at elevated temperatures. This parameter is defined as the minimum applied load divided by the maximum applied load. For a given stress intensity factor range ΔK, the crack-growth rate generally increases with increasing R. For a given maximum stress intensity factor K_{max}, time-dependent crack growth becomes relatively more important at higher load ratios (30). As the load ratio increases for a given K_{max}, the mean stress intensity level increases and the stress intensity range ΔK decreases, leading to the increased contribution of time-dependent crack growth.

The load-cycle waveshape affects fatigue crack growth. Most tests are performed using a simple triangular wave at a low R with equal loading and unloading rates. Clavel and Pineau (32) observed slightly higher crack-growth rates in Inconel 718 at 550°C under triangular cycling than under square wave cycling of the same frequency. These two wave forms are shown in Figure 2.2.

They accounted for this difference by proposing that the hold times in the square wave cycle had little effect on the crack growth rate at 550°C. They also proposed that the environmentally-assisted portion of crack-growth damage occurs essentially during the loading and/or unloading part of the cycle. The longer time of these parts of the triangular wave as compared to the square wave was used to account for the higher growth rates.

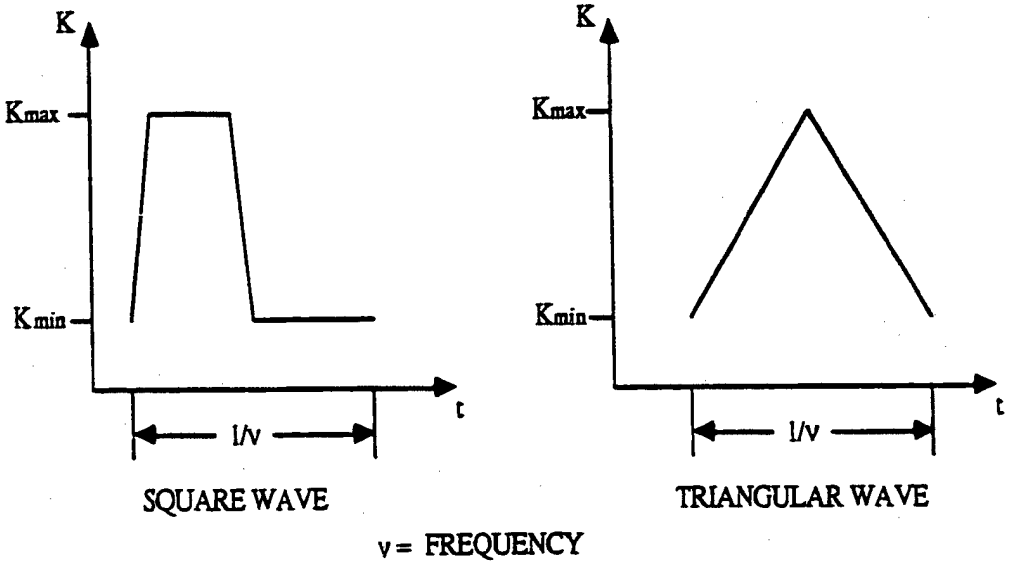

Figure 2.2: Square and Triangular Waveforms of the Same Frequency

Nicholas, Weerasooriya, and Ashbaugh (30) examined the effects of loading and unloading rates of triangular waves on crack growth in Inconel 718 at 649°C. With the loading duration held constant at 0.5 second, they noted no changes in crack growth per cycle for unloading durations ranging from 0.5 second to 5 seconds. For lower unloading rates, the cyclic crack-growth rate increased slightly. The cyclic crack-growth rate appeared to be a function only of the loading rate unless the unloading duration was very much longer than the loading duration. They suggested that most crack-growth damage occurs during the loading portion of the cycle. The unloading portion of the cycle becomes progressively more important with increasing stress ratio and decreasing unloading frequency.

Runkle and Pelloux (34) also noted that the elevated temperature fatigue crack-growth rate in nickel-based superalloys is dependent upon the rate of the loading portion of

the cycle and not the overall cycle frequency, thereby indicating that time-dependent damage occurs during the loading portion of the cycle.

Thermal-Mechanical Fatigue Crack Growth

Virtually all crack-growth testing to date has been performed under isothermal conditions. To understand TMF crack growth, one must examine the effect of temperature variations on sustained-load crack growth and fatigue crack growth. Robinson (35) examined thermal cycling effects on the creep strength of steel and predicted rupture lives by summing the life expenditures at the temperatures in a thermal cycle. He ignored transient and history effects. J. Miller (36) experimentally found the life-to-rupture of various high-temperature alloys and compared results with predictions from Robinson's model. In general, the predicted results were accurate and conservative.

Haritos, D. Miller, and Nicholas (37) measured crack-growth rates in Inconel 718 under a sustained load while varying the temperature and developed a linear cumulative-damage model to predict the results. They measured sustained-load crack-growth rates at 537°C, 593°C, and 648°C and obtained da/dt versus K plots for each temperature. They used these curves to obtain da/dt versus T in °C at given K levels. On a log-log scale, da/dt versus T was nearly linear at a given K, suggesting the form :

$$da/dt = CT^n \quad \text{for fixed K, T in °C} \tag{2.1}$$

where

C, n = Functions of K only

Assuming linear cumulative damage, the total crack growth in a thermal cycle Δa was found by integrating da/dt over the cycle:

$$\Delta a = \int_{t_1}^{t_2} C\,T^n\,dt \tag{2.2}$$

They tested triangular thermal profiles with no hold times, hold time at maximum temperature, hold time at minimum temperature, hold time at both temperatures, and non-symmetric hold times and thermal cycling rates. The linear cumulative-damage model predicted crack-growth rates within a factor of two of the experimental results. This was within the data scatter range for tests of this type.

Several TMF crack-growth studies have been performed on very high temperature turbine-blade materials. Rau, Gemma, and Leverant (38) evaluated TMF crack growth in cast cobalt-base, cast nickel-base, and directionally-solidified nickel-base alloys with load/temperature in and out-of-phase at a frequency of 0.5 cycles per minute and temperatures ranging from 316°C to 1038°C. The phase relationships of basic TMF cycles are shown in Figure 2.3. The 180° out-of-phase strain/temperature cycle (maximum temperature at maximum compressive strain) produced the highest crack-growth rate, higher than both the isothermal crack-growth rate at the minimum test temperature and the in-phase TMF crack-growth rate. A 90° out-of-phase TMF cycle produced crack-growth rates between the in-phase and 180° out-of-phase rates. Raising the minimum TMF temperature from 316°C to 426°C did not significantly affect crack-growth rates, but raising the maximum TMF temperature from 927°C to 1038°C produced higher crack-growth rates.

Thus, in that study, out-of-phase TMF appeared to be more damaging than in-phase TMF and the crack-growth damage was particularly sensitive to the maximum temperature in the TMF cycle. Rau, et. al. (38) used the strain intensity factor K_ε as the crack-growth correlation parameter and concluded that LEFM was applicable for these materials and test conditions. The strain intensity factor is similar to the stress intensity factor with remote stress replaced by remote strain, and has units $\sqrt{in}$ or $\sqrt{m}$. Gemma, Ashland, and

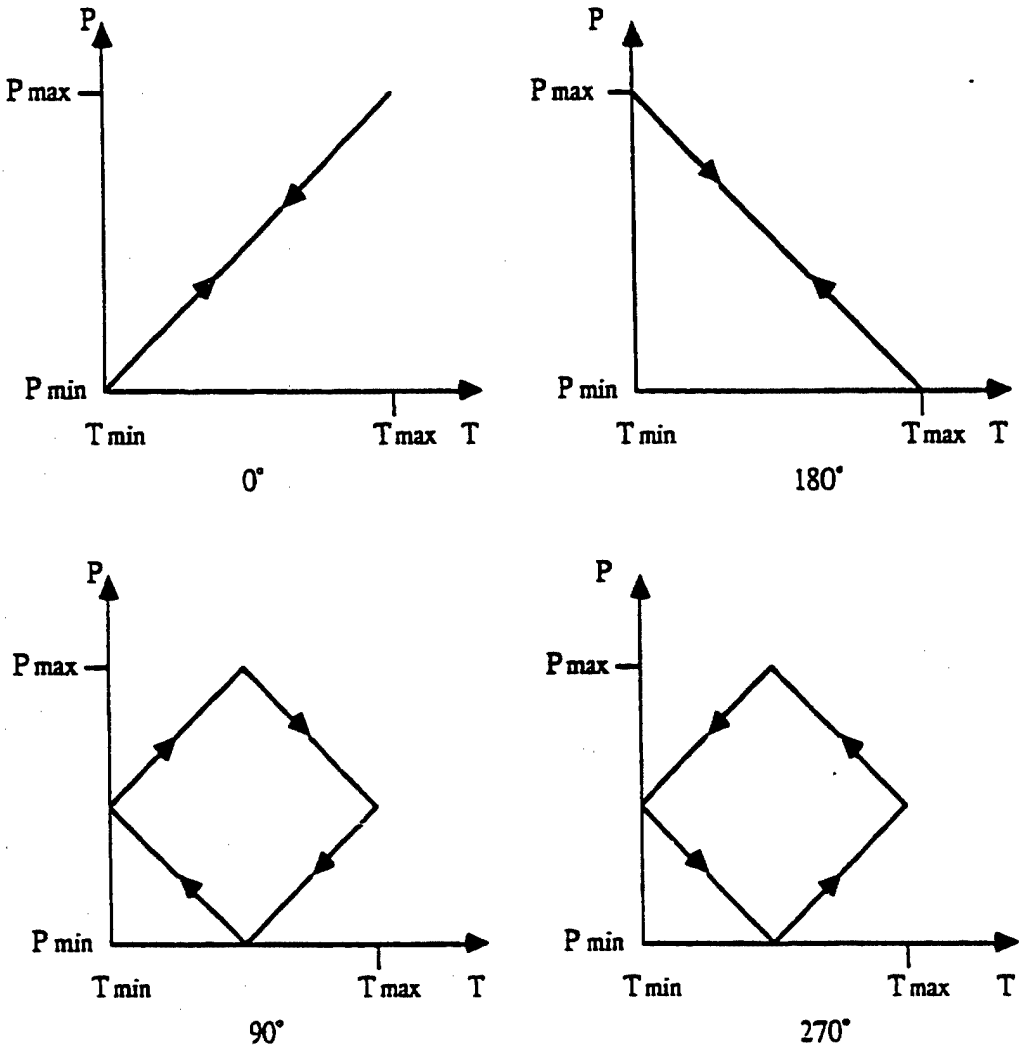

Figure 2.3: Basic TMF Cycle Phase Diagrams (Load Control)

Masci (39) also successfully applied the strain intensity factor to correlate TMF crack growth data in two nickel-base alloys.

DeLuca and Cowles (40) performed crack initiation and crack-growth TMF tests on an advanced cast single crystal turbine blade alloy. In-phase and 180° out-of-phase tests were conducted between 427°C and 982°C at a frequency of 0.0083 Hz. They found the 180° out-of-phase cycle to be the most damaging for crack initiation. However, the in-phase cycling was found to produce more rapid crack growth than out-of-phase cycling. At higher stress intensity factor ranges, the in-phase TMF crack-growth rate was found to be greater than the isothermal crack-growth rate at the upper cycle temperature.

Wright, Jang, and Popp (41) performed TMF fatigue crack-growth tests under load control on the single crystal superalloy René N4. The temperature was cycled between 649°C and 1093°C with the load 180° out-of-phase. The total cycle time of 180 seconds included a 60-second hold time at maximum temperature and minimum load. Using the elastic stress intensity factor as a correlating parameter, they found the TMF crack-growth rate to be slightly greater than the isothermal rate for the minimum cycle temperature, but significantly less than the isothermal rate for the maximum cycle temperature.

Gemma, Langer, and Leverant (42) performed the TMF crack-growth tests on a directionally-solidified nickel-base superalloy at 0.0074 Hz from 427°C to 1038°C. They also (successfully) applied LEFM using both stress and strain intensity factors.

Meyers (27) and Jordan and Meyers (43) predicted TMF crack-growth rates in Hastalloy with reasonable accuracy using a linear cumulative-damage model. Temperatures were cycled between 426°C and 982°C and the strain intensity factor was used as the crack-growth correlation parameter in the model. The cyclic crack growth rate Δa was assumed to be a simple function of the maximum strain intensity factor:

$$\Delta a = C K_\varepsilon^B \tag{2.3}$$

where

C and B = functions of temperature only.

The differential growth was integrated over the loading portion of the TMF cycle:

$$\Delta a = \int_0^{K_{\varepsilon max}} \frac{d(\Delta a)}{dK_\varepsilon} dK_\varepsilon = \int_0^{K_{\varepsilon max}} B C K_\varepsilon^{B-1} dK_\varepsilon \tag{2.4}$$

The crack-growth rates predicted by this model were closer to the actual test results than the isothermal crack-growth rates at the maximum cycle temperature. Jordan and Meyers also found that the elastic stress intensity factor did a reasonable job of correlating TMF crack growth data.

Marchand and Pelloux (44) performed in-phase and 180° out-of-phase load-controlled TMF crack growth tests on Inconel X-750 in the temperature range from 300°C to 650°C. At a test load ratio of 0.05, they found the in-phase TMF crack growth to be slightly lower than the isothermal crack growth at 650°C. They successfully applied the elastic stress intensity factor as a crack-growth correlation parameter.

To predict TMF crack growth, the tendency has been to use isothermal crack-growth data at the maximum temperature of the TMF cycle (27). However, Larsen, Schwartz, and Annis (5) found that the TMF crack-growth rates in IN100 under 0.0167-Hz triangular cycling, 180° out-of-phase, with R=0.1 and the temperature varying from 427°C to 704°C, correlated well with isothermal crack-growth rates at 427°C. They attributed this to the importance of the temperature at the time of the peak load and suggested that TMF behavior is more closely related to isothermal fatigue crack growth than originally thought.

General Electric (45) conducted the TMF crack-growth tests on 0.1-inch thick Inconel 718 specimens under 0.0083-Hz triangular cycling to a maximum stress of 100 ksi and at temperatures ranging from 399°C to 593°C. They compared TMF test results with isothermal crack growth at 399°C and 593°C under 0.0083-Hz triangular loading with no hold times. They found in-phase loading to be somewhat more damaging than 180° out-of-phase loading, pointing out the influence of time-dependent crack growth at elevated temperatures. Partially out-of-phase loading (90°) was found to be no less damaging than in-phase loading. Hold times at the maximum temperature were found to be the most damaging, particularly if the load was simultaneously high. Hold times at low stress and low temperature had negligible effect on crack growth. No attempt was made to develop a predictive model from the data.

A review of previous work in elevated temperature crack growth indicates the following:

1) The stress intensity factor, K, is generally considered a valid crack-growth correlation parameter for fatigue crack growth and sustained-load crack growth in Inconel 718 for temperatures up to about 650°C.

2) Three types of damage appear to contribute to elevated temperature crack growth in Inconel 718:

a. Purely cycle-dependent damage, which is transgranular and independent of the loading frequency and test temperature. This damage dominates at all loading frequencies at low temperatures and at high loading frequencies at high temperatures. Cycle-dependent damage dominates at 537°C and below (9).

b. Purely time-dependent damage, which is intergranular, environmentally enhanced, and dependent upon the period of the loading cycle and test temperature. This damage dominates at very low loading frequencies at high temperatures. Time-dependent damage dominates at 649°C at loading frequencies below about 0.01 Hz (20).

c. Mixed-mode damage, which is a mixture of transgranular and intergranular damage and appears to result from the interaction of cycle-dependent and time-dependent behaviors. This damage is observed at frequencies between the cycle-dependent and time-dependent regions at temperatures between 427°C and 649°C.

III. Experimental Apparatus and Procedure

In order to investigate thermal-mechanical fatigue crack growth behavior and develop a predictive model, a series of experiments were conducted on equipment in the Metals Behavior Branch of the Air Force Wright Aeronautical Laboratories' Materials Laboratory. This section discusses the test apparatus and the procedure used to obtain all experimental data. The test equipment was developed by Mr. George Hartman and Mr. David Johnson of the University of Dayton Research Institute (46, 47).

Description of Test Apparatus

The thermal-mechanical test equipment consists of the following major components:

1) Center-cracked tension specimen
2) Five K-type thermocouples
3) Micricon 82300 microcomputer
4) Four quartz lamp heaters
5) Cooling air jets
6) IBM 9000 computer
7) MTS servohydraulic loading machine
8) D.C. potential drop crack measuring system
9) Traveling microscope

All tests were conducted on standard center-cracked panel specimens of Inconel 718, approximately 50 millimeters wide by 2.41 millimeters thick. This specimen geometry was chosen because of its high surface-to-volume ratio, which allows maximum heating/cooling rates and minimum through-the-thickness temperature variations. The

specimen geometry is shown in Figure 3.1. The exact specimen dimensions are listed in Table 3.1.

The stress intensity factor solution for the center-cracked panel specimen is given by ASTM Standard Test Method E647-83 (48) as:

$$\Delta K = \frac{\Delta P}{B} \sqrt{\frac{\pi}{2} \frac{\alpha}{w} \sec\left(\frac{\pi}{2} \frac{\alpha}{w}\right)} \qquad (3.1)$$

$$\alpha = \frac{2a}{w} \qquad (3.2)$$

where: a = Crack length

w = Specimen width

ΔK = Stress intensity range

ΔP = Load range

B = Specimen thickness

Five K-type thermocouples are spotwelded to the specimen at the locations shown in Figure 3.1. The one closest to the center of the crack provides temperature data to the test observer. The other four provide temperature feedback to the Micricon microcomputer. The Micricon independently controls four 1000 watt quartz heating lamps to maintain a desired thermal profile. Each lamp is associated with a thermocouple and provides a 50.8 mm by 38.1 mm heating zone on the specimen as shown in Figure 3.2 (49).

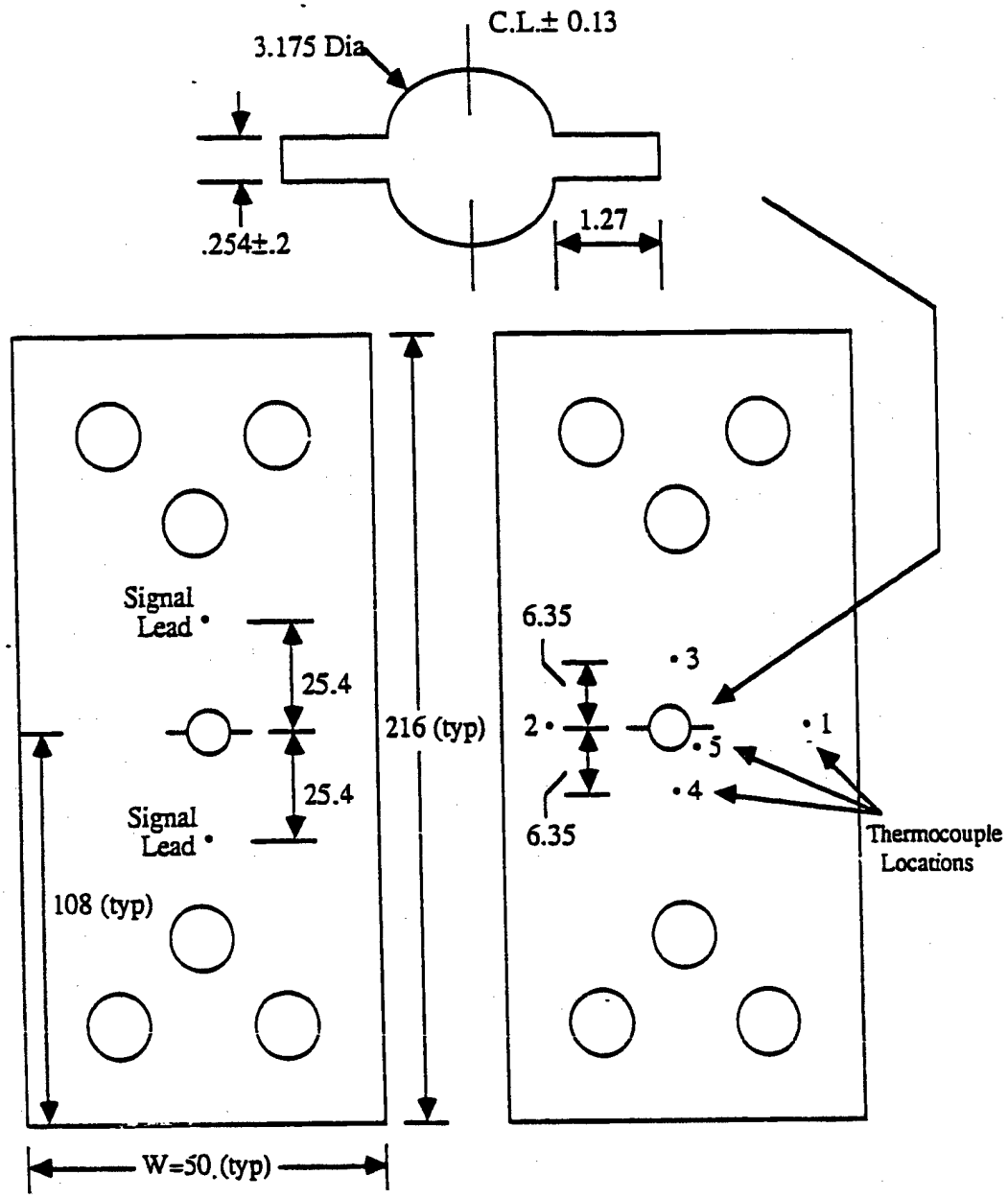

Figure 3.1: Specimen Geometry (all dimensions in millimeters)

Table 3.1

Exact Specimen Dimensions and Total Precrack Length

Specimen No.	Width (mm)	Thickness (mm)	Precrack 2a (mm)
85-209	50.8	2.41	10.16
85-298	50.24	2.36	10.77
85-300	50.65	2.39	12.04
85-303	50.55	2.29	10.74
85-304	50.7	2.31	10.73
85-306	50.62	2.39	11.07
85-307	50.37	2.36	10.68
85-308	50.37	2.34	10.49
85-309	50.24	2.34	10.67
85-310	50.52	2.36	10.73
85-312	50.37	2.36	10.61
85-313	50.44	2.34	10.57
85-314	50.62	2.29	10.39
85-315	50.52	2.36	11.29
85-316	50.50	2.29	10.27
85-317	50.09	2.36	10.53
85-318	50.47	2.36	10.40
85-319	50.67	2.36	10.76

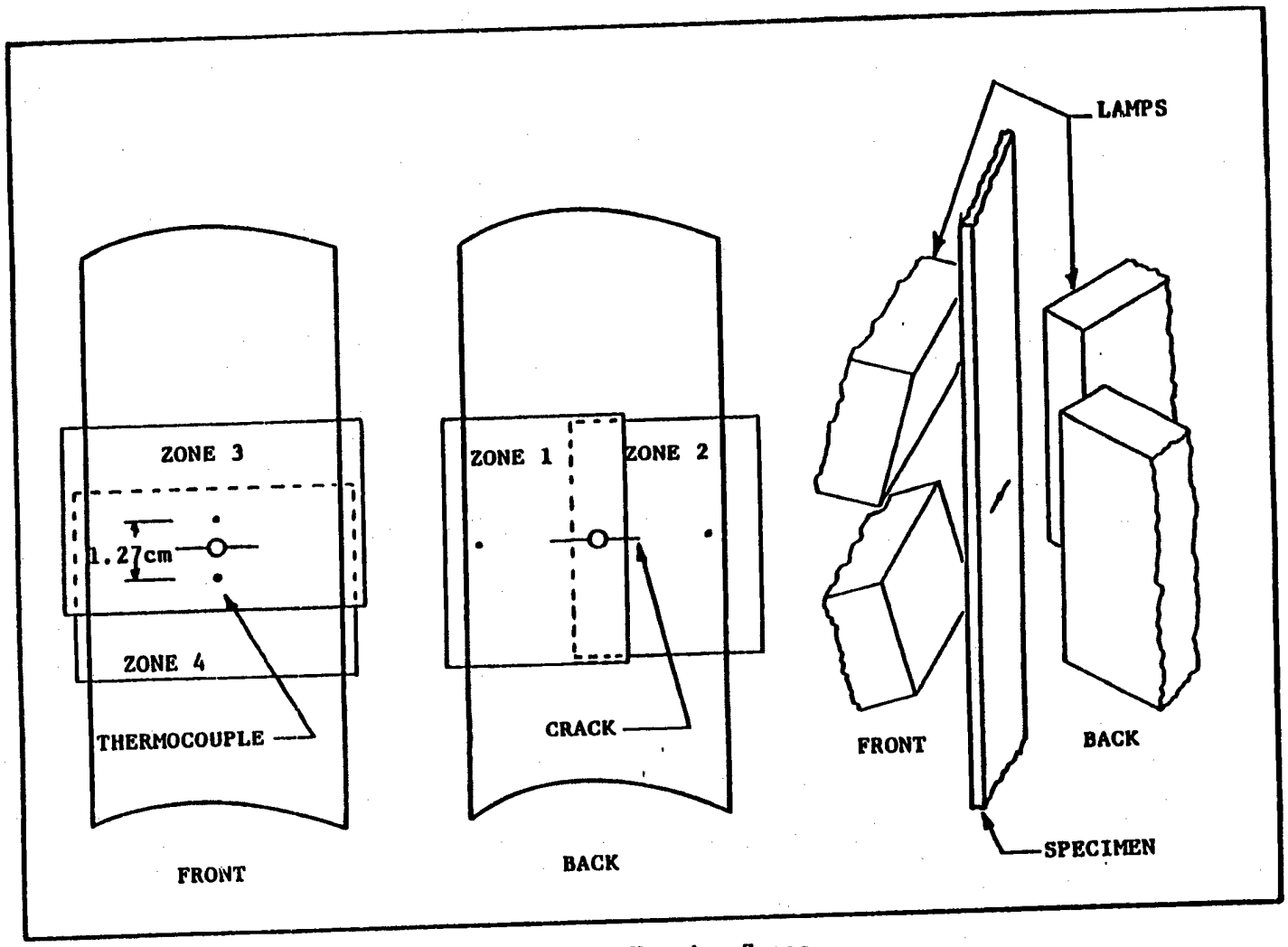

Figure 3.2: Lamp Heating Zones

The Micricon also controls an on/off solenoid to provide room temperature compressed air to the cooling jets. Two 6.35 mm diameter copper tubes with 1.27 mm outlet holes provide an updraft of cooling air on the back side and a downdraft of air on the front side of the specimen as shown in Figure 3.3. It was found that applying cooling air during the heating and cooling portions of a thermal cycle and compensating with the lamps provided the best temperature control of the specimen. The closed loop heating and cooling system is able to heat and cool the crack-tip region of the specimen at a rate of 8°C per second while maintaining a temperature variation over the specimen width of 5°C or less (49). A typical programmed thermal cycle and actual specimen temperature response is shown in Figure 3.4. The lag time between programmed and actual system response is one second or less with a temperature variance of 5°C or less (49).

The desired thermal cycle characteristics (waveshape, period, and temperature limits) are provided to the Micricon by an IBM 9000 computer. This computer controls all aspects of a thermal-mechanical fatigue crack-growth test. The operator enters specimen characteristics (type, dimensions, material properties), thermal cycle characteristics (waveshape, period, and temperature limits), mechanical cycle characteristics (waveshape, period, load ratio, maximum load, and phase relationship with temperature), and the data acquisition interval. The load is applied to the specimen by a MTS servohydraulic testing machine.

The crack length in the specimen is automatically measured using a D.C. electric potential drop technique. A direct current of 10 amps is imposed through the specimen and a voltmeter measures the potential drop across the crack through two leads spotwelded to the specimen (shown in Figure 3.1). The IBM 9000 computer uses the potential drop to calculate the crack length using H. H. Johnson's closed form analytic solution for the electric potential field in a finite width plate with a central crack (47).

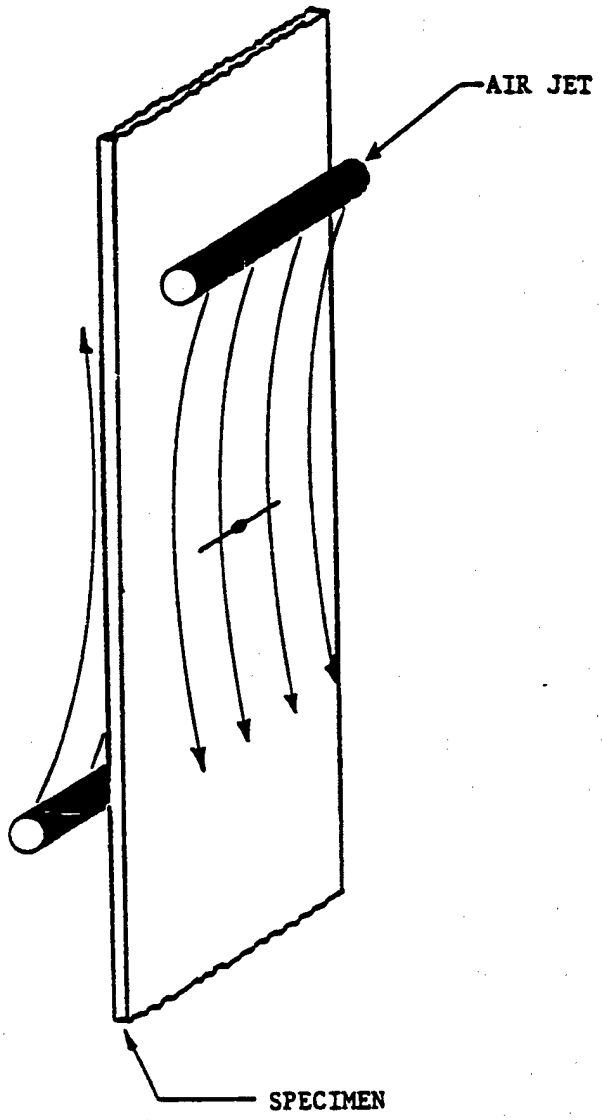

Figure 3.3: Air Cooling

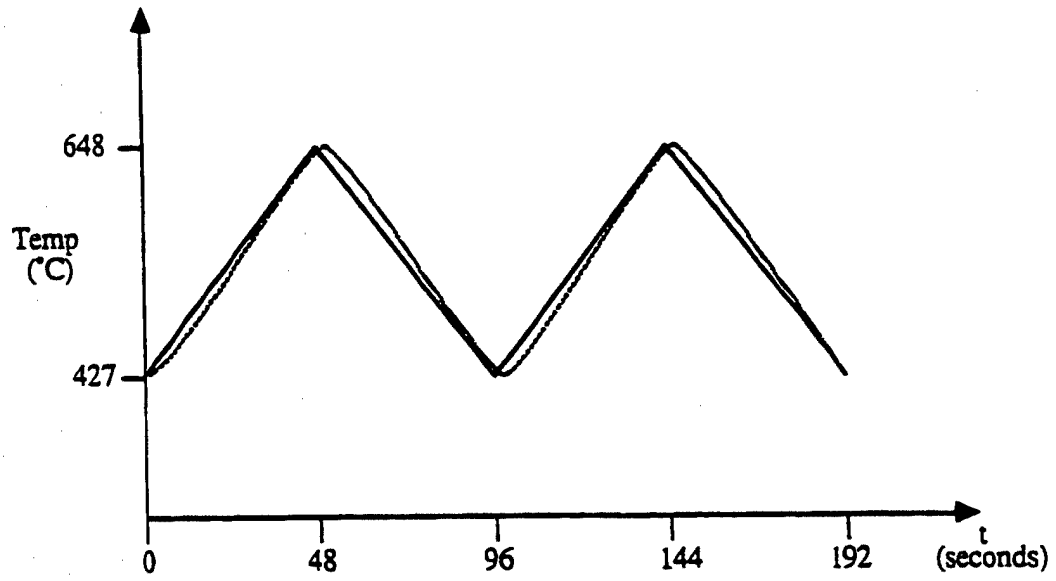

Figure 3.4: Typical Programmed versus Actual Temperature Response

The IBM 9000 computer automatically saves the appropriate data (cycle number, maximum load, and crack length) on a hard disk. The calculated crack lengths are periodically verified with a Gaertner 10X traveling microscope. The electric potential drop system was evaluated by Hartman and Johnson on this specimen type and found to produce crack length data accurate within ±0.1 mm for isothermal and thermal-mechanical fatigue crack growth tests (47).

Test Procedure

Eighteen Inconel 718 center-cracked panel specimens were tested. A through-the-thickness starter notch, approximately 5.71 mm long, was machined in the center of the specimen in accordance with the requirements for this specimen type given in ASTM Standard E647 (48). The notch geometry is shown in Figure 3.1. The specimens were heat treated as shown in Appendix A. A band, approximately 9.5 mm wide, was polished to a mirror-like finish across the width of the specimen in the region of the starter notch to improve the visibility of the crack tip. The thermocouples and electric potential drop leads

were spotwelded to the specimen at the locations shown in Figure 3.1. The specimen is precracked at room temperature to a final crack length of approximately 5.334 mm on a decreasing stress intensity factor schedule to a final maximum stress intensity level of 14.3 $MPa\sqrt{m}$. All precracking was performed in accordance with ASTM Standard E647. The final precrack lengths for each specimen are listed in Table 3.1.

To perform a crack growth test, the following test parameters are entered into the IBM 9000 computer:

1) Specimen type, identification number, and dimensions
2) Initial crack length
3) Final crack length (test will automatically stop upon reaching this length)
4) Test temperature (isothermal tests), or temperature-time profile (thermal-mechanical tests)
5) Material modulus and yield stress at maximum test temperature
6) Test type (constant maximum load or decreasing K threshold). Constant maximum load tests were used for this investigation.
7) Load ratio
8) Load waveform (triangle or sine, isothermal tests), or load-time profile and phase relationship with temperature (thermal-mechanical tests)
9) Load frequency (isothermal tests)
10) Data acquisition interval (time increment or crack-length increment)

After the test is started, all data acquisition is fully automated. The operator may update the crack length using the traveling microscope at any time. The operator can plot crack length, a, versus cycle number, N, or crack-growth rate da/dN, versus stress intensity factor range, ΔK, on a video screen as the test is running. Data were acquired up to the point of specimen failure. All data which exceeded the following ASTM Standard E647 plastic zone size restriction were discarded (48):

$$P_{max} \leq \frac{(w - 2a)\, B}{1.25}\, \sigma_{ys} \qquad (3.3)$$

w = Specimen width

2a = Total crack length

B = Specimen thickness

σ_{ys} = Specimen yield strength

After the test is completed, the test data are transferred to a PDP 11/24 computer for processing. For sustained-load crack growth tests, the raw data consisted of crack length, time of data acquisition, and applied load. For fatigue crack-growth tests, the raw data were crack length, cycle number, load ratio, and maximum load applied. These data were reduced to crack growth per second versus stress intensity factor (sustained-load crack growth) or crack growth per cycle versus stress intensity factor range (fatigue crack growth) using a least squares sliding polynomial fit of seven or more points in accordance with ASTM Standard E647 (48).

Isothermal test results are discussed in Chapter IV. Thermal-mechanical fatigue test results are discussed in Chapter V.

IV. Crack Growth Predictive Model Development

Mechanistic Basis of Linear Cumulative Damage Model

The micro-mechanisms of elevated temperature crack growth in Inconel 718 provide a conceptual basis for the development of a mathematical model to predict crack growth under conditions of varying load and temperature (thermal-mechanical cycling). The contribution to crack growth of each of two dominant mechanisms during a thermal-mechanical cycle is addressed in a predictive model. In addition, the model addresses the effect of mechanism interactions. A linear cumulative damage concept is proposed for the model development.

The two dominant mechanisms contributing to elevated temperature crack growth in Inconel 718 are environmental interaction (oxidation) and mechanical fatigue. A third mechanism, creep damage due to grain boundary cavitation and triple point cracking, can also occur (20). Since the contribution to crack growth due to creep is several orders of magnitude below that of the environment at temperatures below 650°C (14,15), this mechanism is not considered in the model development. Only the contributions to crack growth of environmental interaction and mechanical fatigue are addressed by the model.

Environmental interaction, one of the two dominant mechanisms of crack growth, occurs when oxygen diffuses into the region ahead of the crack tip along grain boundaries (20). The material along the grain boundaries oxidizes and becomes brittle. The stress field ahead of the crack fractures the embrittled grain boundaries, allowing further oxide penetration (55). The grain boundaries are the preferred path for oxide penetration and cracking because they are regions of high strain energy and high defect concentration and thus provide a rapid diffusion path. Furthermore, they are regions rich in highly oxidizable carbides (56). The state of stress ahead of the crack enhances oxidation and oxidation-induced crack growth. The strain energy associated with the stress field encourages

chemical reactions, and the increased number of vacancy sources due to stress enhances oxidation (17). Since the environmentally-enhanced fracture occurs along the grain boundaries, the resulting fracture surface is intergranular. A photograph of such a fracture surface is shown in Figure 14 of Reference 19.

The crack growth rate due to environmental interaction is controlled by the diffusion rate of oxygen ahead of the crack tip. Since diffusion is a thermally activated process, the crack growth rates at high temperature are higher than those at low temperature. Since diffusion is a time-dependent process, environmentally-enhanced crack growth is also time-dependent. The crack growth resulting from this mechanism is thus a linear function of the cycle period. The region dominated by this mechanism is called time-dependent. A plot on log-log pa of crack growth rate versus loading frequency for a constant value of K_{max} in the time- ndent region has a slope of -1, as shown previously in Figure 2.1 (20). Environmentally enhanced crack growth is dominant at high temperatures and low loading frequencies (20).

The second dominant mechanism in elevated temperature crack growth is mechanical fatigue. At high loading frequencies, the time for oxygen diffusion and environmentally enhanced damage to develop during a cycle is low, so little time dependent damage develops. In this situation, the mechanical fatigue crack growth mechanism dominates. At low temperatures, the diffusion-controlled environmentally-enhanced crack growth process is very slow, so the mechanical fatigue crack growth mechanism dominates (9).

Mechanical fatigue occurs due to a complex process described below. The stresses near the crack tip in an elastic body under load a square-root singular. Since infinite stresses cannot develop in an actual material, plastic strain develops near the crack tip under cyclic loading. During the loading portion of the cycle, localized flow occurs along favorable slip paths in both maximum shear directions at the crack tip. Crack extension

occurs by shear decohesion at the inner edge of the crack tip flow bands during the tensile strain increment. As the load increases, work hardening of the flow bands will occur and the increasing stress will activate other parallel slip planes (57).

At the crack tip, a small plastic zone is surrounded by elastic material. During load release, the surrounding elastic material will contract and exert compressive stresses on the plastic zone, which is too large for its surroundings. The compressive stresses are above yield at the crack tip, leading to fully reversed plastic deformation which closes and resharpens the crack tip (58). The cyclic opening and closing of the crack causes the development of a pattern of ripples on the fracture surface, called fatigue striations. Crack growth proceeds through the grains and the resulting fracture surface is transgranular (9, 11). The transgranular fracture surface resulting from mechanical fatigue crack growth is shown in Figure 3 of Reference 11.

Since the mechanism causing mechanical fatigue crack growth is not controlled by a rate dependent process such as diffusion, the crack growth rate due to mechanical fatigue is independent of the loading cycle period.

The amount of crack growth from mechanical fatigue depends upon the number of cycles applied and not the cycle frequency. The region dominated by this mechanism is called cycle-dependent, as shown previously in Figure 2.1 (20). Further, since the mechanism is not a thermally activated process, temperature will not have a large effect upon cycle-dependent damage (20, 32). Any minor effect due to temperature is attributed solely to small changes in the modulus of elasticity and yield strength (32).

The mechanical fatigue and environmentally-enhanced crack growth mechanisms are always active. In the cycle dependent region, the mechanical fatigue process dominates and in the time dependent region, the environmentally-enhanced crack growth process dominates. Since both processes are active, a simple linear summation of the damage

effects over a cycle will provide a measure of the total crack growth damage for that cycle. This basic concept is applied in the development of a linear cumulative damage model.

In Inconel 718, cycle dependent crack growth is independent of the test temperature and loading frequency for temperatures below 650°C. Since mechanical fatigue is the dominant mechanism at 427°C, the cycle dependent damage contribution to crack growth for a mechanical cycle of any frequency at any temperature below 650°C can be identified from a fatigue crack growth test at 427°C.

The environmentally-enhanced crack growth rate, da/dt, for a given temperature and stress intensity level can be identified from elevated temperature sustained-load crack growth tests. Previous research has shown that time-dependent damage occurs only during the loading portion of the cycle (30, 32, 34). The compressive stresses at the crack tip as the load starts to decrease inhibit oxide cracking, diffusion, and oxidation, thereby inhibiting environmentally-enhanced crack growth. Therefore, it is proposed that the time-dependent damage over a cycle be calculated by integrating the sustained-load crack growth rate over the loading portion of the mechanical cycle:

$$\left(\frac{da}{dN}\right)_{\substack{\text{time-}\\\text{dependent}}} = \int_{\substack{\text{loading}\\\text{portion}}} \left(\frac{da}{dt}\right) dt \qquad (4.1)$$

A simple summation of cycle dependent damage identified from a low temperature fatigue crack growth test and time dependent damage calculated with equation (4.1) has been shown to provide good predictions of isothermal fatigue crack growth rates in the time-dependent and cycle-dependent regions (30). At high temperatures and low loading frequencies (time-dependent region), the time-dependent damage calculated by equation (4.1) is much larger than the cycle-dependent damage. At high temperatures and high frequencies or low temperatures (cycle-dependent region), the time dependent damage

calculated by equation (4.1) is much smaller than the cycle-dependent damage. Thus, each term dominates in the appropriate region.

In intermediate regions where both mechanisms contribute similar amounts to crack growth, interactive effects have been observed. For Inconel 718 at 649°C and loading frequencies between 0.01 Hz and 10 Hz, experimentally observed crack growth rates are shown by the inclined line in the "mixed-mode" region of Figure 2.1 (20). This line lies somewhat above the sum of the cycle-dependent damage line (horizontal line from the "cycle-dependent" region) and the time-dependent damage line (inclined line of -1 slope from the "time-dependent" region). It is proposed to add a mixed-mode damage term to the linear cumulative damage model to account for this additional experimentally observed damage:

$$\left(\frac{da}{dN}\right)_{total} = \left(\frac{da}{dN}\right)_{cycle\text{-}dependent} + \left(\frac{da}{dN}\right)_{time\text{-}dependent} + \left(\frac{da}{dN}\right)_{mixed\text{-}mode} \qquad (4.2)$$

The additional mixed-mode damage shown in Figure 2.1 is small and decreases to zero at frequencies above 10 Hz, where cycle-dependent damage dominates, and frequencies below 0.01 Hz, where time-dependent damage dominates. The fracture surface in the mixed-mode region has a mixture of transgranular and intergranular damage (20). Such a fracture surface is also observed in Inconel 718 at intermediate temperatures (538°C) and low loading frequencies (32).

Synergistic interactions between environmentally enhanced crack growth and mechanical fatigue crack growth contribute to the additional mixed-mode damage. Possible fatigue-environment interactions that lead to mixed-mode crack growth include:

1) The point defects generated during fatigue cycling enhance oxidation and time-dependent crack growth (19).

2) Fatigue cycling spalls off the oxide film on the crack surface, leading to further oxidation.

3) Slip due to fatigue cycling exposes additional material to oxidation attack.

The proposed linear cumulative damage model developed above is based upon the dominant mechanisms of elevated temperature crack growth in Inconel 718. Similar modeling concepts have been applied to isothermal fatigue crack growth and non-isothermal sustained load crack growth (30, 37). However, this concept has never been applied to predict crack growth under thermal-mechanical cycling.

The two dominant mechanisms of elevated temperature crack growth were used to determine the temperature limits of the thermal-mechanical cycles used in the experimental portion of this investigation. The lower limit was set at a temperature where the mechanical fatigue mechanism dominates at all loading frequencies (427°C). The upper limit was set at a temperature where the environmentally assisted mechanism dominates at low loading frequencies (649°C). The thermal-mechanical cycle period was set at 96 seconds to allow accurate temperature control of the test specimen over these temperature limits. Thus, the dominant crack growth mechanism transitions from mechanical fatigue to environmental interaction during a thermal-mechanical cycle. During this transition, the mechanisms may interact to produce additional mixed-mode damage. Each contribution is addressed by the proposed linear cumulative damage model.

Since cycle-dependent damage is independent of temperature and loading frequency, the contribution of this damage in a thermal-mechanical cycle is found from an isothermal fatigue crack growth test at low temperature. The calculation of time-dependent damage in a thermal-mechanical cycle using equation (4.1) requires sustained load crack growth data, da/dt, at all temperatures within the cycle. Sustained load crack growth tests are conducted at three temperatures and an interpolative model is applied to interpolate crack growth rate data between the test temperatures.

Interpolative Models

Two curve-fit models have been developed to interpolate crack growth rate data between different test conditions. The models empirically fit a function to crack growth rate data. Plots of experimental cyclic fatigue crack-growth data, da/dN, versus stress intensity range, ΔK, typically assume a sigmoidal shape on log-log paper. This shape is shown in Fig. 4.1. Pratt and Whitney's SINH model fits a hyperbolic sine curve to test data using four coefficients that are simple functions of the test parameters. The coefficient-parameter functional relationships were empirically developed to provide good interpolations of crack growth rate data. General Electric's MSE model uses a modified sigmoidal equation with six coefficients to fit data. Given a limited set of data, both models do a reasonable job of describing crack-growth rates between ranges of load frequency, load ratio, temperature, and hold time (50). In addition to fatigue crack-growth rate data, plots of sustained-load crack-growth rate, da/dt, versus K are also often sigmoidal (5) and could be modeled with SINH or MSE. The MSE curve fit model was used in this investigation.

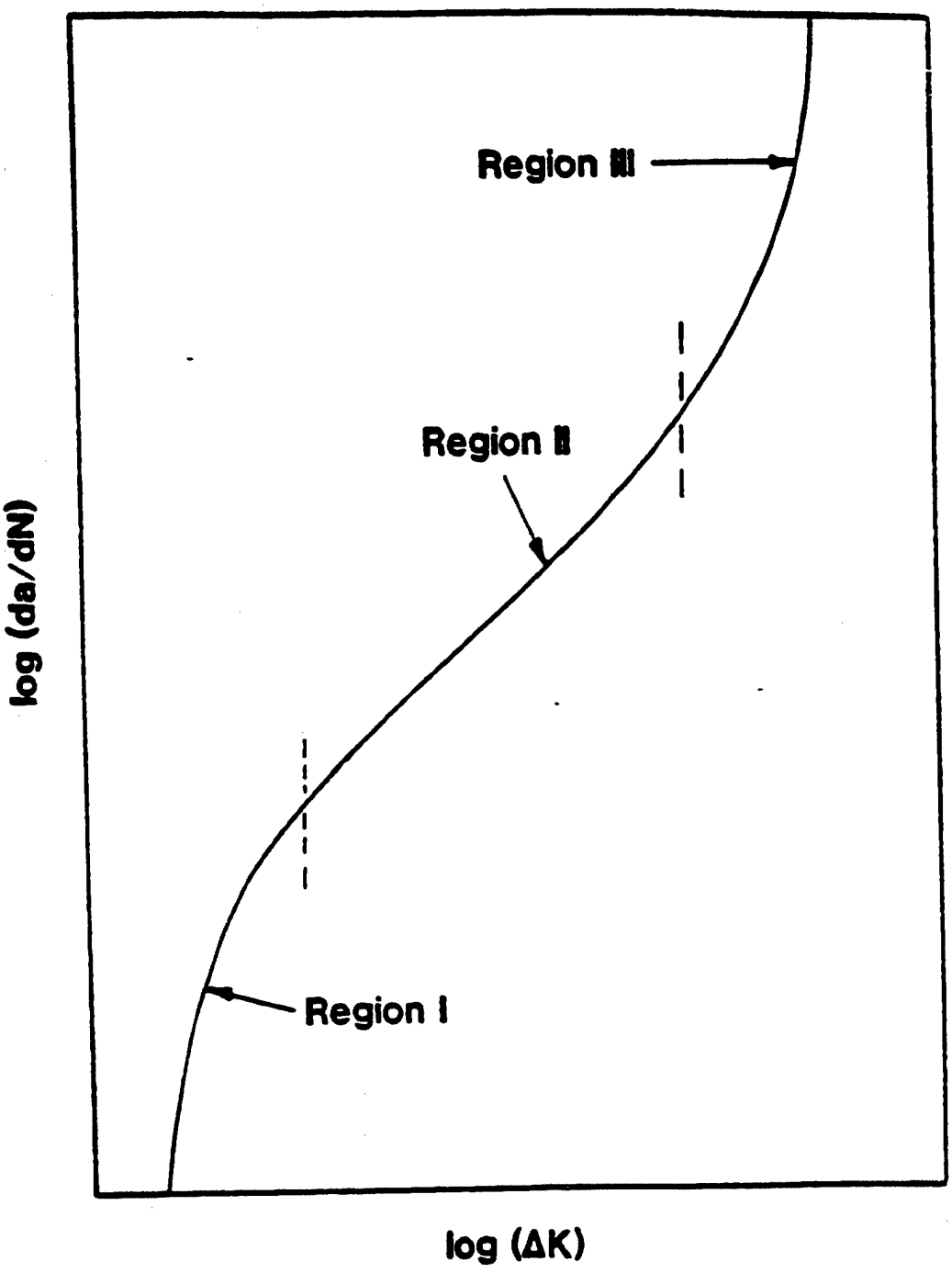

Figure 4.1: Sigmoidal Shape of Fatigue Crack Growth Rate Data

The Modified Sigmoidal Equation Model

The modified sigmoidal equation (MSE) model fits da/dN versus ΔK data with a modified sigmoidal curve (51):

$$\frac{da}{dN} = \exp B' \left(\frac{\Delta K}{\Delta K_i}\right)^P \left[\ln\left(\frac{\Delta K}{\Delta K^*}\right)\right]^Q \left[\ln\left(\frac{\Delta K_c}{\Delta K}\right)\right]^D \tag{4.3}$$

$$\text{where } D = -\left[Q^{1/2} \ln\left(\frac{\Delta K_i}{\Delta K_c}\right) \Big/ \ln\left(\frac{\Delta K_i}{\Delta K^*}\right)\right]^2 \tag{4.4}$$

$$P = \left(\frac{da}{dN_i}\right)' - \frac{Q}{\ln\left(\frac{\Delta K_i}{\Delta K^*}\right)} + \frac{D}{\ln\left(\frac{\Delta K_c}{\Delta K_i}\right)} \tag{4.5}$$

$$B' = \ln\left(\frac{da}{dN_i}\right) - Q \ln\left[\ln\left(\frac{\Delta K_i}{\Delta K^*}\right)\right] - D \ln\left[\ln\left(\frac{\Delta K_c}{\Delta K_i}\right)\right] \tag{4.6}$$

The six independent parameters in the MSE model are Q, ΔK_i, ΔK^*, ΔK_c, (da/dN_i), and $(da/dN_i)'$. The physical meanings of these parameters on a MSE curve are shown in Figure 4.2.

The parameters Q and D control the sharpness of the transition from the inflection point to the asymptotes. Decreasing the absolute value of the parameters will increase the sharpness of the transition (52). The MSE curve can be made symmetric about the inflection point by setting Q equal to –D:

$$Q = -D \tag{4.7}$$

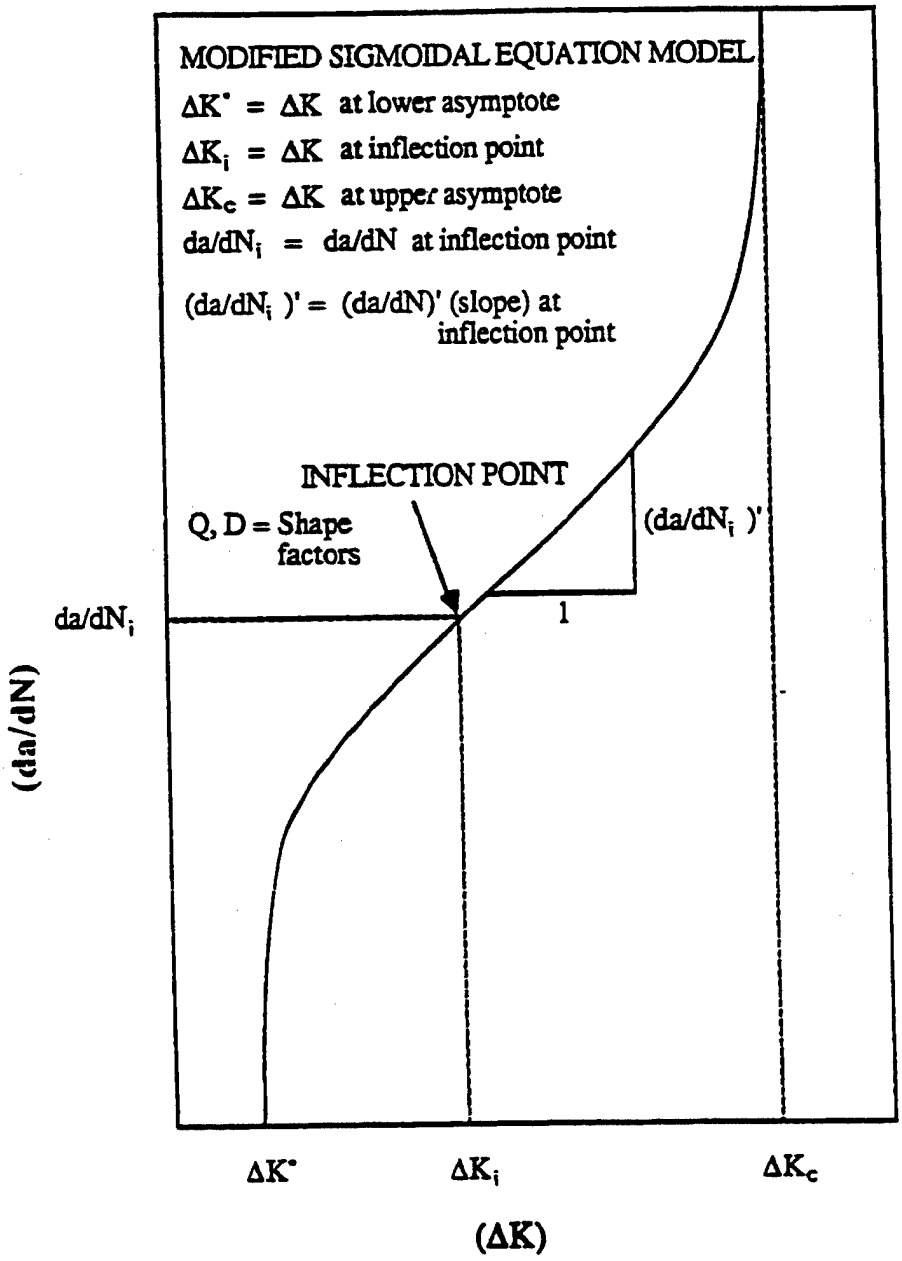

Figure 4.2: Definition of MSE Parameters

Substituting (4.7) in (4.4):

$$Q = Q \left[\ln \left(\frac{\Delta K_i}{\Delta K_c} \right) \Big/ \ln \left(\frac{\Delta K_i}{\Delta K^*} \right) \right]^2 \qquad (4.8)$$

Dividing by Q and taking the square root of both sides, get:

$$\ln \left(\frac{\Delta K_i}{\Delta K^*} \right) - \ln \left(\frac{\Delta K_i}{\Delta K_c} \right) = 0 \qquad (4.9)$$

$$\ln \left(\frac{\Delta K_i}{\Delta K^*} \right) + \ln \left(\frac{\Delta K_i}{\Delta K_c} \right) = 0 \qquad (4.10)$$

Taking the exponential of both sides of (4.9) and (4.10), get:

$$\Delta K^* = \Delta K_c \quad \text{(Trivial solution)} \qquad (4.11)$$

$$\frac{\Delta K_i^2}{\Delta K_c \, \Delta K^*} = 1 \qquad (4.12)$$

Solving (4.12) for ΔK_c, get:

$$\Delta K_c = \frac{\Delta K_i^2}{\Delta K^*} \qquad (4.13)$$

Equation (4.13) reduces the number of independent parameters to five and does not impair the ability of the model to fit da/dN versus ΔK data (53). In addition, Painter found that setting the shaping parameter Q equal to a constant for a given material and set of test conditions did not impair the modeling process (52).

The functional relationships between the four MSE parameters (excluding Q) and test temperature T, loading frequency f, hold time t_H, and load ratio R were investigated by

Utah (51) and Painter (52). They found that a simple linear relationship between the parameter and test variable existed on a log-log scale [ΔK^*, ΔK_i, (da/dN_i) and R, f, t_H], log-linear scale [ΔK^*, ΔK_i, (da/dN_i) and T], linear-log scale [$(da/dN_i)'$ and R, f, t_H], and linear-linear scale [$(da/dN_i)'$ and T]. These relationships can be depicted in a matrix equation:

$$\begin{pmatrix} \log \Delta K^* \\ \log \Delta K_i \\ \log(da/dN_i) \\ (da/dN_i)' \end{pmatrix} = \begin{pmatrix} \log \Delta K^*_{base} \\ \log (\Delta K_i)_{base} \\ \log(da/dN_i)_{base} \\ (da/dN_i)'_{base} \end{pmatrix} + \begin{bmatrix} C_{11} & C_{12} & C_{13} & C_{14} \\ C_{21} & C_{22} & C_{23} & C_{24} \\ C_{31} & C_{32} & C_{33} & C_{34} \\ C_{41} & C_{42} & C_{43} & C_{44} \end{bmatrix} \begin{pmatrix} \log \left(\frac{1-R}{1-R_{base}} \right) \\ \log(f/f_{base}) \\ \log(t_h + 1) \\ (T - T_{base}) \end{pmatrix} . \quad (4.14)$$

The application of the MSE model to sustained load crack growth data is discussed in the Time Dependent Damage Term Development section of this chapter.

Cycle-Dependent Damage Term Development

To give an approximate prediction for the TMF crack growth rate over a given thermal-mechanical cycle, each of the three terms of the model must be found for that cycle. Since cycle-dependent damage is independent of temperature and loading frequency, the contribution of this damage in a thermal-mechanical cycle is found from isothermal fatigue crack growth tests at a low temperature (427°C). To find the load-ratio dependence of this term using the MSE model, tests are conducted at two load ratios. Two tests were conducted under triangular 10 Hz loading to define the cycle-dependent term: 427°C, R=0.1, and 427°C, R=0.5. The specimens used for the tests and test conditions are listed in Table 4.1. The maximum load in the cycle was held constant during these tests. Specimen 85-307 had a longer initial crack length than 85-304 due to crack growth during

an earlier decreasing load test at 427°C, R=0.5. The maximum cycle load for each test was chosen to provide an initial ΔK above threshold. The da/dN versus ΔK data for the two constant maximum load tests at 427°C are shown in Figure 4.3.

Table 4.1

Cycle-Dependent Term Test Conditions

Specimen	Temp (°C)	Load Ratio	Load Freq. (Hz)	Initial Crack Length (mm)	Maximum Cycle Load (KN)
85-304	427	0.1	10	7.18	13.4
85-307	427	0.5	10	12.24	12.5

A symmetric MSE model was used to fit the test data shown in Figure 4.3. The five MSE parameters ΔK^*, ΔK_i, (da/dN_i), $(da/dN_i)'$, and Q were iterated until a best visual fit of the data was obtained. The MSE parameters for the cycle-dependent term tests are listed in Table 4.2. The experimental data and MSE fits are shown in Figures 4.4 and 4.5. Since the tests were conducted under constant maximum load cycling, the data and MSE fits do not represent threshold values. The computer program used to generate the MSE curves is listed as PROGRAM FCG in Appendix B.

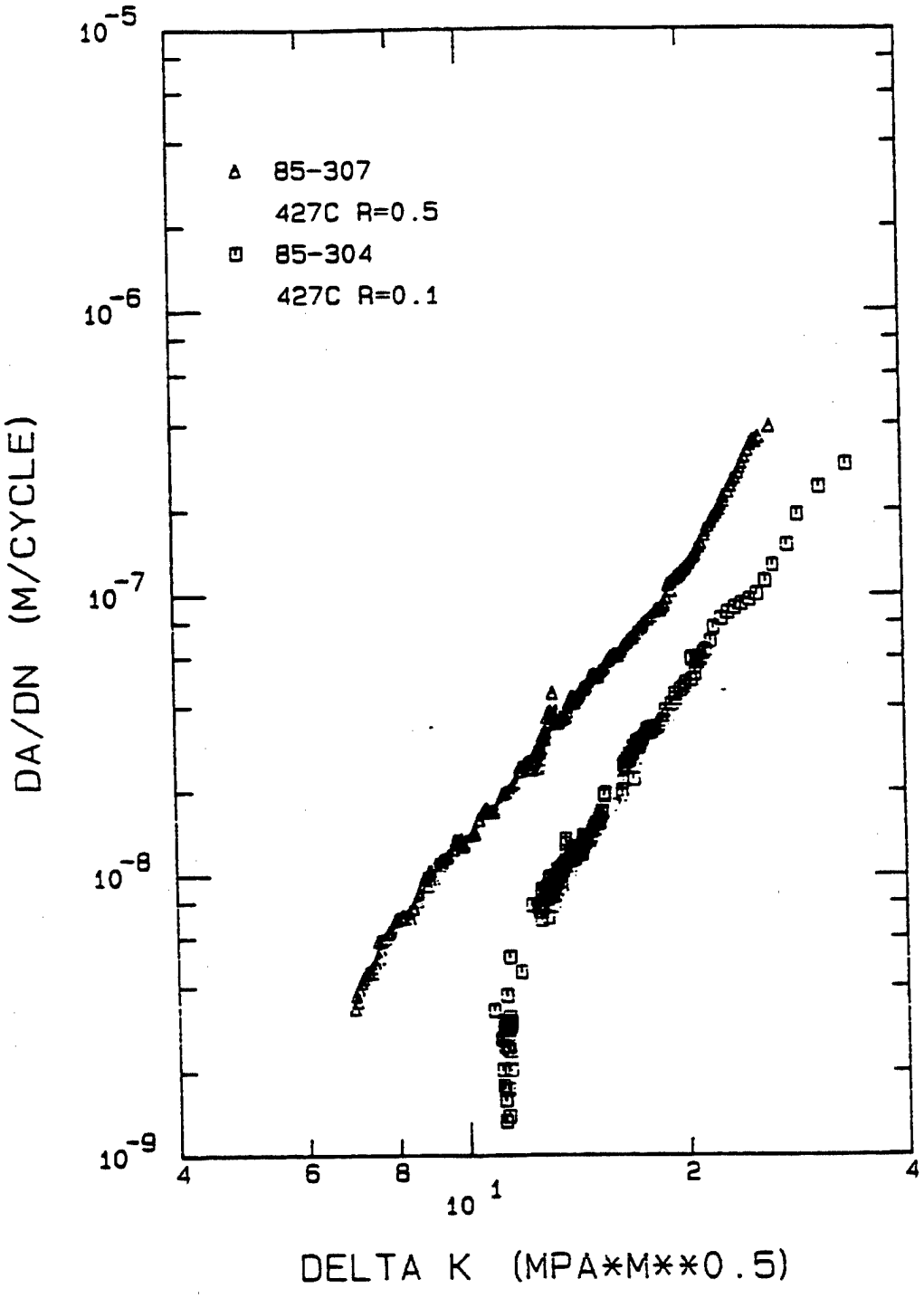

Figure 4.3: Fatigue Crack Growth at 427°C, R=0.1, and 427°C, R=0.5

Table 4.2

Cycle-Dependent Term MSE Parameters

Test	ΔK^* ($MPa\sqrt{m}$)	ΔK_i ($MPa\sqrt{m}$)	da/dN_i (m/cycle)	$(da/dN_i)'$	Q
427°C R=0.1 10 Hz	11.0	40.0	5.5×10^{-7}	3.5	0.4
427°C R=0.5 10 Hz	6.0	28.0	3.5×10^{-7}	3.0	0.4

The interpolative relations for MSE parameters are listed previously in equations (4.14). For the cycle-dependent term, only the R-ratio is varied and R=0.1 is chosen as the base value. Equations (4.14) simplify to:

$$\begin{pmatrix} \log \Delta K^* \\ \log \Delta K_i \\ \log(da/dN_i) \\ (da/dN_i)' \end{pmatrix} = \begin{pmatrix} \log \Delta K^*_{R=0.1} \\ \log (\Delta K_i)_{R=0.1} \\ \log(da/dN_i)_{R=0.1} \\ (da/dN_i)'_{R=0.1} \end{pmatrix} + \begin{pmatrix} C_1 \\ C_2 \\ C_3 \\ C_4 \end{pmatrix} \left[\log \left(\frac{1-R}{0.9} \right) \right] \qquad (4.15)$$

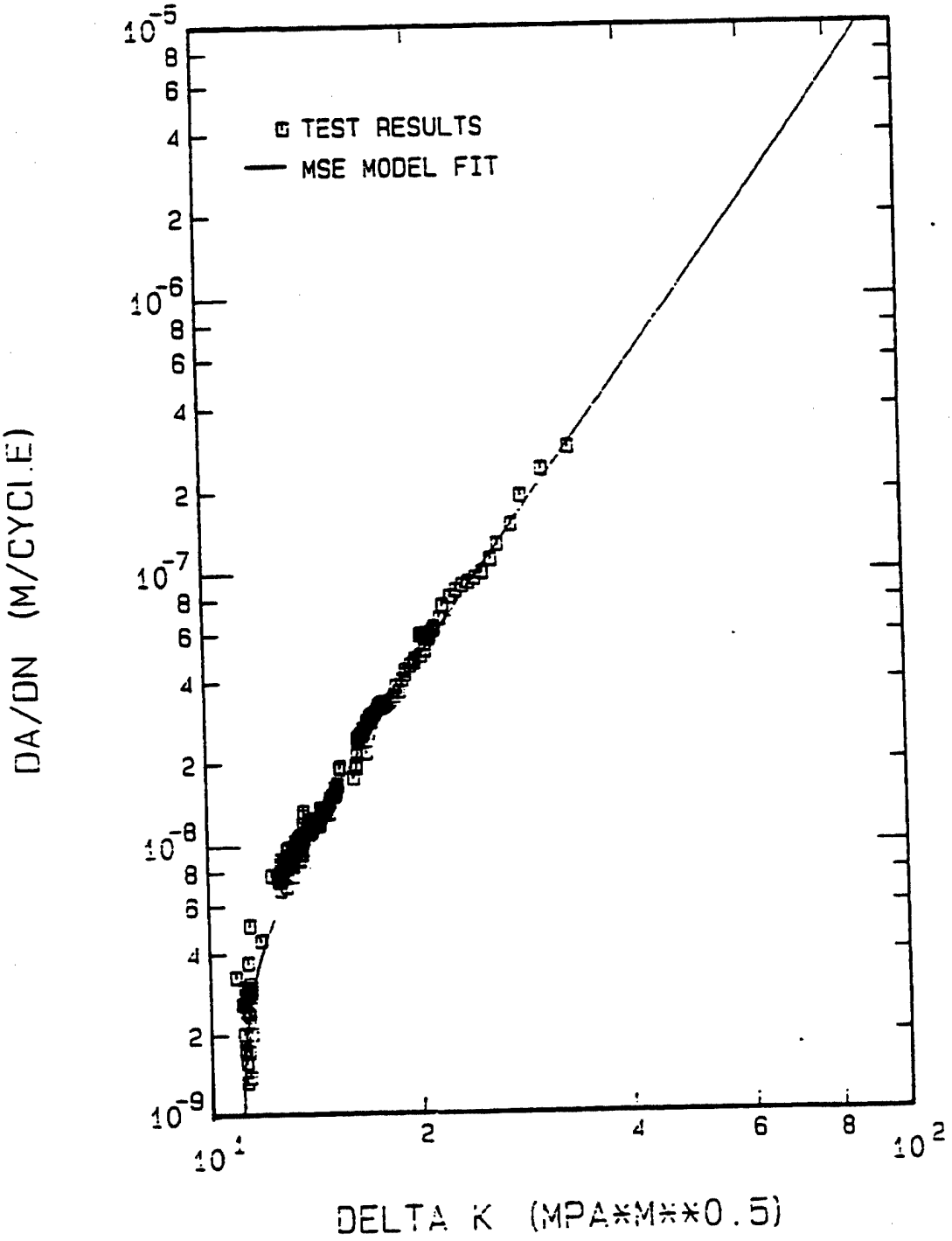

Figure 4.4: MSE Fit of Fatigue Crack Growth at 427°C, R=0.1

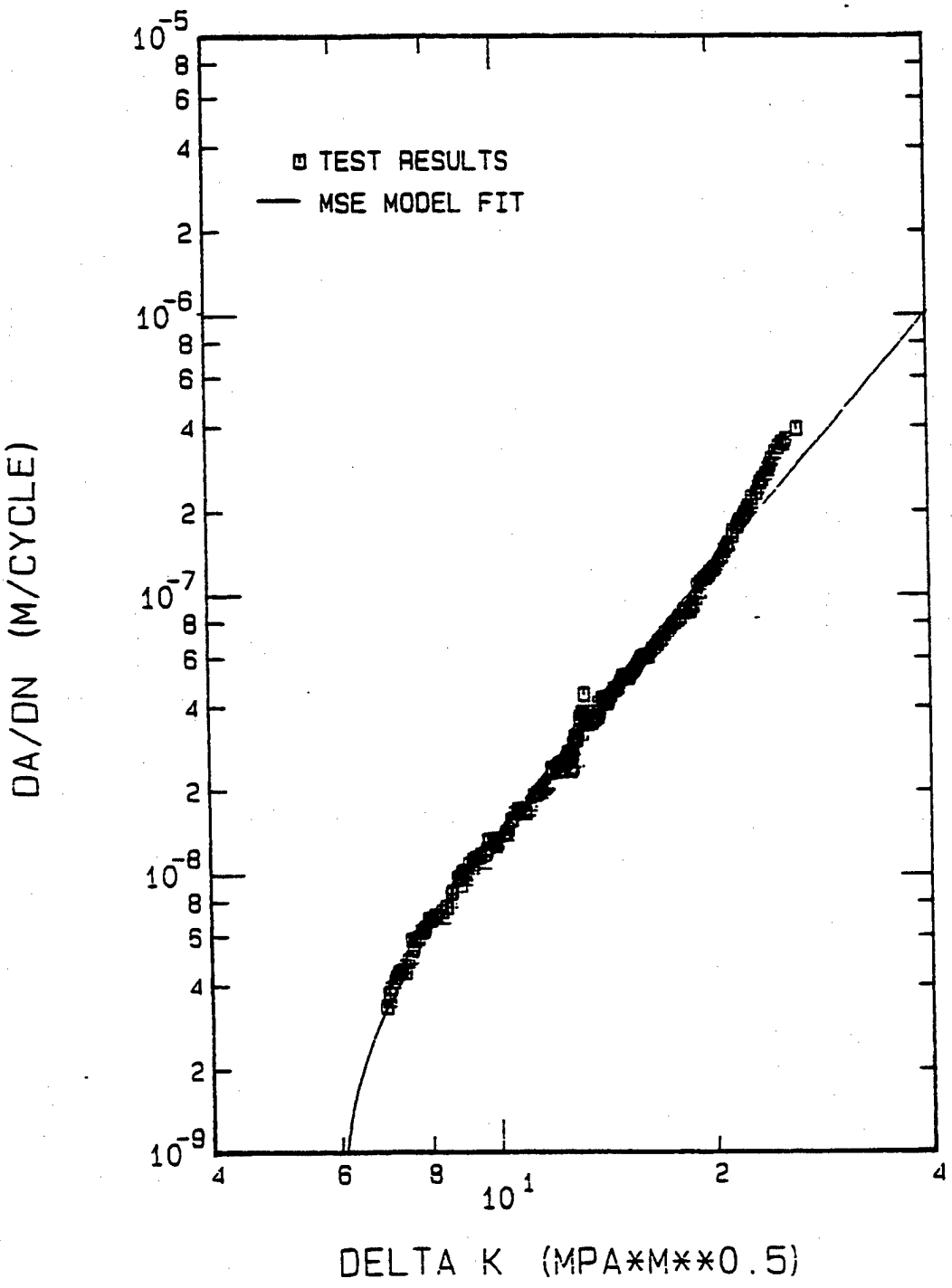

Figure 4.5: MSE Fit of Fatigue Crack Growth at 427°C, R=0.5

The MSE parameters listed in Table 4.1 were used to generate the matrix constants of equations (4.15). The cycle-dependent term MSE parameter interpolative relations on R-ratio were found to be:

$$\begin{pmatrix} \log \Delta K^* \\ \log \Delta K_i \\ \log (da/dN_i) \\ (da/dN_i)' \end{pmatrix} = \begin{pmatrix} 1.0414 \\ 1.0621 \\ -6.2596 \\ 3.5 \end{pmatrix} + \begin{pmatrix} 1.0312 \\ 0.6068 \\ 0.7690 \\ 1.9587 \end{pmatrix} \log \left(\frac{1-R}{0.9} \right) \qquad (4.16)$$

A computer program was written to use the MSE model to provide the cycle-dependent damage term of the linear cumulative damage model for a given thermal-mechanical cycle. This program is listed as FUNCTION DADN in Appendix C.

Time-Dependent Damage Term Development

At temperatures above 427°C, time-dependent and mixed-mode damages become increasingly important. The time-dependent damage term is found by integrating the sustained-load crack-growth rate over the loading portion of the cycle. Because the temperature and stress intensity factor are changing over a thermal-mechanical cycle, the sustained-load crack-growth rate must be expressed as a function of these two variables:

$$\frac{da}{dt} = \frac{da}{dt}(K, T) \qquad (4.17)$$

To find this functional dependence, sustained-load crack growth tests were conducted at three temperatures: 538°C, 593°C, and 649°C. A constant sustained load was applied to the precracked specimen and crack growth was monitored until the specimen

failed. The specimens used for the tests and the test conditions are listed in Table 4.3. Specimens 85-209 and 85-300 have longer initial crack lengths because of crack growth during previous unrelated testing. The constant sustained load values used during testing were chosen to produce initial stress intensity levels high enough to initiate crack growth.

Table 4.3

Sustained Load Crack Growth Test Conditions

Specimen	Temp (°C)	Initial Crack Length (mm)	Sustained Load (KN)
85-303	538	5.61	31.2
85-306	593	5.95	24.5
85-209	649	14.6	9.8
85-300	649	11.7	15.2

The sustained load crack growth rate, da/dt, versus applied stress intensity factor, K, data for the tests are shown in Figure 4.6. At temperatures below 538°C, the sustained-load crack-growth rate drops off rapidly. Due to time constraints, no sustained load tests were conducted at 427°C. Sustained-load crack-growth rate test results at 427°C from Sadananda and Shahinian (11) were used in the model development.

A symmetric modified sigmoidal equation (MSE) model was used to find the temperature dependence of the sustained-load crack-growth rate. The model fits da/dt versus K data with the modified sigmoidal function of equation (4.3):

$$\frac{da}{dt} = \exp B' \left(\frac{K}{K_i}\right)^P \left[\ln\left(\frac{K}{K^*}\right)^P\right] \left[\ln\left(\frac{K_c}{K}\right)\right]^D \qquad (4.18)$$

where D, P, and B' are defined in equations (4.4) through (4.6) with da/dN replaced by da/dt and ΔK replaced by K. The physical meanings of the MSE parameters as applied to

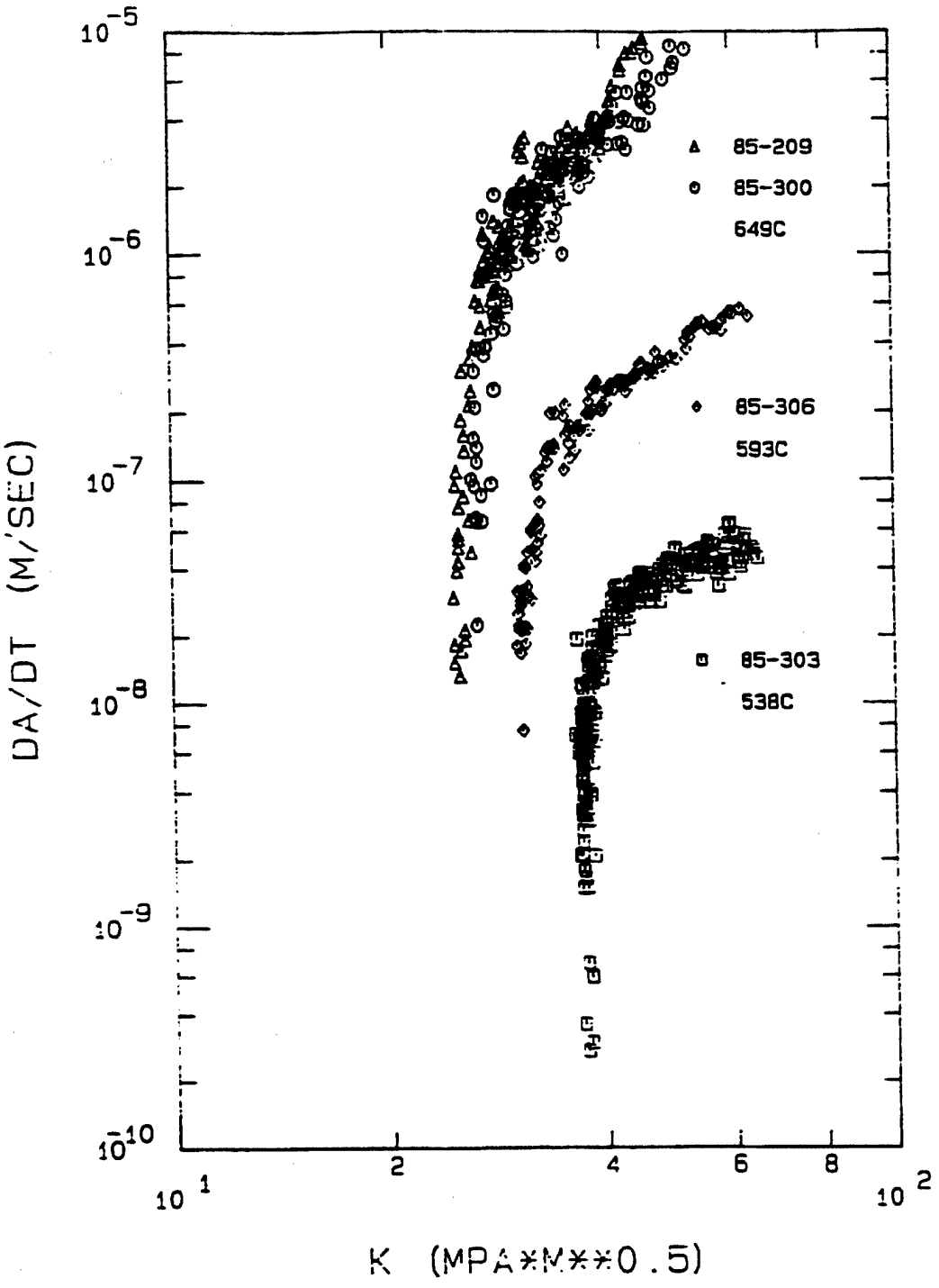

Figure 4.6: Sustained Load Crack Growth Tests

sustained-load crack growth are shown in Figure 4.7. Once again, a symmetric MSE curve can be used with a constant shaping parameter Q without impairing the model's ability to fit da/dt versus K data. The five MSE parameters K^*, K_i, (da/dt_i), $(da/dt_i)'$, and Q were iterated until a best usual fit of the test data was obtained. The MSE parameters for the sustained load crack growth tests (including Sadananda and Shahinian's 427°C test) are listed in Table 4.4. The experimental data and MSE fits are shown in Figure 4.8. The computer program used to generate the MSE curves is listed as PROGRAM SLCG in Appendix B.

Table 4.4

Sustained Load Crack Growth MSE Parameters

Test	K^* (MPa$\sqrt{m}$)	K_i (MPa$\sqrt{m}$)	da/dt_i (m/sec)	$(da/dt_i)'$	Q
427°C	50.0	100.0	2.8×10^{-9}	1.2	0.4
538°C	37.0	76.0	6.5×10^{-8}	1.2	0.4
593°C	30.5	73.0	8.0×10^{-7}	2.0	0.4
649°C	25.4	60.0	1.1×10^{-5}	3.0	0.4

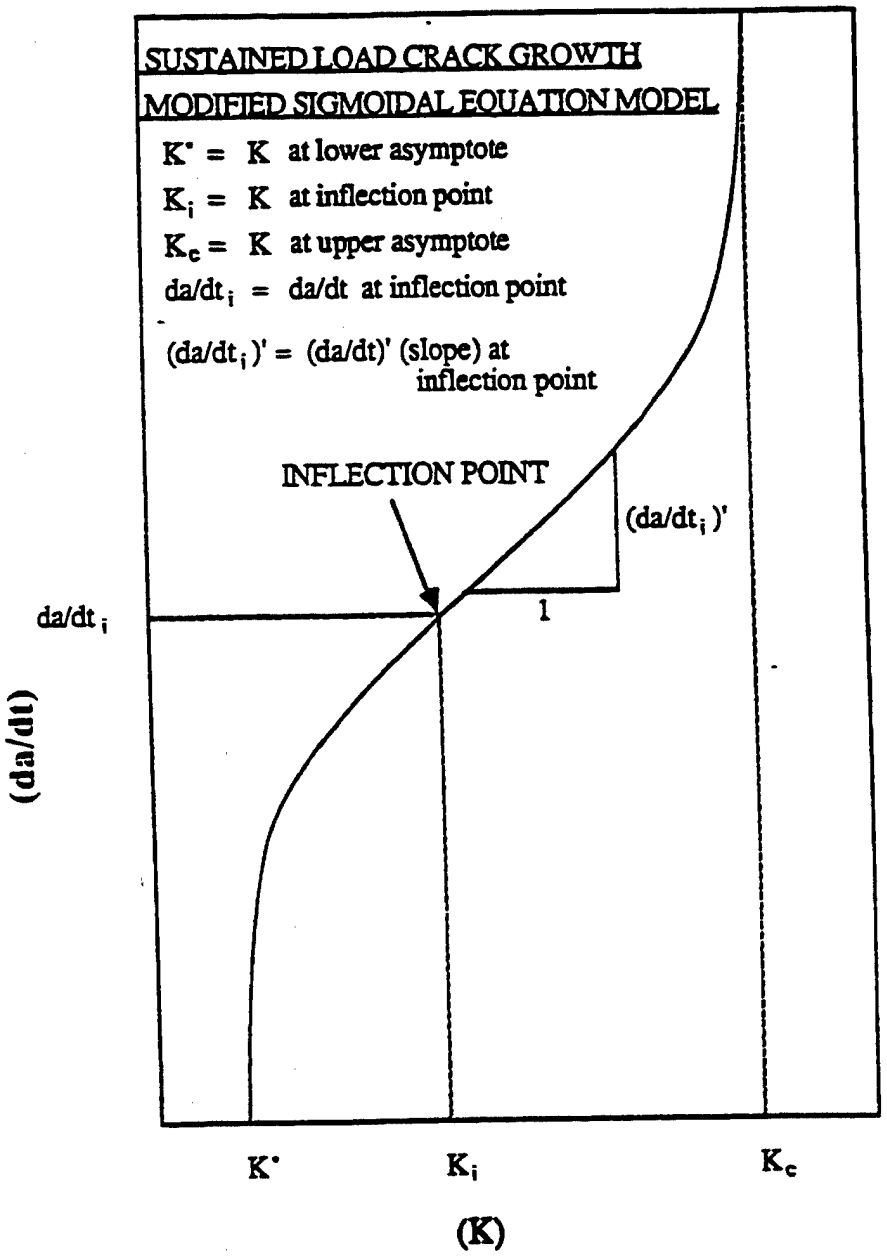

Figure 4.7: MSE Model Applied to Sustained Load Crack Growth

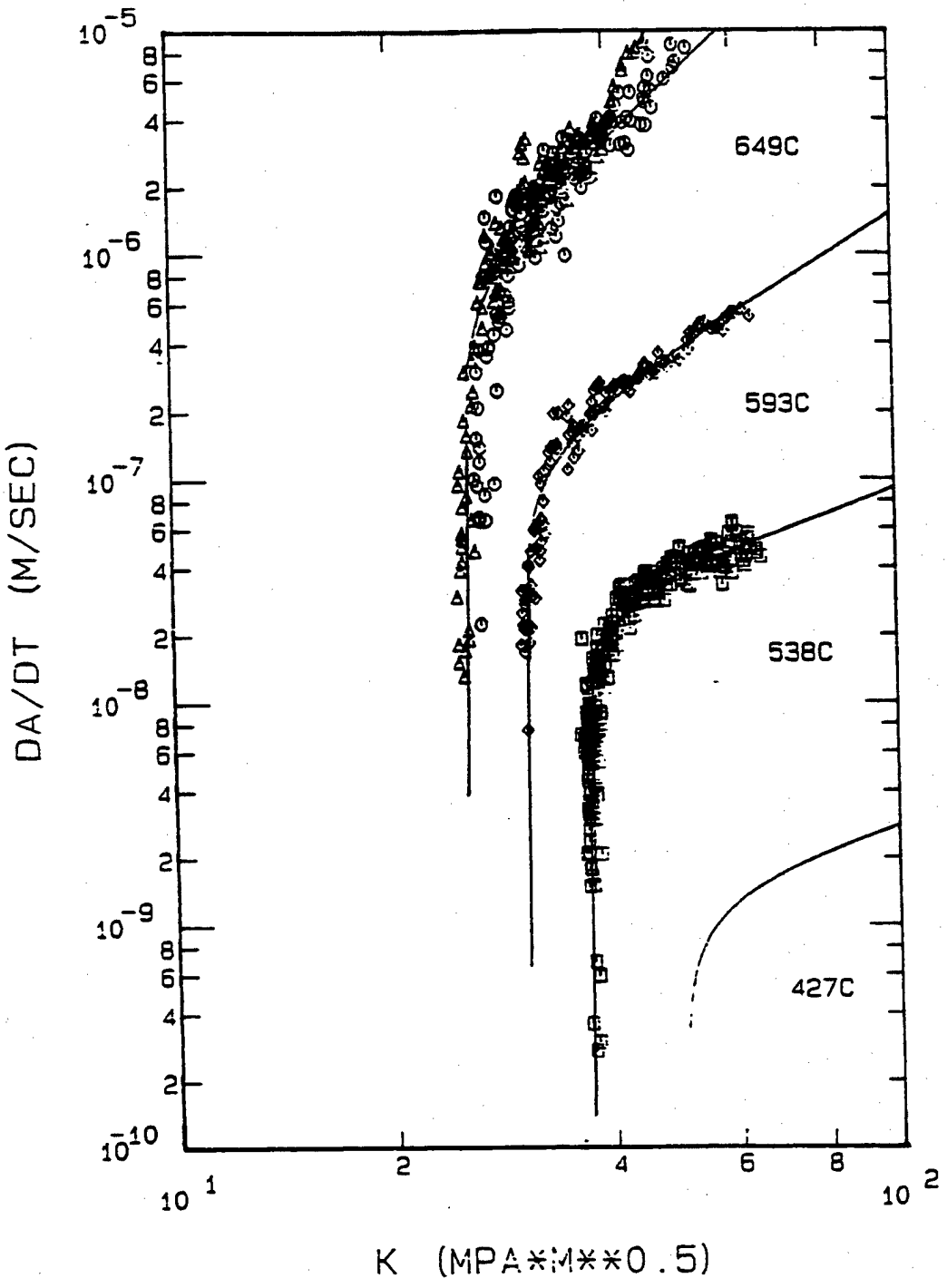

Figure 4.8: MSE Fits of Sustained Load Crack Growth Data

As in the case of fatigue crack growth, a linear relationship is assumed to exist between the MSE parameters and temperature for a given temperature range:

$$\begin{pmatrix} \log \Delta K^* \\ \log \Delta K_i \\ \log(da/dt_i) \\ (da/dt_i)' \end{pmatrix} = \begin{pmatrix} \log \Delta K^*_{base} \\ \log (\Delta K_i)_{base} \\ \log(da/dt_i)_{base} \\ (da/dt_i)'_{base} \end{pmatrix} + \begin{pmatrix} C_1 \\ C_2 \\ C_3 \\ C_4 \end{pmatrix} [(T - T_{base})] \qquad (4.19)$$

This linear relationship was tested over the temperature range of 538°C to 649°C. Using the MSE parameters from Table 4.4, the interpolative relations of equations (4.19) become:

$$\begin{pmatrix} \log \Delta K^* \\ \log \Delta K_i \\ \log(da/dt_i) \\ (da/dt_i)' \end{pmatrix} = \begin{pmatrix} 1.5682 \\ 1.8808 \\ -7.1871 \\ 1.2 \end{pmatrix} + \begin{pmatrix} -1.472 \times 10^{-3} \\ -9.249 \times 10^{-4} \\ 2.008 \times 10^{-2} \\ 1.622 \times 10^{-2} \end{pmatrix} (T - 538) \qquad (4.20)$$

The predicted MSE parameters for sustained load crack growth at 593°C using the interpolative relations of equations (4.20) are compared to the actual best fit parameters in Table 4.5. The predicted MSE model curve is compared to the actual 593°C test data in Figure 4.9. The simple linear interpolation of MSE parameters on temperature provides a reasonable prediction of sustained-load crack-growth rates.

Table 4.5

Predicted versus Actual Sustained Load Crack Growth

MSE Parameters, 593°C.

	K^* (MPa$\sqrt{m}$)	K_i (MPa$\sqrt{m}$)	da/dt_i (m/sec)	$(da/dt_i)'$	Q
Predicted	30.66	67.53	8.46×10^{-7}	2.1	0.4
Actual	30.5	73.0	8.0×10^{-7}	2.0	0.4

Since the sustained load crack growth tests were conducted under a constant load, growth rates near threshold were not obtained. The apparent thresholds in the data were the result of slow crack growth upon initial application of the sustained load. With time, this slow crack growth accelerates to a steady state value. This transient effect has been observed in sustained load testing on other nickel-base superalloys (54).

The experimental sustained load crack growth data at 538°C, 593°C, and 649°C were compared with earlier data obtained at the same temperatures by Haritos, Miller, and Nicholas (37) and Sadananda and Shahinian (11). Although the agreement of the data sets was generally good, the earlier data tended to show somewhat lower threshold stress intensity values for sustained load crack growth.

Elevated temperature fatigue crack growth in Inconel 718 in the time-dependent region (very low loading frequencies) may be predicted by integrating the sustained load crack growth rate over the loading portion of the cycle (30). The apparent threshold value of sustained load crack growth was iterated in predicting low frequency fatigue crack growth test data. It was found that the lower apparent thresholds observed by Haritos, Miller, and Nicholas (37) and Sadananda and Shahinian (11) provided better crack growth predictions in the lower stress intensity factor ranges. Because of this, the lower

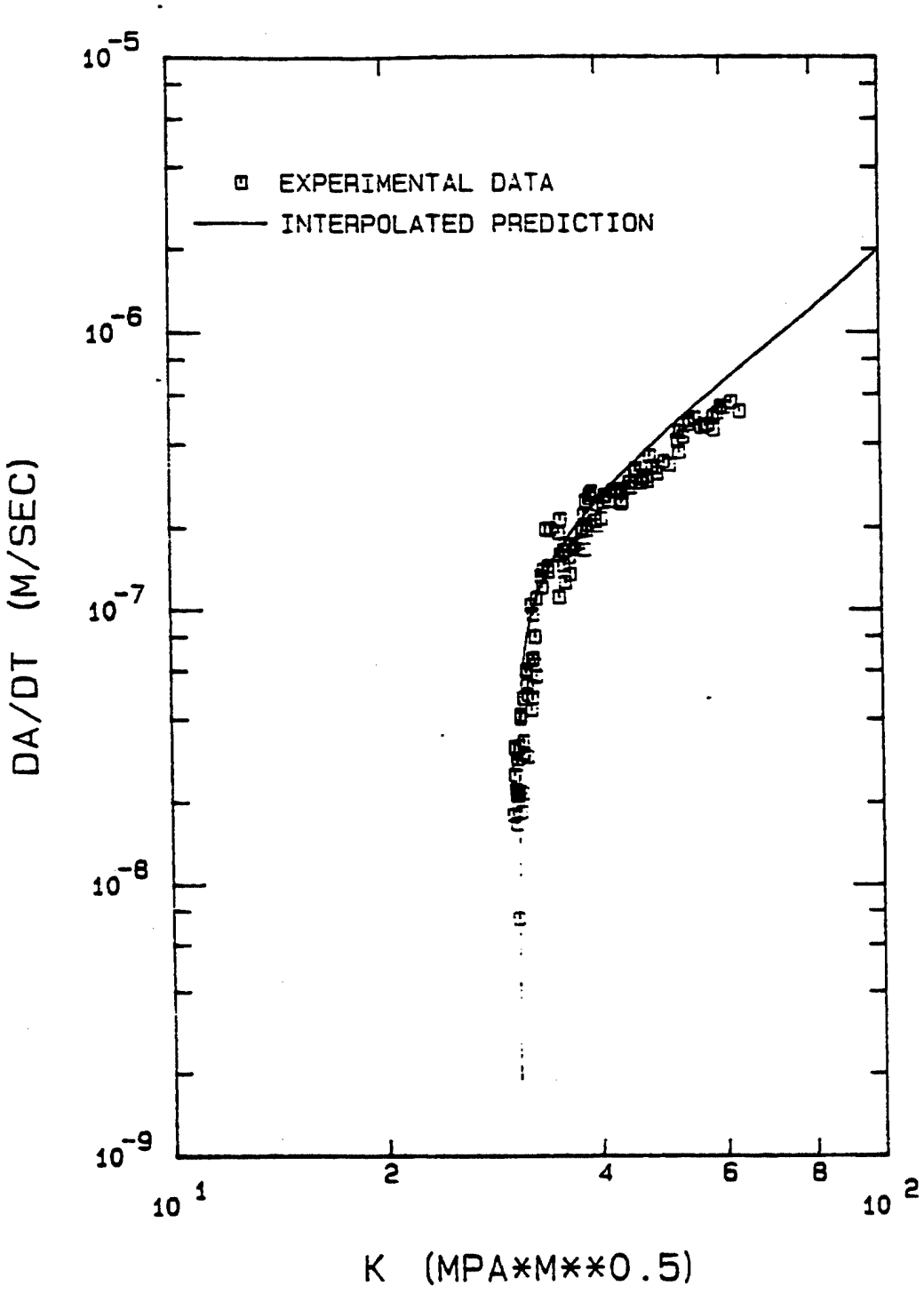

Figure 4.9: Predicted versus Actual Sustained Load Crack Growth at 593°C. Predictions Obtained from Interpolation Between 538°C and 649°C Model Fits.

thresholds were used in developing the time dependent damage term of the linear cumulative-damage model. The threshold stress intensity factor for sustained load crack growth is represented by the parameter K^* in the MSE model. The updated K^* values are listed in Table 4.6.

Table 4.6

Updated Sustained Load Crack Growth MSE Parameters

Test	Original K^* ($MPa\sqrt{m}$)	Updated K^* ($MPa\sqrt{m}$)	K_i ($MPa\sqrt{m}$)	da/dt_i (m/sec)	$(da/dt_i)'$	Q
427°C	50.0	50.0	100.0	2.8×10^{-9}	1.2	0.4
538°C	37.0	24.0	76.0	6.5×10^{-8}	1.2	0.4
593°C	30.5	21.0	73.0	8.0×10^{-7}	2.0	0.4
649°C	25.4	19.0	60.0	1.1×10^{-5}	3.0	0.4

The updated MSE parameters listed in Table 4.6 were used to develop interpolative relations over three temperature ranges: 427°C to 538°C, 538°C to 593°C, and 593°C to 649°C. These relations are listed in equations (4.21) through (4.23).

$427°C \le T \le 538°C$

$$\begin{pmatrix} \log K^* \\ \log K_i \\ \log(da/dt_i) \\ (da/dt_i)' \end{pmatrix} = \begin{pmatrix} 1.699 \\ 2.0 \\ -8.553 \\ 1.2 \end{pmatrix} + \begin{pmatrix} -2.872 \times 10^{-3} \\ -1.074 \times 10^{-3} \\ 1.230 \times 10^{-2} \\ 0 \end{pmatrix} (T - 427) \qquad (4.21)$$

$538°C \le T \le 593°C$

$$\begin{pmatrix} \log K^* \\ \log K_i \\ \log(da/dt_i) \\ (da/dt_i)' \end{pmatrix} = \begin{pmatrix} 1.3802 \\ 1.8808 \\ -7.1871 \\ 1.2 \end{pmatrix} + \begin{pmatrix} -1.054 \times 10^{-3} \\ -3.180 \times 10^{-4} \\ 1.982 \times 10^{-2} \\ 1.455 \times 10^{-2} \end{pmatrix} (T - 538) \qquad (4.22)$$

$593°C \le T \le 649°C$

$$\begin{pmatrix} \log K^* \\ \log K_i \\ \log(da/dt_i) \\ (da/dt_i)' \end{pmatrix} = \begin{pmatrix} 1.3222 \\ 1.8633 \\ -6.0969 \\ 2.0 \end{pmatrix} + \begin{pmatrix} -7.762 \times 10^{-4} \\ -1.521 \times 10^{-3} \\ 2.033 \times 10^{-2} \\ 1.786 \times 10^{-2} \end{pmatrix} (T - 593) \qquad (4.23)$$

Equations (4.18) and (4.21) through (4.23) express the sustained load crack growth rate, da/dt, as a function of the applied stress intensity factor, K, and temperature,

T, for any temperature between 427°C and 649°C. Following the suggestion of Nicholas, Weerasooriya, and Ashbaugh (30), the time-dependent damage term of the linear cumulative damage model is found by integrating this rate over the loading portion of the thermal-mechanical cycle:

$$\left.\frac{da}{dN}\right)_{\substack{\text{Time-}\\\text{Dependent}}} = \int_{\substack{\text{Loading}\\\text{Portion}}} \left(\frac{da}{dt}\right) dt \qquad (4.1)\ \text{(repeated)}$$

A computer program was written to perform the integration of equation (4.1) for a given thermal-mechanical cycle using Simpson's rule. This program is listed as FUNCTION DADNTD in Appendix C.

Mixed-Mode Damage Term Development

At 427°C, cycle-dependent crack growth damage dominates. At higher temperatures, sustained-load crack growth and fatigue crack growth interact to produce additional crack growth damage (mixed-mode damage). Sadananda and Shahinian suggest that the point defects generated during fatigue cycling enhance the diffusion controlled sustained-load crack growth process, resulting in mixed-mode damage (19).

It is assumed that the mixed-mode damage term for a given thermal-mechanical cycle can be obtained by integrating a differential damage term $f(K,T)$ over the loading portion of the cycle:

$$\left.\frac{da}{dN}\right)_{\substack{\text{TMF}\\\text{mixed-mode}}} = \int_{K_{min}}^{K_{max}} f(K, T)\, dK \qquad (4.24)$$

To find this damage function, the mixed-mode damage term is identified from isothermal fatigue crack growth tests using equation (4.25):

$$\left.\frac{da}{dN}\right)_{\substack{\text{Isothermal}\\ \text{mixed-mode}}} = \left.\frac{da}{dN}\right)_{\text{total}} - \left.\frac{da}{dN}\right)_{\substack{\text{cycle-}\\ \text{dependent}}} - \left.\frac{da}{dN}\right)_{\substack{\text{time-}\\ \text{dependent}}} \tag{4.25}$$

$\left.\frac{da}{dN}\right)_{\text{total}}$: Total fatigue crack growth rate (from test)

$\left.\frac{da}{dN}\right)_{\substack{\text{cycle-}\\ \text{dependent}}}$: From high frequency tests at 427°C

$\left.\frac{da}{dN}\right)_{\substack{\text{time-}\\ \text{dependent}}}$: Calculated using Eq. (4.1)

For the isothermal case, Eq. (4.24) simplifies to:

$$\left.\frac{da}{dN}\right)_{\substack{\text{Isothermal}\\ \text{mixed-mode}}} = \int_{K_{min}}^{K_{max}} f(K)\, dK \tag{4.26}$$

To find the damage function $f(K)$, consider the effect upon mixed-mode crack growth of an incremental variation h in the minimum stress intensity factor value while holding K_{max} constant.* The integration to find this effect is illustrated in Fig. (4.10).

* The maximum stress intensity factor K_{max} may also be varied while holding K_{min} constant to find the damage function. This derivation is performed in Appendix D.

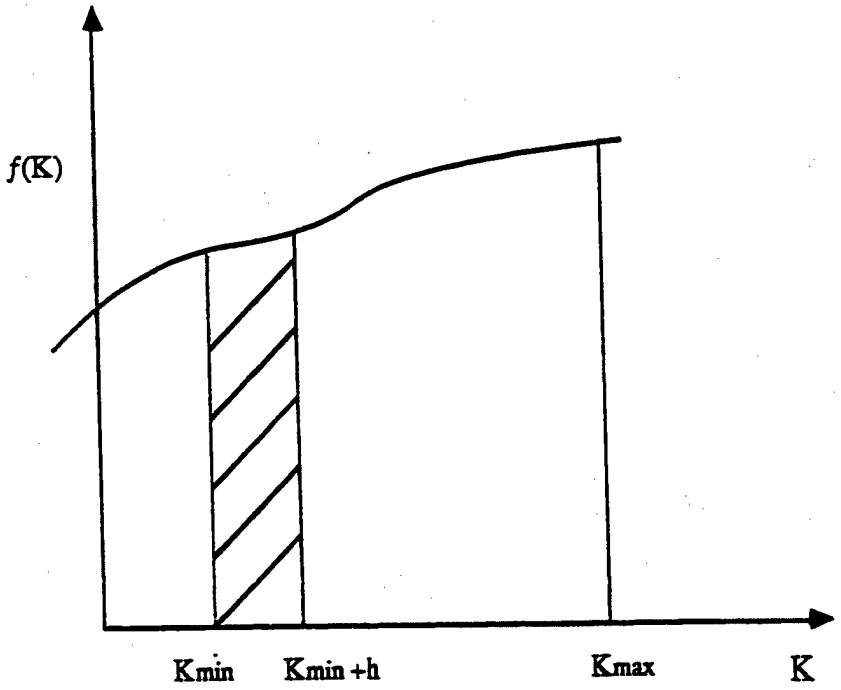

Figure 4.10: Integration for an Incremental Variation h in K_{min}

The shaded area shown in Figure 4.10 is expressed in terms of crack growth rates:

$$\left.\frac{da}{dN}\right)_{K_{min}+h} = \int_{K_{min}+h}^{K_{max}} f(K)\,dK \qquad (4.27)$$

$$\left.\frac{da}{dN}\right)_{K_{min}} = \int_{K_{min}}^{K_{max}} f(K)\,dK \qquad (4.28)$$

$$\text{Shaded Area} = \left.\frac{da}{dN}\right)_{K_{min}} - \left.\frac{da}{dN}\right)_{K_{min}+h} = \int_{K_{min}}^{K_{min}+h} f(K)\,dK \qquad (4.29)$$

Apply the mean value theorem:

$$\left.\frac{da}{dN}\right)_{K_{min}+h} - \left.\frac{da}{dN}\right)_{K_{min}} = -f(K_{min}+\alpha h)\, h \;, 0 \le \alpha \le 1 \qquad (4.30)$$

Take the limit as h approaches zero

$$\lim_{h\to 0} \frac{\left.\frac{da}{dN}\right)_{K_{min}+h} - \left.\frac{da}{dN}\right)_{K_{min}}}{h} = \lim_{h\to 0} \{ -f(K_{min}+\alpha h) \} \;, 0 \le \alpha \le 1 \qquad (4.31)$$

$$\frac{\partial(da/dN)}{\partial K_{min}} = -f(K_{min}) \qquad (4.32)$$

$$f(K_{min}) = -\frac{\partial(da/dN)}{\partial K_{min}} \qquad (4.33)$$

The overall cycle minimum stress intensity factor is a constant (K'_{min}). Equation (4.26) becomes:

$$\left.\frac{da}{dN}\right)_{\text{mixed-mode}} = \int_{K_{min}}^{K_{max}} f(K)\, dK = -\int_{K_{min}}^{K_{max}} \frac{\partial(da/dN)}{\partial K_{min}}\, dK_{min} \qquad (4.34)$$

K_{min} can be defined in terms of load ratio R:

$$K_{min} = R\, K_{max} \qquad (4.35)$$

Using (4.35) in (4.34) while holding K_{max} constant:

$$\left(\frac{da}{dN}\right)_{\text{mixed-mode}} = -\int_{R'}^{1} \frac{\partial(da/dN)}{\partial R}\, dR \quad \text{where } R' = \frac{K'_{min}}{K_{max}} \tag{4.36}$$

(da/dN) is the mixed-mode crack growth rate which is defined as the total crack growth rate minus the cycle-dependent and time-dependent damage terms:

$$\left(\frac{da}{dN}\right)_{\text{mixed-mode}} = \left(\frac{da}{dN}\right)_{\text{total}} - \left(\frac{da}{dN}\right)_{\substack{\text{cycle-}\\\text{dependent}}} - \left(\frac{da}{dN}\right)_{\substack{\text{time-}\\\text{dependent}}}$$

(4.25)
(repeated)

To apply Eq. (4.36) to calculate the mixed-mode damage for a given thermal-mechanical cycle, $(da/dN)_{\text{mixed-mode}}$ must be expressed as a function of load ratio and temperature.

Since essentially all crack-growth damage at 427°C is cycle-dependent, no mixed-mode term is expected at that temperature (9). Fatigue crack growth rate tests were conducted under 0.01 Hz triangular loading at T=538°C, R=0.1 and R=0.5, and T=649°C, R=0.1 and R=0.5, to provide the temperature and load ratio dependence of the mixed-mode term. The maximum load in the cycle was held constant during the tests. The specimens used for the tests and test conditions are listed in Table 4.7. The da/dN versus ΔK data for the tests are shown in Figures 4.11 through 4.14.

Table 4.7

Mixed-Mode Term Test Conditions

Specimen	Temp (°C)	Load Ratio	Load Freq. (Hz)	Initial Crack Length (mm)	Maximum Cycle Load (KN)
85-309	538	0.1	0.01	6.42	20.1
85-315	538	0.5	0.01	6.12	26.7
85-310	649	0.1	0.01	5.93	16.1
85-308	649	0.5	0.01	5.73	17.8

The MSE parameters for a best visual fit of those test data are listed in Table 4.8. The experimental data and MSE fits are shown in figures (4.15) through (4.18). The computer program used to generate the MSE curves is listed as PROGRAM FCG in Appendix B.

Table 4.8

Mixed-Mode Test MSE Parameters

Test	ΔK^* ($MPa\sqrt{m}$)	ΔK_i ($MPa\sqrt{m}$)	da/dN_i (m/cycle)	$(da/dN_i)'$	Q
538°C R=0.1 0.01 Hz	21.8	60.0	5.4×10^{-6}	2.7	0.4
538°C R=0.5 0.01 Hz	12.9	42.0	4.6×10^{-6}	2.4	0.4
649°C R=0.1 0.01 Hz	17.0	60.0	1.4×10^{-4}	2.1	1.0
649°C R=0.5 0.01 Hz	10.4	27.0	1.1×10^{-4}	2.6	1.0

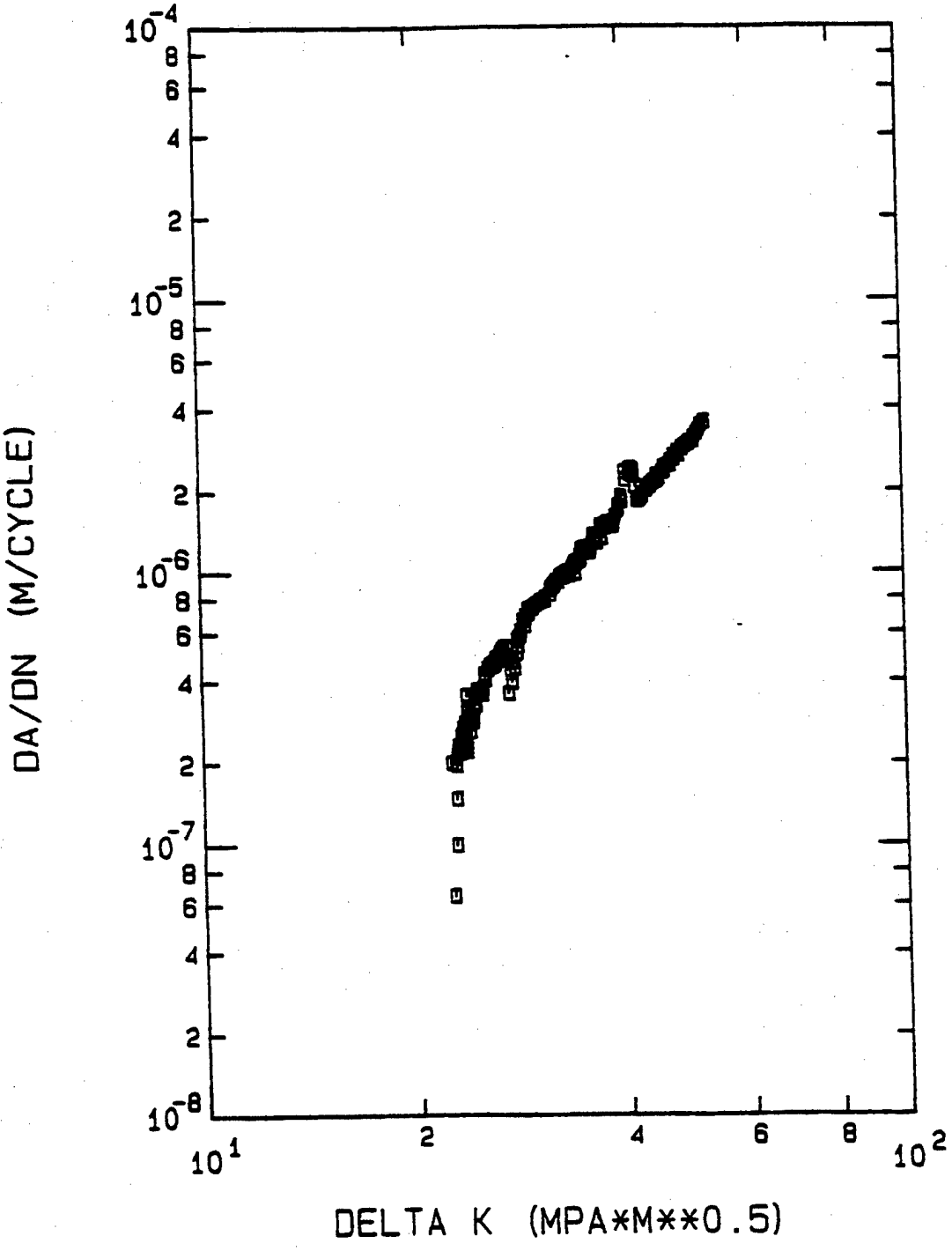

Figure 4.11: Fatigue Crack Growth at 538°C, R=0.1

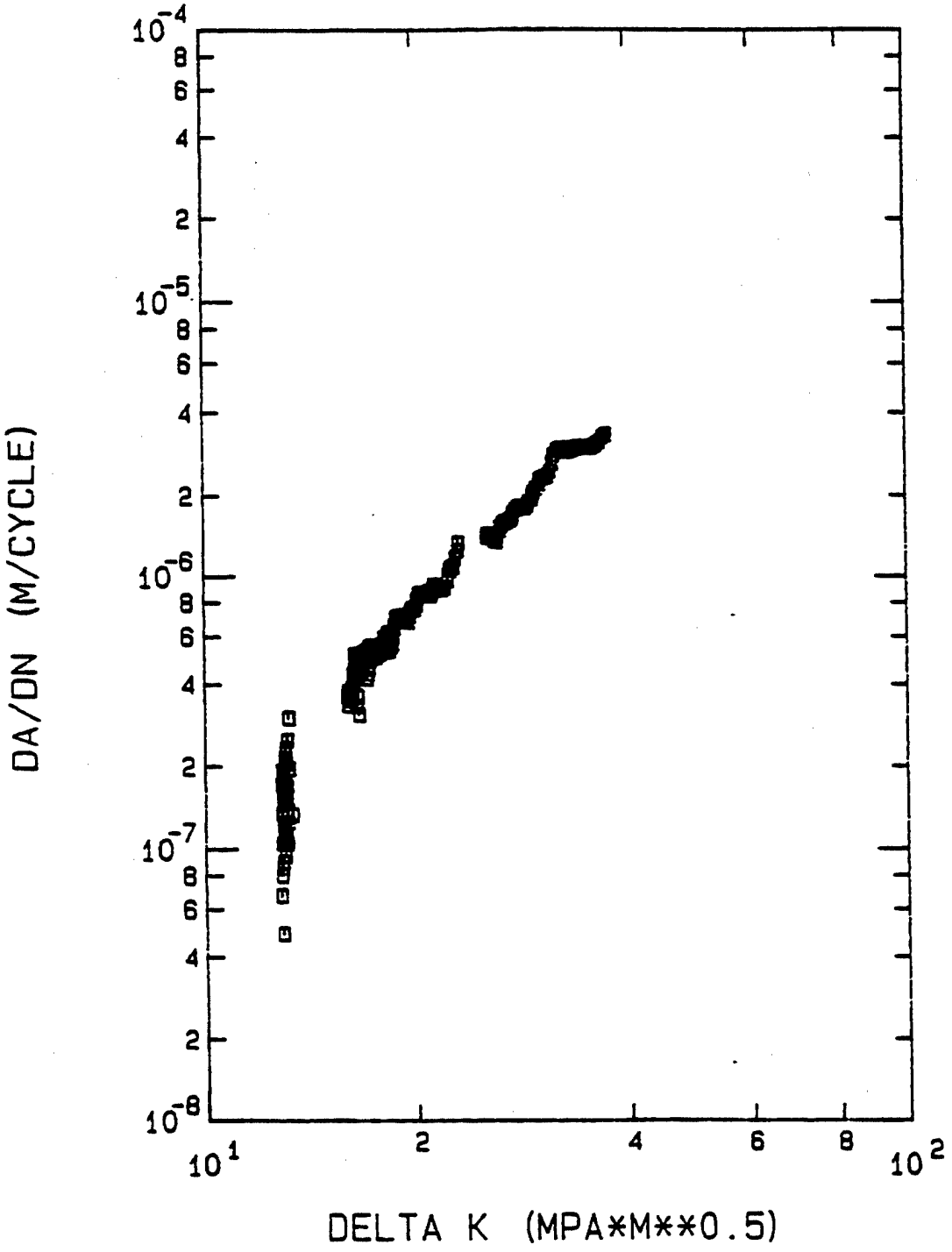

Figure 4.12: Fatigue Crack Growth at 538°C, R=0.5

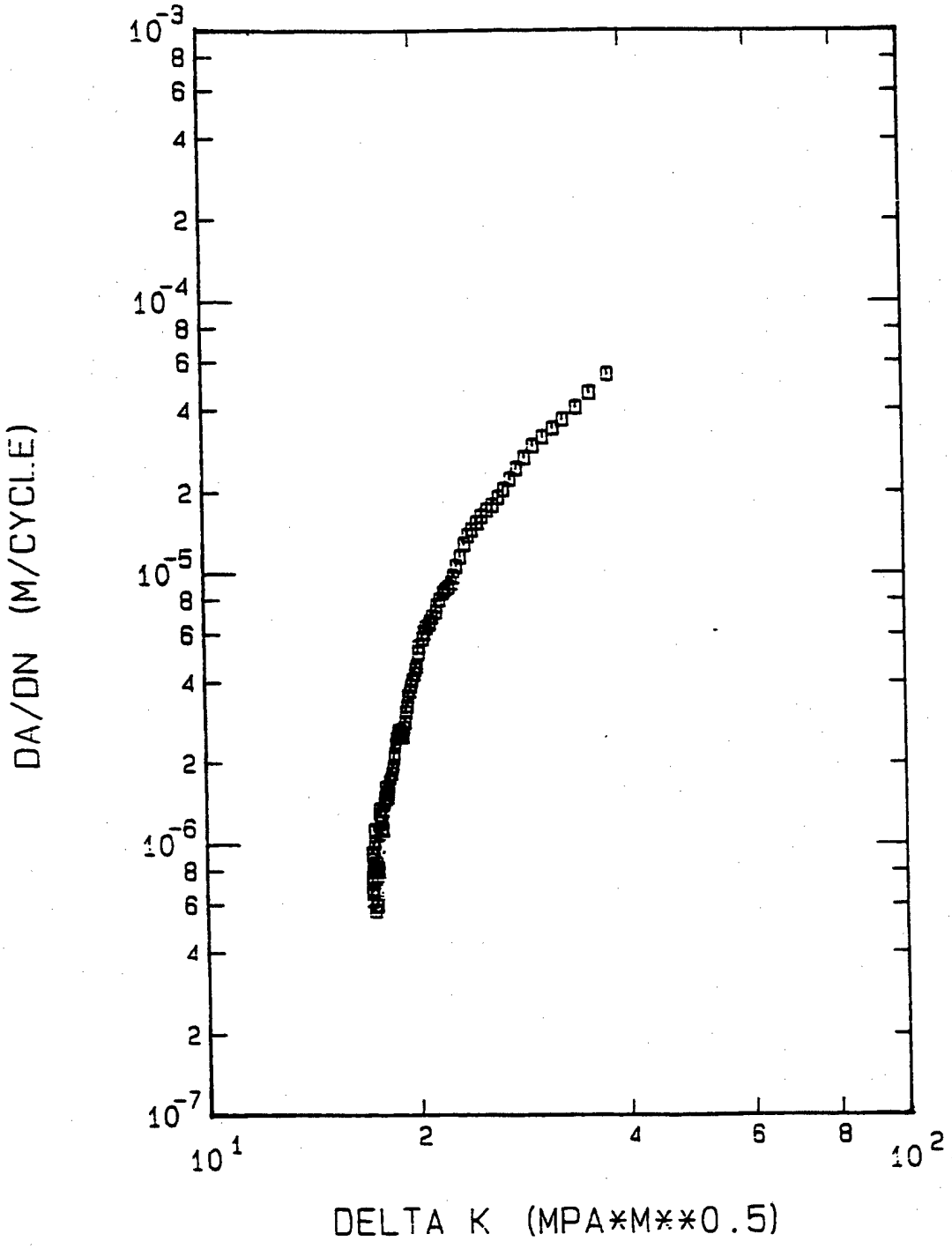

Figure 4.13: Fatigue Crack Growth at 649°C, R=0.1

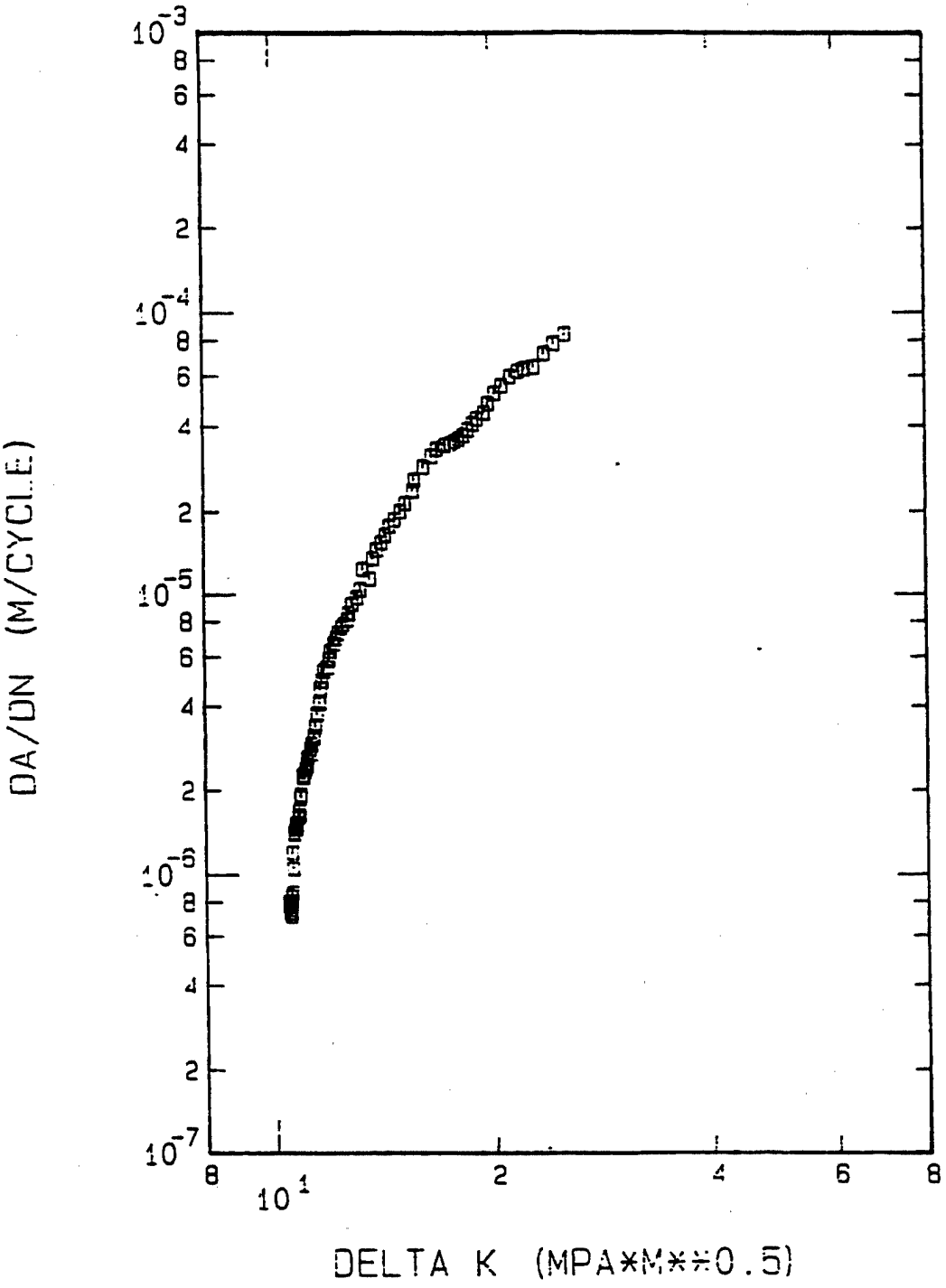

Figure 4.14: Fatigue Crack Growth at 649°C, R=0.5

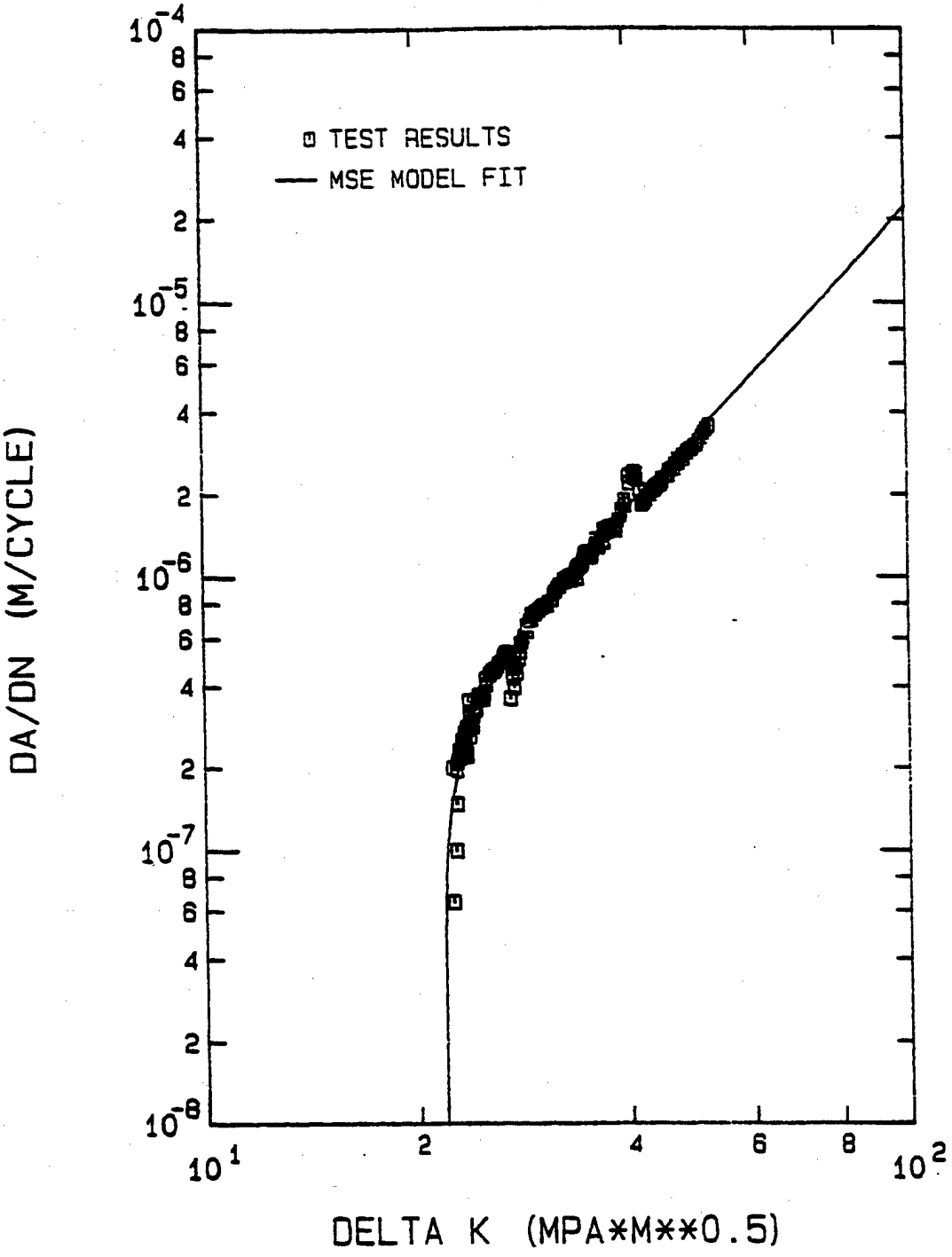

Figure 4.15: MSE Fit of Fatigue Crack Growth at 538°C, R=0.1

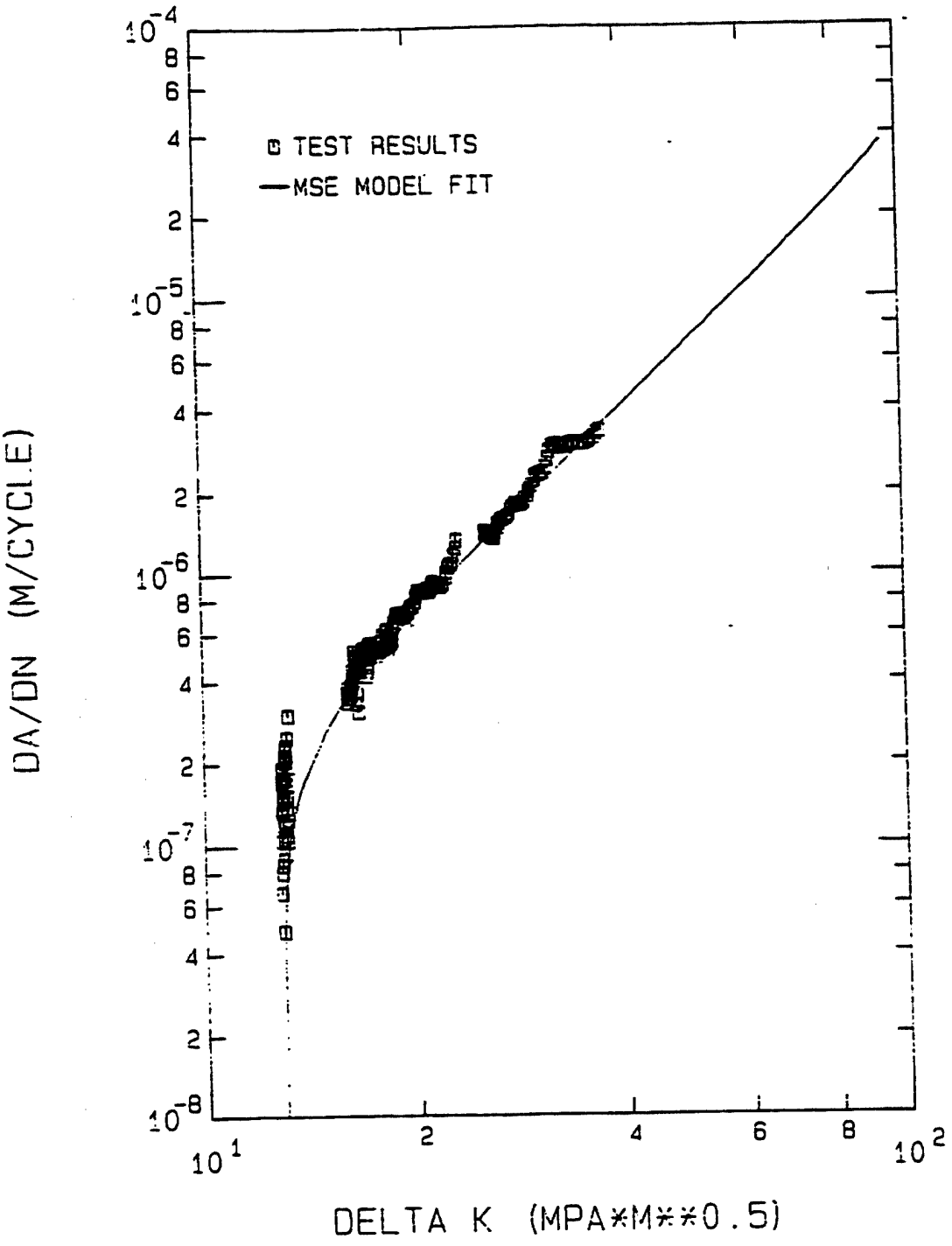

Figure 4.16: MSE Fit of Fatigue Crack Growth at 538°C, R=0.5

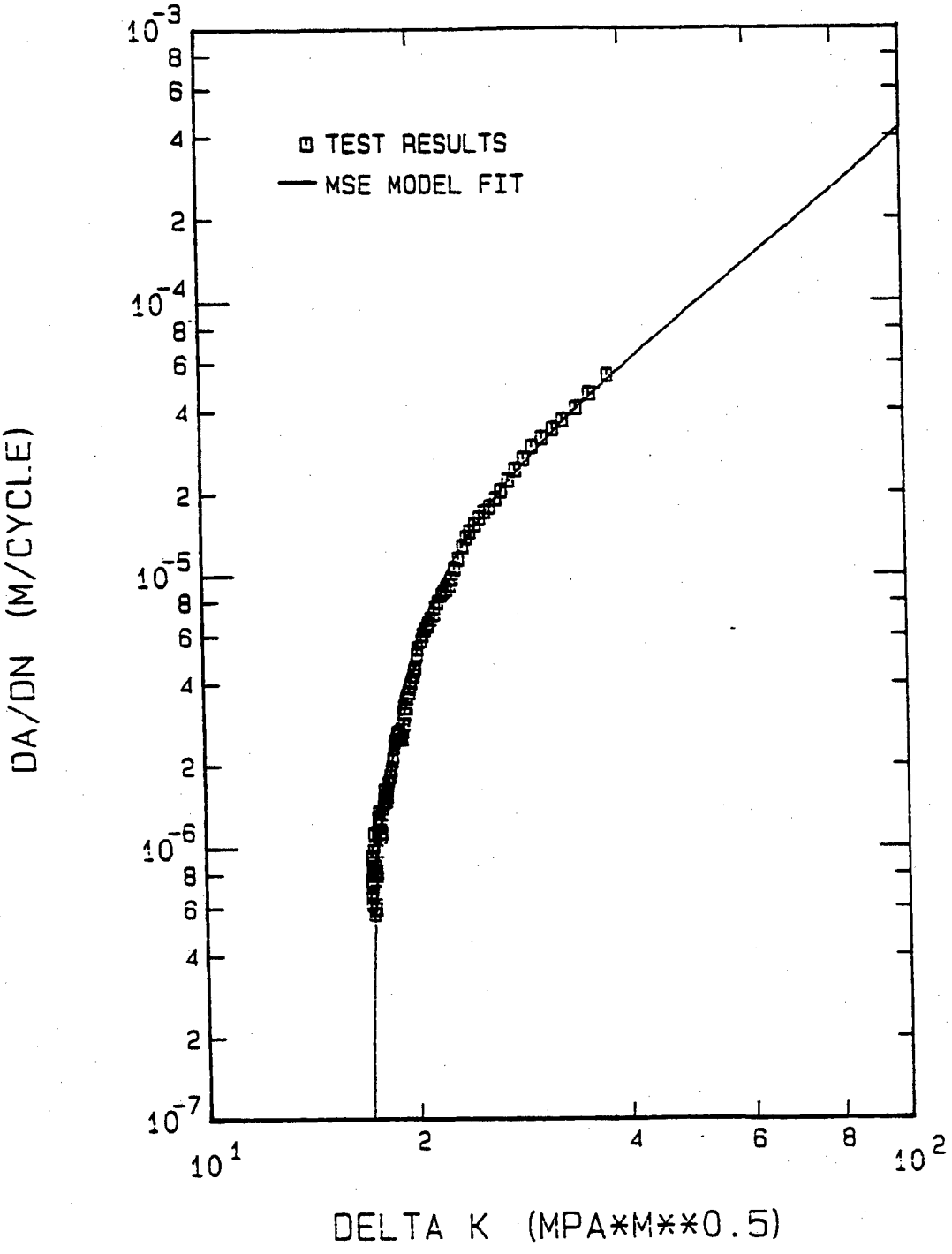

Figure 4.17: MSE Fit of Fatigue Crack Growth at 649°C, R=0.1

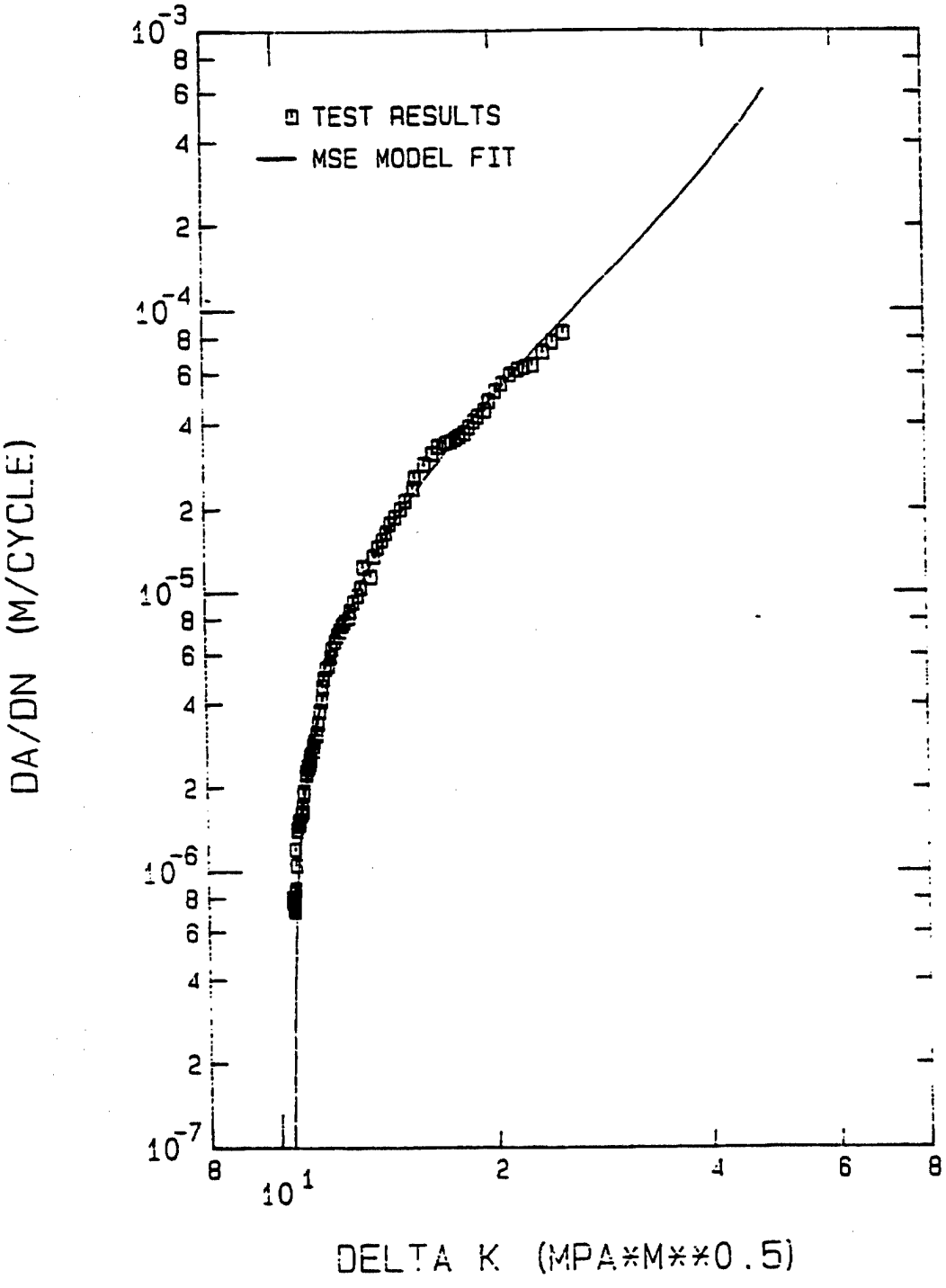

Figure 4.18: MSE Fit of Fatigue Crack Growth at 649°C, R=0.5

To apply Eq. (4.25) to calculate the mixed-mode damage for each of the four tests, the total, cycle-dependent, and time-dependent damages must be calculated for that test. The cycle-dependent damage for each test was calculated using the MSE model with parameters defined by equations (4.16). The time-dependent damage for each test was calculated by integrating sustained-load crack growth over the loading portion of the cycle. The MSE model with parameters defined by equations (4.21) to (4.23) was used to calculate sustained load crack growth and Simpson's rule was used to perform the integration. The total damage for each test was calculated using the MSE model with parameters defined in Table 4.8, and cycle-dependent and time-dependent damages were subtracted from this total to give the mixed-mode damage term. The computer program used to calculate the mixed-mode term for each test is listed as PROGRAM MM in Appendix B.

The total crack growth rate, sum of cycle-dependent and time-dependent damages, and mixed-mode damage for each test are plotted versus ΔK in Figures 4.19 through 4.22. By definition, the total crack growth rate equals the sum of cycle-dependent, time-dependent, and mixed-mode damages.

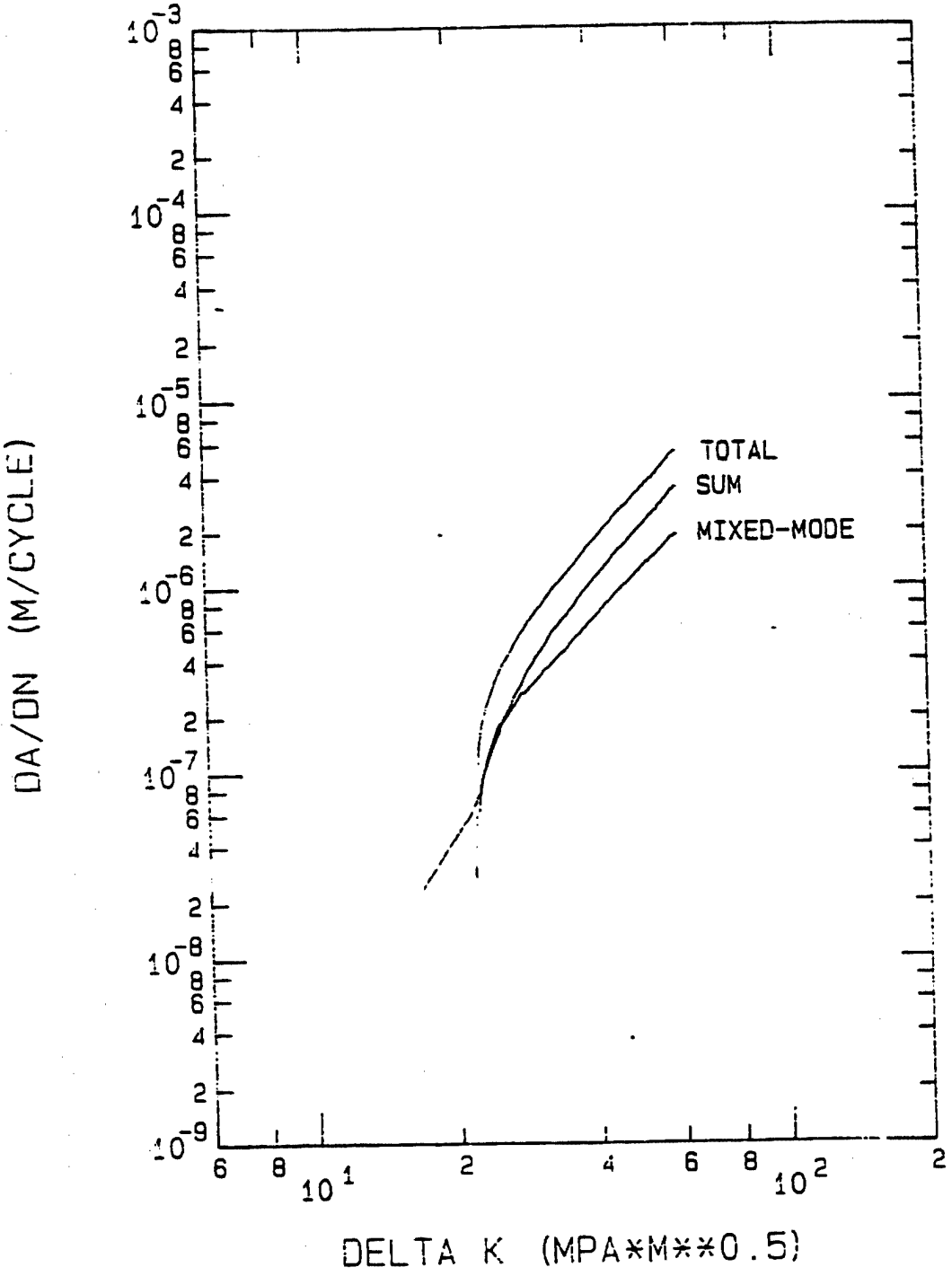

Figure 4.19: Mixed-mode Term at 538°C, R=0.1

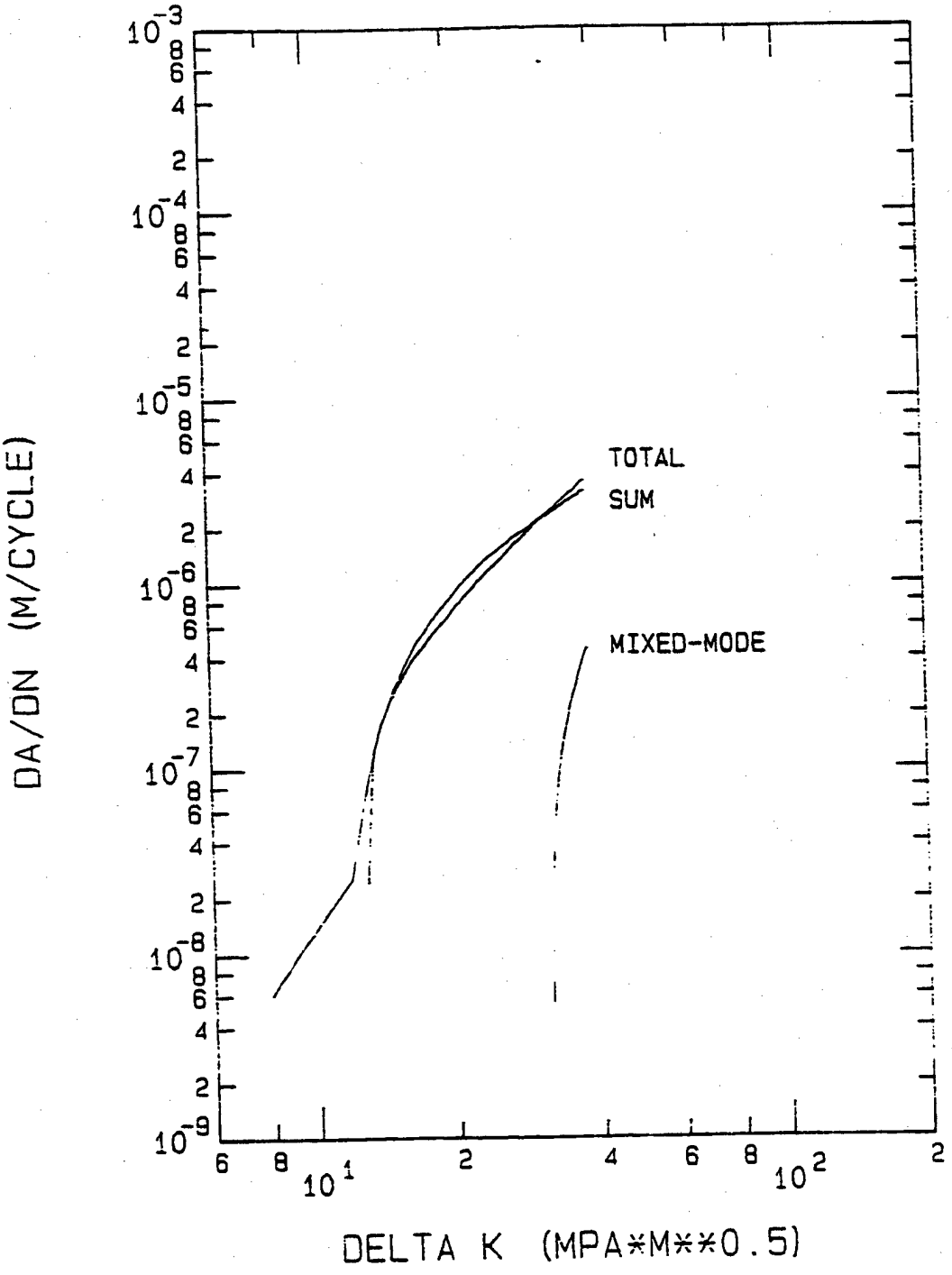

Figure 4.20: Mixed-Mode Term at 538°C, R=0.5

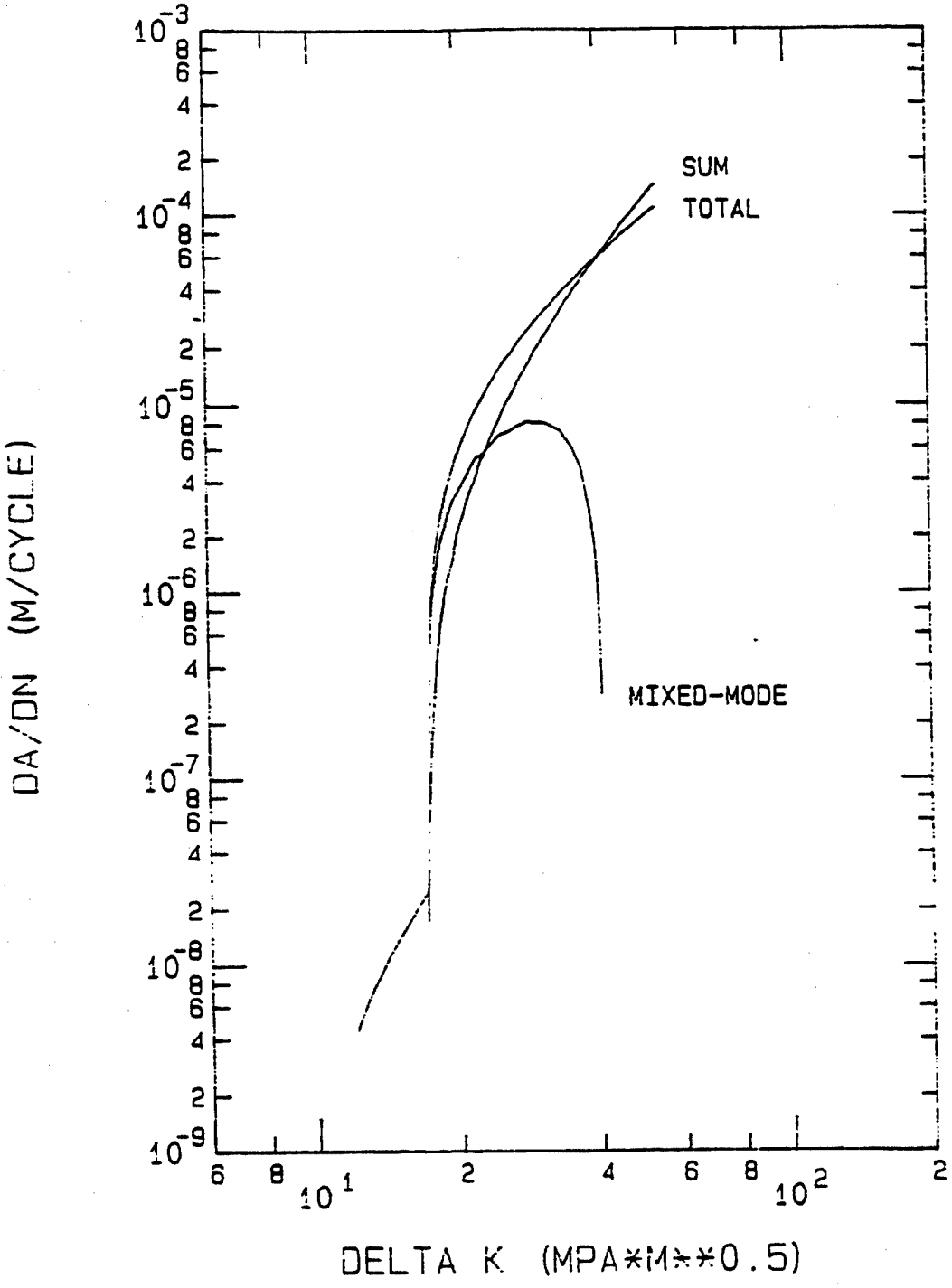

Figure 4.21: Mixed-Mode Term at 649°C, R=0.1

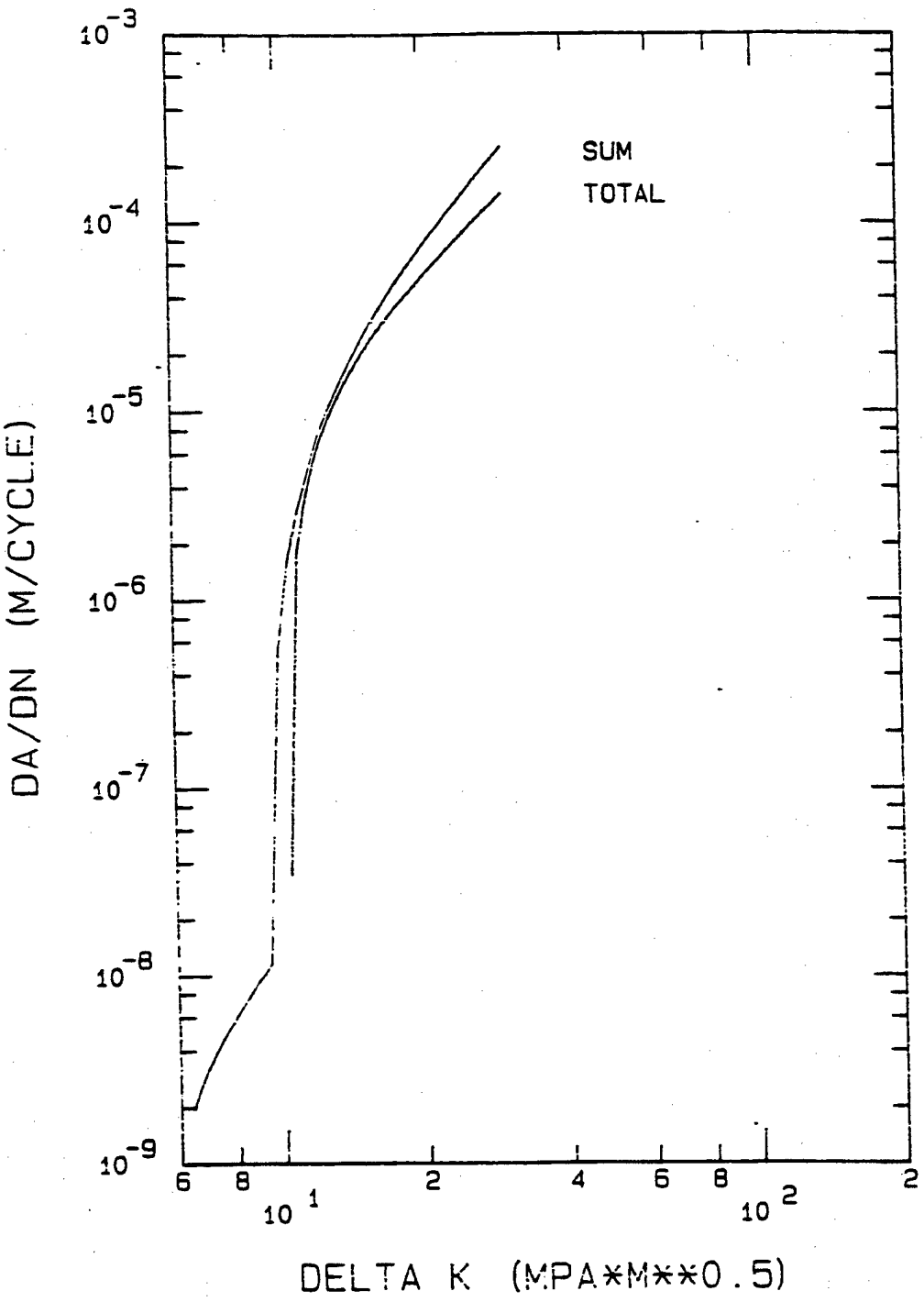

Figure 4.22: Total Crack Growth Rate and Sum of Cycle- and Time-Dependent Damage at 649C, R=0.5 (Mixed-Mode Term is Negative)

At 538°C, R=0.1, the sum of cycle-dependent and time-dependent damages falls below the total test crack growth rate. Therefore, the mixed-mode damage is significant for this test. The MSE model was used to fit this mixed-mode damage. The MSE parameters of the fit are listed in Table 4.9. The mixed-mode damage and MSE model fit of the damage are shown in Figure 4.23.

At 538°C, R=0.5, the sum of cycle-dependent and time-dependent damages is greater than the total test crack growth rate at the lower stress intensity ranges. Three possible explanations for this behavior are:

1. The mixed-mode term is actually negative in this region, indicating a retardation effect upon crack growth.

2. Experimental errors make the mixed-mode term appear to be negative. The sum of the cycle-dependent and time-dependent damages falls within a factor of two of the total crack growth, which is within the experimental scatter band for tests of this type.

3. For this set of test conditions, the simple linear cumulative-damage model inadequately describes the actual crack-growth behavior.

A negative (or retarding) mixed-mode effect has not been previously reported in the literature. Mechanisms leading to such an effect have not been described. Since the retarding effect is small in relation to the total crack growth and the MSE model does not account for negative crack growth rates, all apparently negative mixed-mode damage contributions were ignored in the mixed-mode term development.

At the higher stress intensity factor ranges, the mixed-mode damage becomes positive. However, the maximum magnitude of the mixed-mode term is much smaller than the total crack growth. Therefore, MSE parameters were selected to define a very small mixed-mode damage term for this test condition. The MSE parameters are listed in Table 4.9.

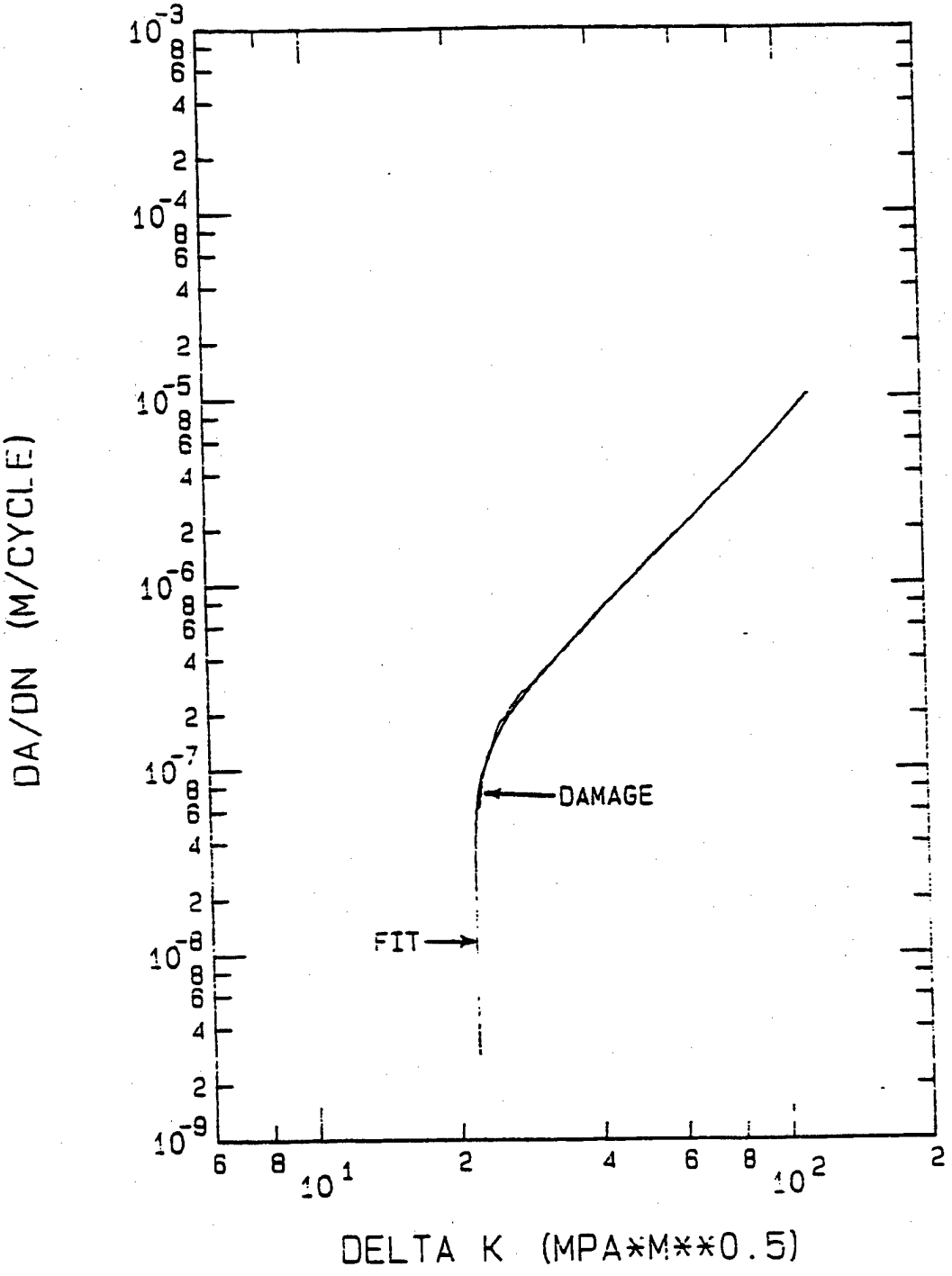

Figure 4.23: Mixed-Mode Damage Term and MSE Model Fit, 538°C, R=0.1

At 649°C, R=0.1, the mixed-mode damage is positive and small relative to the total crack growth at the lower stress intensity factor ranges and negative at the higher stress intensity factor ranges. Time-dependent damage dominates as reported by Weerasooriya (20). Therefore, no mixed-mode damage was included for this test condition.

At 649°C, R=0.5, the mixed-mode damage is relatively small and negative at all stress intensity factor ranges. Therefore, no mixed-mode damage was included for this test condition.

The MSE model parameters for the mixed-mode damage term are listed in Table 4.9. No mixed-mode damage is modeled at 427°C and 649°C.

Table 4.9

Mixed-Mode Term MSE Parameters

Test	ΔK^* ($MPa\sqrt{m}$)	ΔK_i ($MPa\sqrt{m}$)	da/dN_i (m/cycle)	$(da/dN_i)'$	Q
427°C R=0.1	No mixed-mode term				
427°C R=0.5	No mixed-mode term				
538°C R=0.1	21.8	59.81	1.908×10^{-6}	2.5	0.3
538°C R=0.5	12.9	40.0	2.0×10^{-8}	2.5	0.3
649°C R=0.1	No mixed-mode term				
649°C R=0.5	No mixed-mode term				

The MSE parameters at 538°C were used to develop interpolative relations on R-ratio. The mixed-mode term MSE parameter interpolative relations were found to be:

$$\begin{pmatrix} \log \Delta K^* \\ \log \Delta K_i \\ \log (da/dN_i) \\ (da/dN_i)' \end{pmatrix} = \begin{pmatrix} 1.3385 \\ 1.7768 \\ -5.7194 \\ 2.5 \end{pmatrix} + \begin{pmatrix} 0.8926 \\ 0.6844 \\ 7.7546 \\ 0 \end{pmatrix} \log \left(\frac{1-R}{0.9} \right) \qquad (4.37)$$

At load ratios above 0.5, the mixed-mode term becomes negligible.

The magnitude of the mixed-mode damage was known at three temperatures: 427°C, 538°C, and 649°C. A simple linear relationship was assumed to exist between mixed-mode damage and temperature. The equations representing mixed-mode damage as a function of temperature are:

427°C ≤ T ≤ 538°C:

$$\left.\frac{da}{dN}\right)_{\text{mixed-mode}} = \left(\frac{T}{111} - 3.847 \right) \left.\frac{da}{dN}\right)_{\text{mixed-mode 538°C}} \qquad (4.38)$$

538°C ≤ T ≤ 649°C:

$$\left.\frac{da}{dN}\right)_{\text{mixed-mode}} = \left(5.847 - \frac{T}{111} \right) \left.\frac{da}{dN}\right)_{\text{mixed-mode 538°C}} \qquad (4.39)$$

Equation (4.36) provides the means of calculating mixed-mode damage for a cycle in which temperature and stress intensity factor are varying (thermal-mechanical cycle).

$$\left.\frac{da}{dN}\right)_{\text{mixed-mode}} = -\int_{R'}^{1} \frac{\partial(da/dN)}{\partial R}\, dR \qquad \text{where } R' = \frac{K'_{min}}{K_{max}} \qquad (4.36)\ \text{(repeated)}$$

The integration and differentiation of equation (4.36) were performed numerically. Dividing the loading portion of a cycle into N increments as shown in Figure 4.24, the derivative $\partial(da/dn)/\partial R$ at the midpoint m' between points (m-1) and (m) can be expressed by:

$$\left.\frac{\partial\,(da/dN)}{\partial R}\right|_{m'} = \frac{\frac{da}{dN}(R_m, T_{m'}) - \frac{da}{dN}(R_{m-1}, T_{m'})}{R_m - R_{m-1}} \qquad (4.40)$$

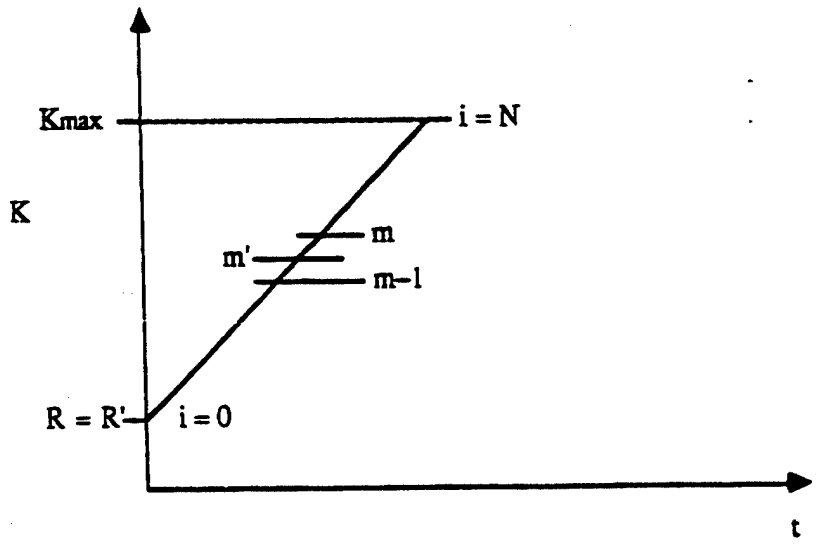

Figure 4.24: Load Cycle Increments

The integration of equation (4.36) is performed numerically using the simple rectangular rule:

$$\left.\frac{da}{dN}\right)_{\substack{TMF \\ mixed\text{-}mode}} = \sum_{i=1}^{N} \left[\frac{da}{dN}(R_{i-1}, T_{i'}) - \frac{da}{dN}(R_i, T_{i'}) \right] \qquad (4.41)$$

Equations (4.3), (4.37), (4.38), and (4.39) provide (da/dN) as a function of R and T.

A computer program was written to perform the summation of equation (4.41). This program is listed as FUNCTION DADNMM in Appendix C.

The total fatigue crack growth over a thermal-mechanical cycle consists of the sum of the cycle-dependent, time-dependent, and mixed-mode damage terms. A FORTRAN computer program was written to calculate each term and sum them to give the total thermal-mechanical fatigue crack growth rate as a function of the cycle stress intensity range. This program is listed as PROGRAM TMF in Appendix C.

Model Application to Isothermal Baseline Tests

Since isothermal fatigue crack growth is a degenerate case of thermal mechanical fatigue crack growth (temperature held constant), the thermal-mechanical fatigue crack growth predictive model should successfully predict isothermal fatigue crack growth. The fatigue crack growth rates predicted by the linear cumulative damage thermal-mechanical fatigue crack growth model were compared with the isothermal fatigue crack growth test results at 427°C, 538°C, and 649°C. The results are shown in Figures 4.25 through 4.30. All model predictions are within a factor of two of the test results, which is the data scatter for tests of this type.

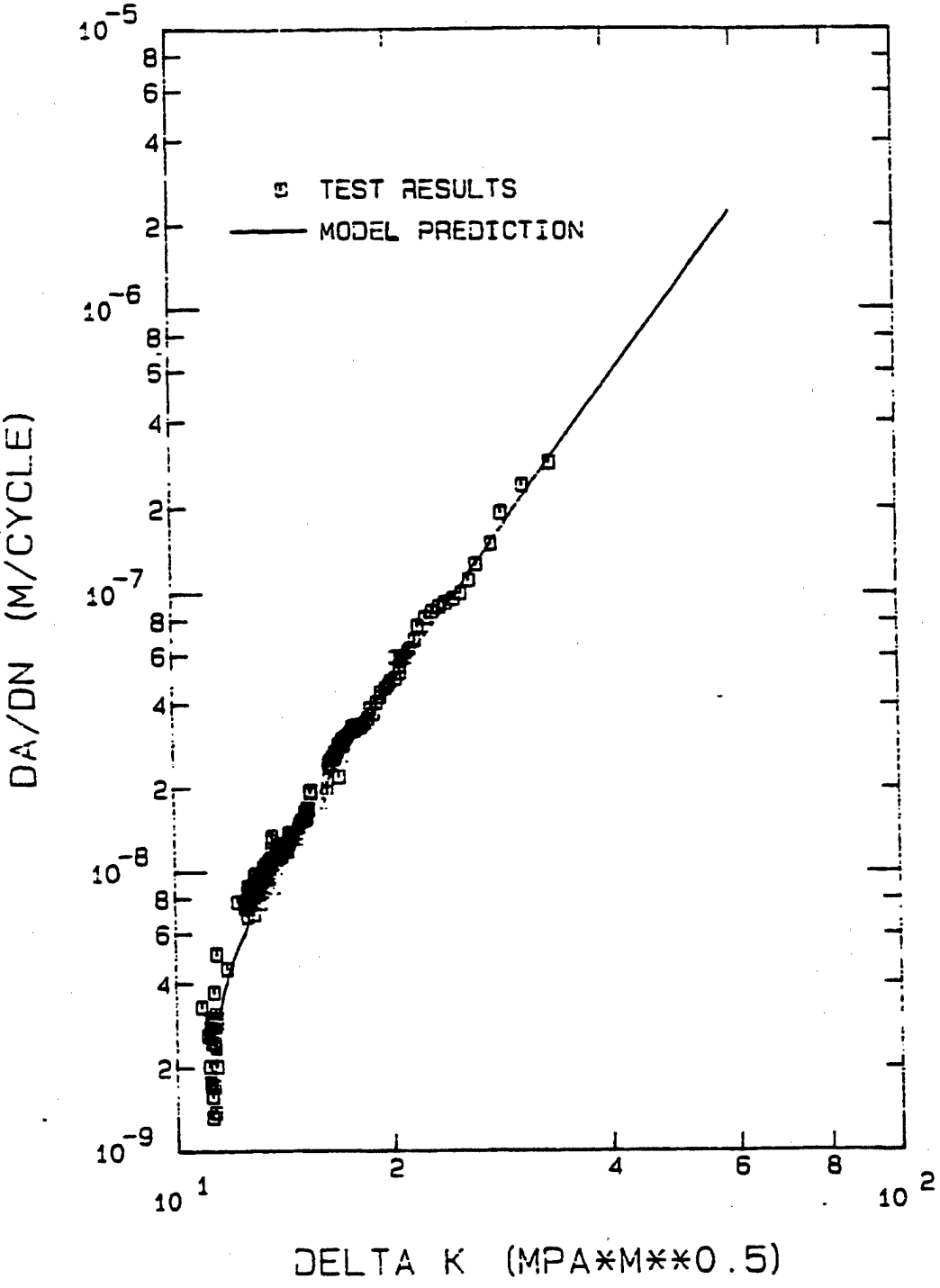

Figure 4.25: Predicted versus Actual Crack Growth, 427°C, R=0.1

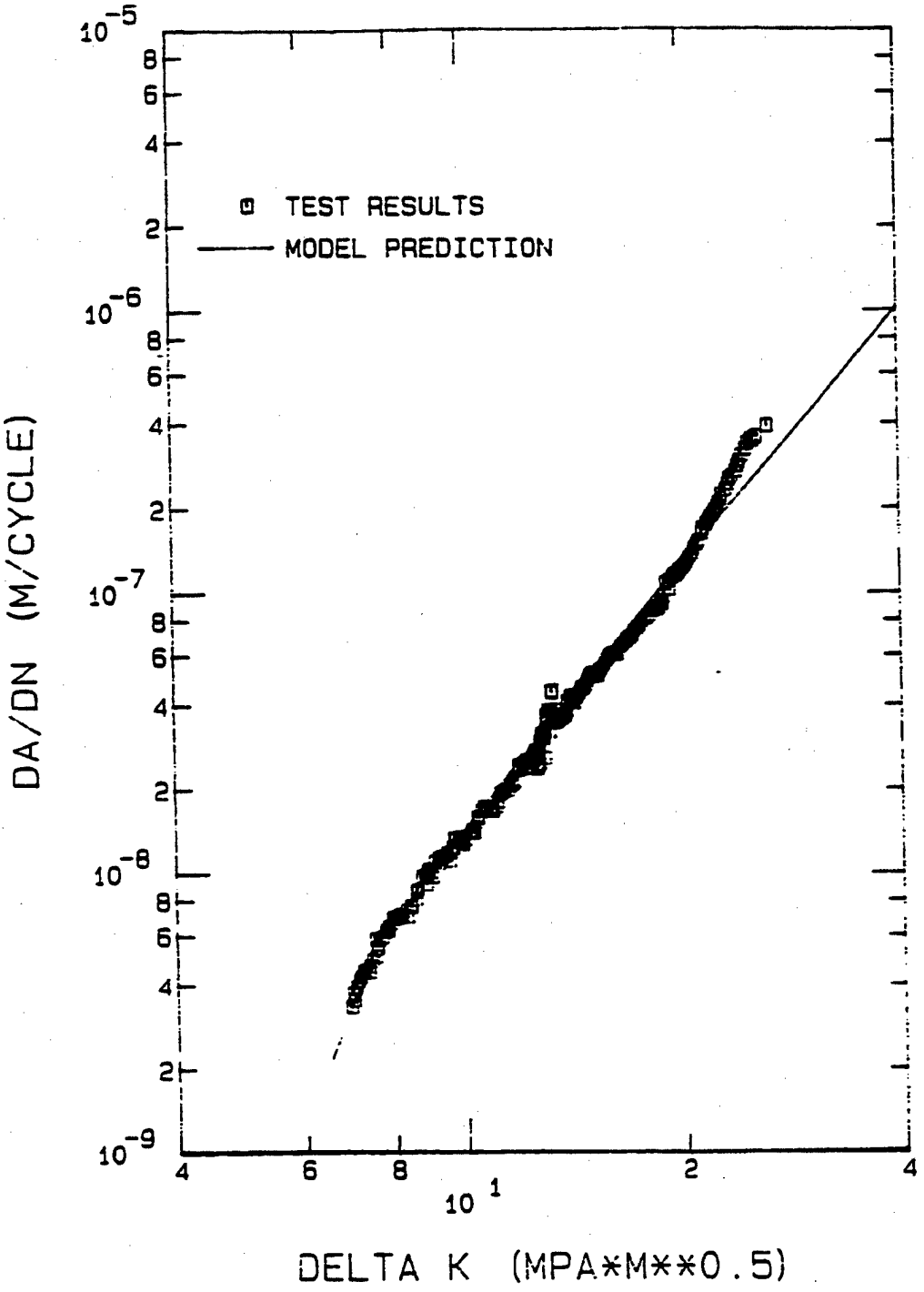

Figure 4.26: Predicted versus Actual Crack Growth, 427°C, R=0.5

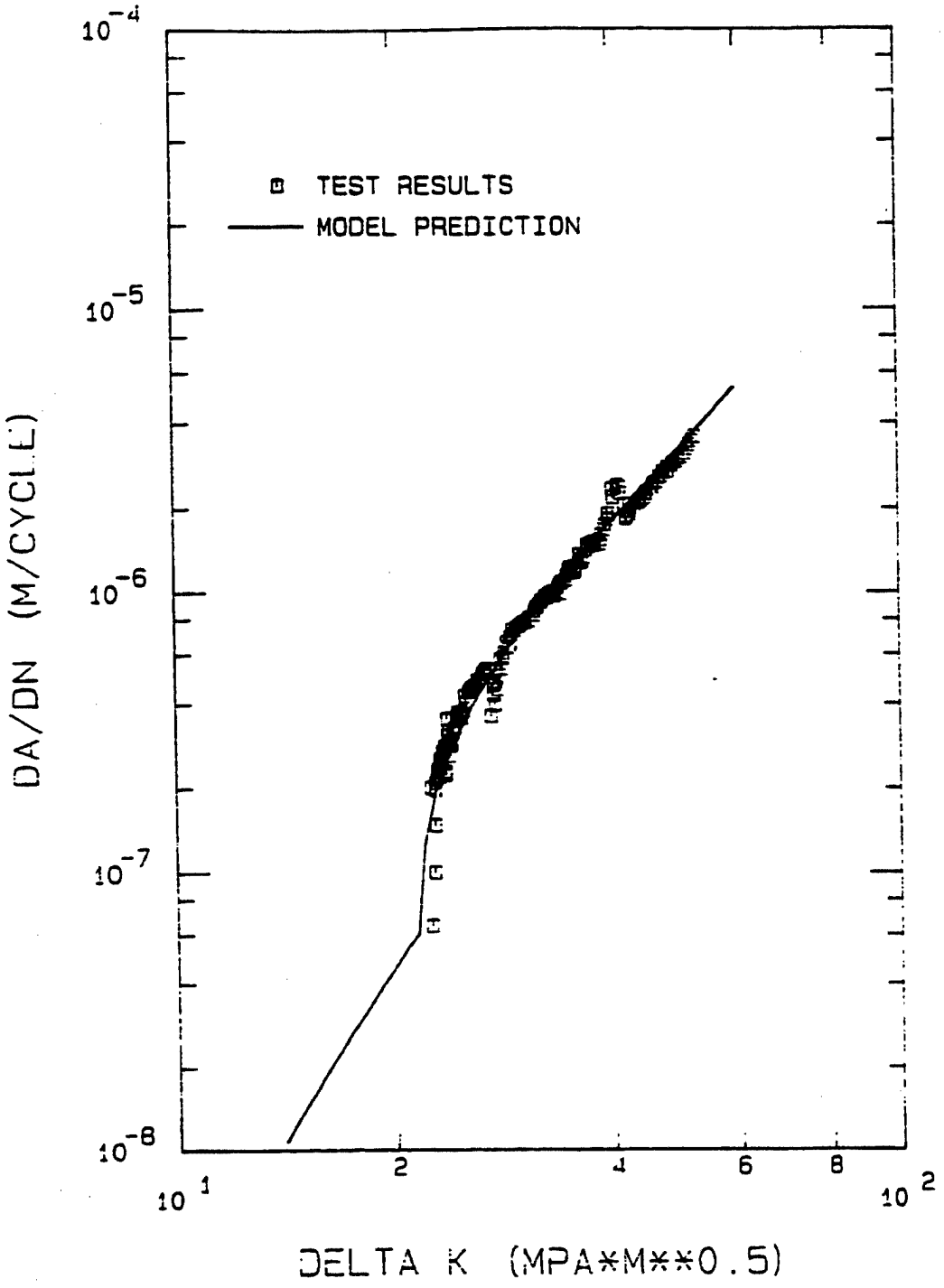

Figure 4.27: Predicted versus Actual Crack Growth, 538°C, R=0.1

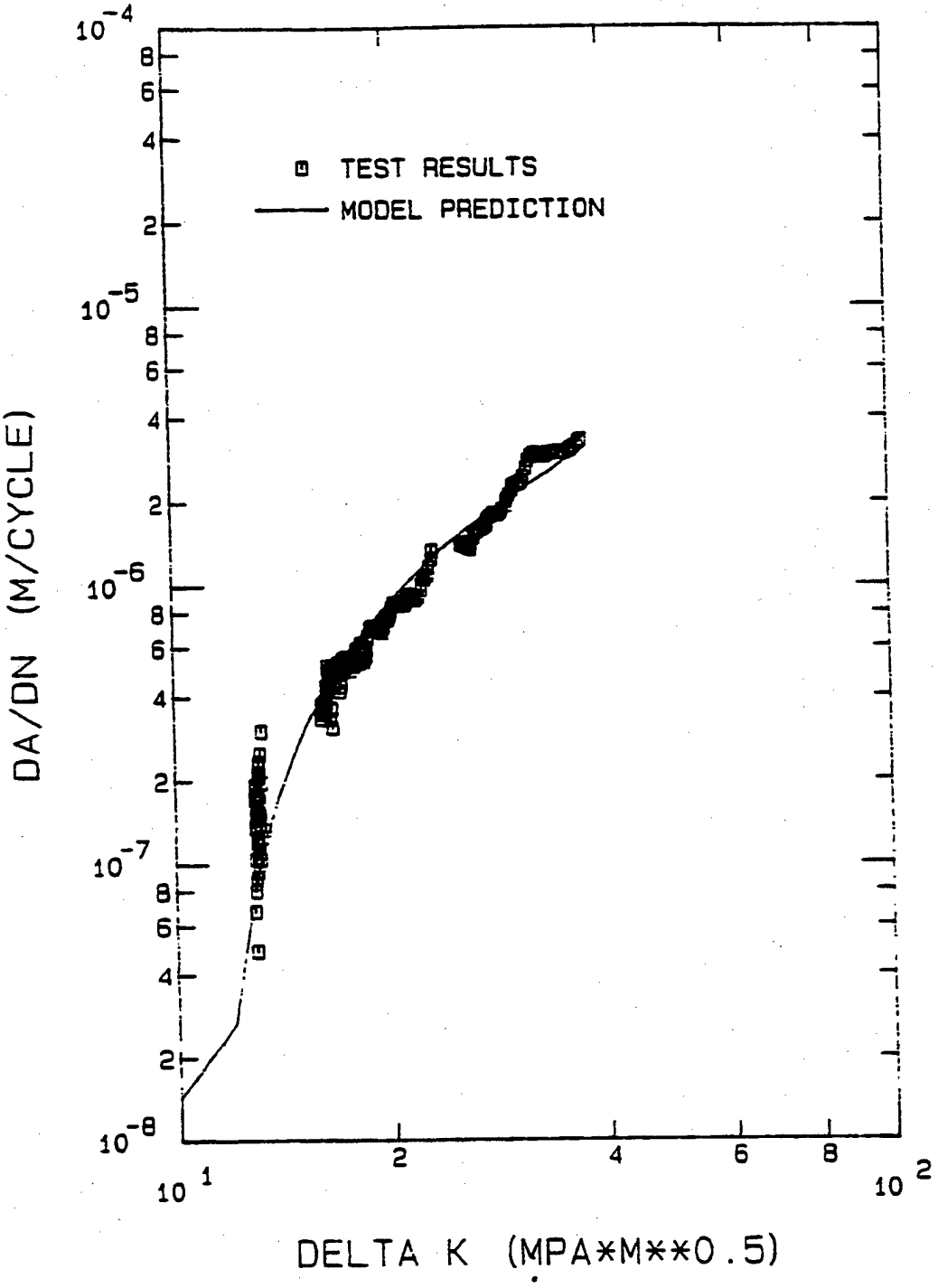

Figure 4.28: Predicted versus Actual Crack Growth, 538°C, R=0.5

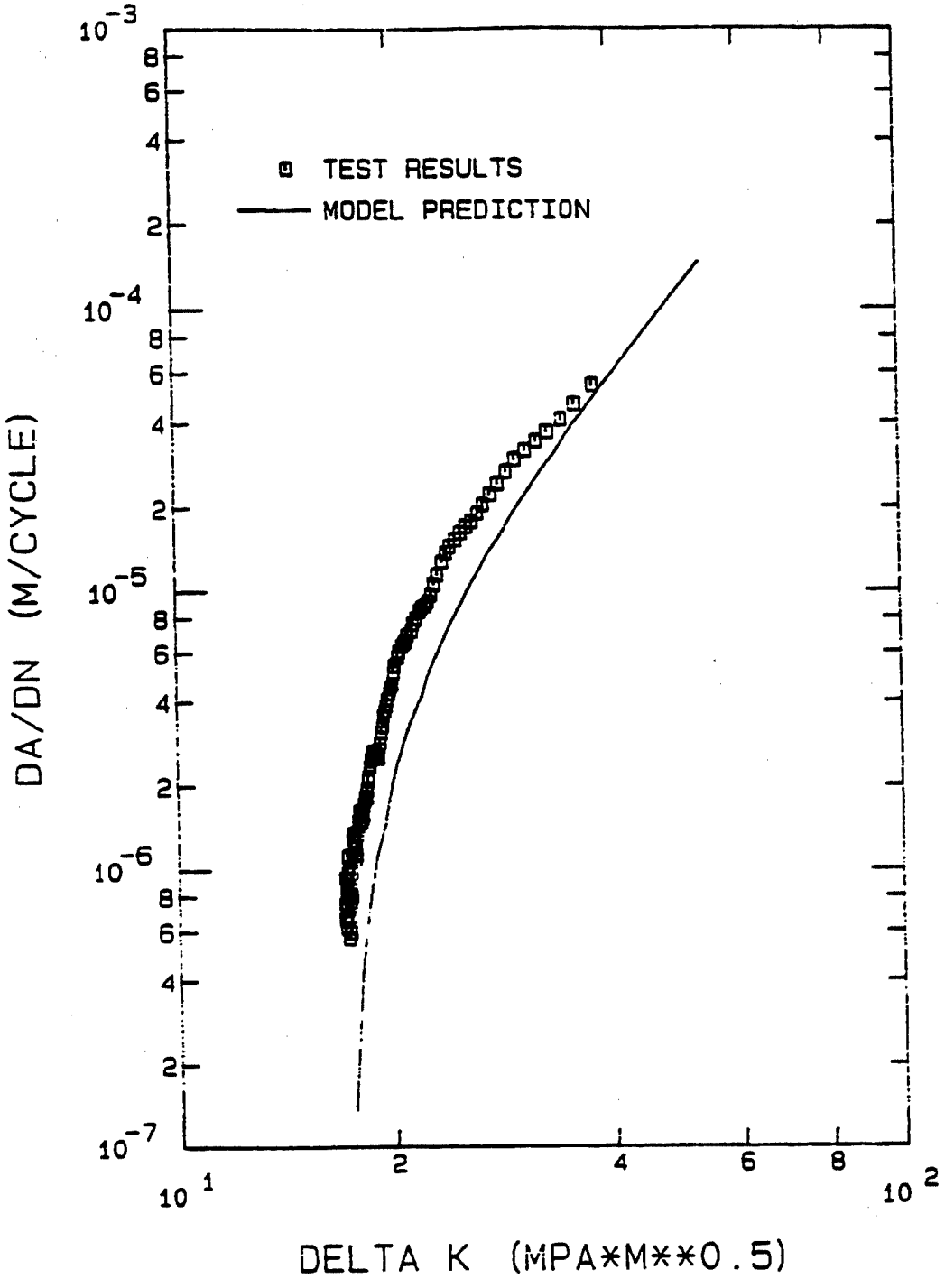

Figure 4.29: Predicted versus Actual Crack Growth, 649°C, R=0.1

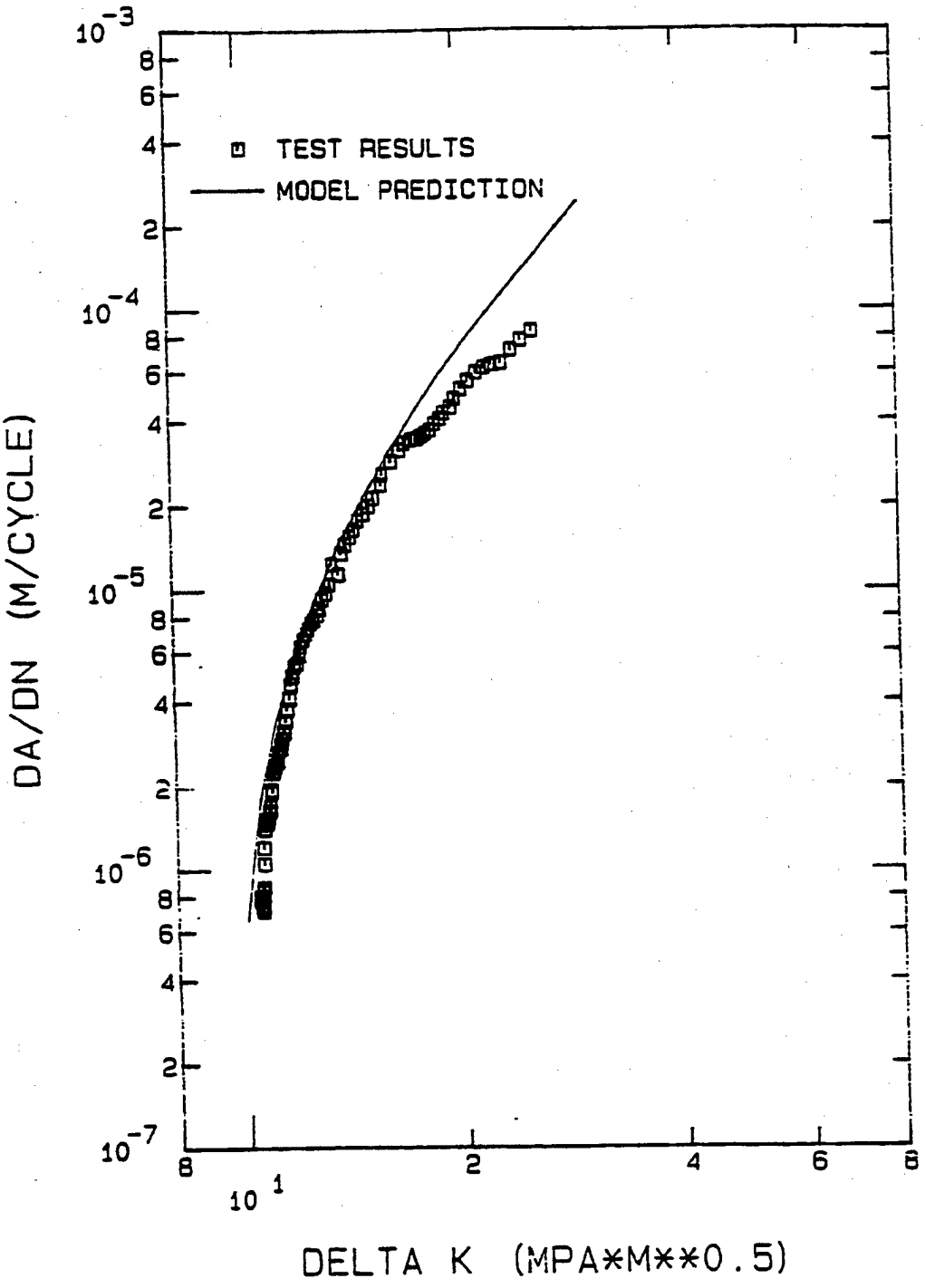

Figure 4.30: Predicted versus Actual Crack Growth, 649°C, R=0.5

V. Thermal Mechanical Fatigue Crack Growth Test Results and Predictions

Baseline TMF Test Results and Predictions

Four baseline thermal-mechanical cycles were chosen to characterize load controlled TMF crack growth in Inconel 718 and evaluate the effectiveness of the linear cumulative-damage model developed in Chapter IV. These cycles are shown in Figure 5.1. The temperature limits of the cycle were 427°C to 649°C and the cycle period was 96 seconds. The cyclic load range was held constant during the tests, resulting in an increasing ΔK test since K increases with crack length for a given load for the center-cracked specimen. The specimens used for the baseline TMF tests and test conditions are listed in Table 5.1. The phase angle is defined as the number of degrees that the maximum temperature lags behind the maximum load.

Table 5.1

Baseline TMF Test Conditions

Specimen	Phase Angle	Load Ratio	Initial Crack Length (mm)	Maximum Cycle Load (KN)
85-313	0°	0.1	5.283	20.0
85-312	0°	0.5	5.304	31.1
85-316	90°	0.1	7.150	26.7
85-314	180°	0.1	6.350	26.7
85-317	270°	0.1	5.644	26.7

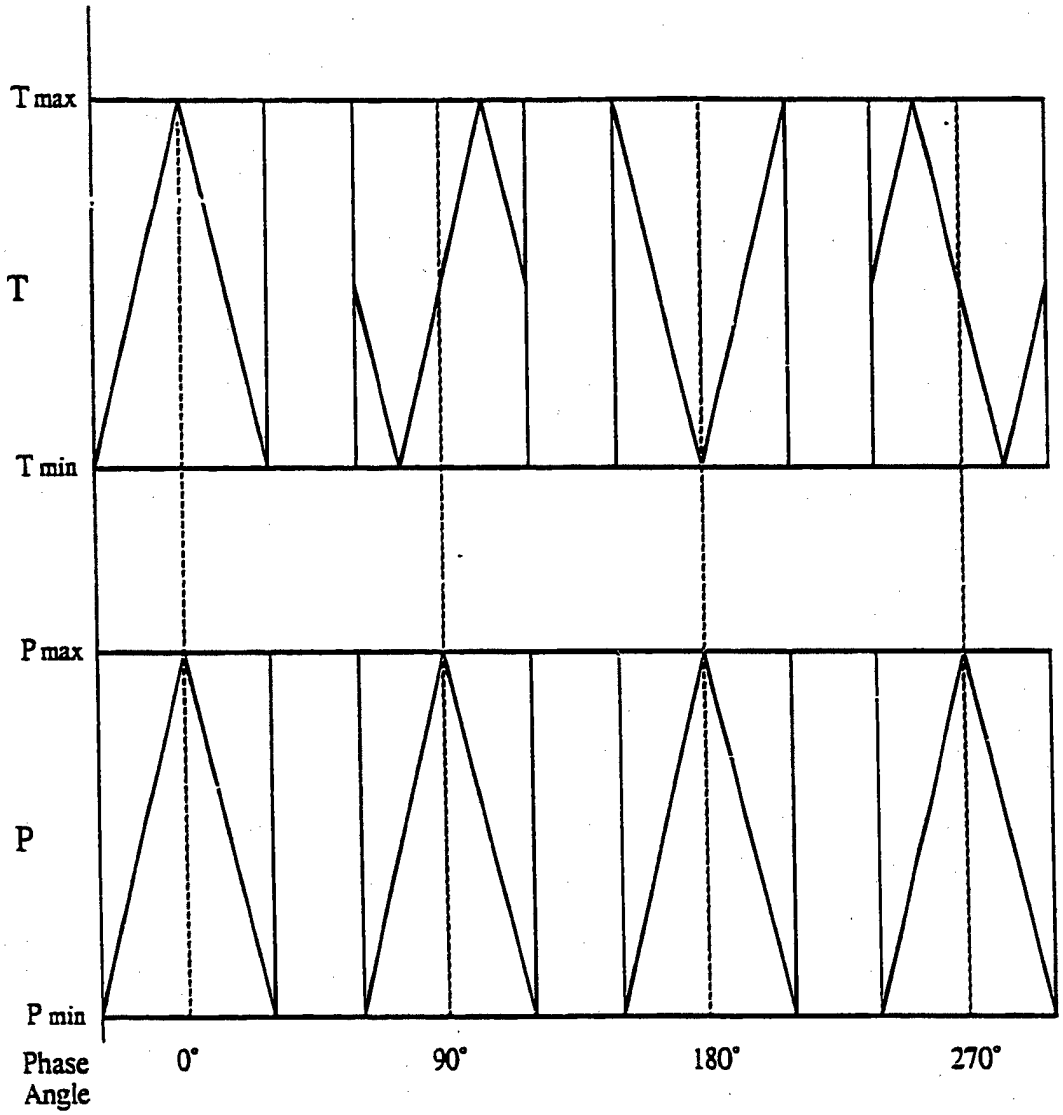

Figure 5.1: Baseline Thermal-Mechanical Cycles

The D.C. electric potential drop system was used to monitor the crack length versus the number of thermal-mechanical cycles and data was reduced to crack growth rate da/dN, versus stress intensity factor range, ΔK, as described in Chapter III.

At a given stress intensity factor level above threshold, the sustained load crack growth rate in Inconel 718 increases by a factor of over 1000 from 427°C to 649°C (see Figure 4.6). Therefore, the temperature during the high load portion of the thermal-mechanical cycle plays an important role in determining time-dependent damage in the linear cumulative-damage model. High temperatures at high loads are predicted to produce rapid crack growth by the model. The test results confirm this observation. A 0° phase angle (maximum load at maximum temperature) produces the fastest crack growth. On the other hand, high loads at the low temperature portion of the cycle (as in the 180° cycle) produce much slower crack growth. For the set of experiments conducted here, the time required to grow the crack from initial size to failure varied from several hours (0°, R=0.5) to several hundred hours (180° and 90°, R=0.1). The resulting growth rates varied by over two decades for a given value of ΔK.

The baseline thermal-mechanical fatigue test results are shown in Figures 5.2 and 5.3. Figure 5.2 compares the 0°, R=0.5 TMF results to isothermal test results at the cycle temperature limits (427°C and 649°C). Figure 5.3 compares the R=0.1 ults for 0°, 90°, 180°, and 270° TMF to the isothermal results at 427°C and 649°C. The TMF results are always bracketed by the isothermal fatigue crack growth rates at the temperature cycle limits.

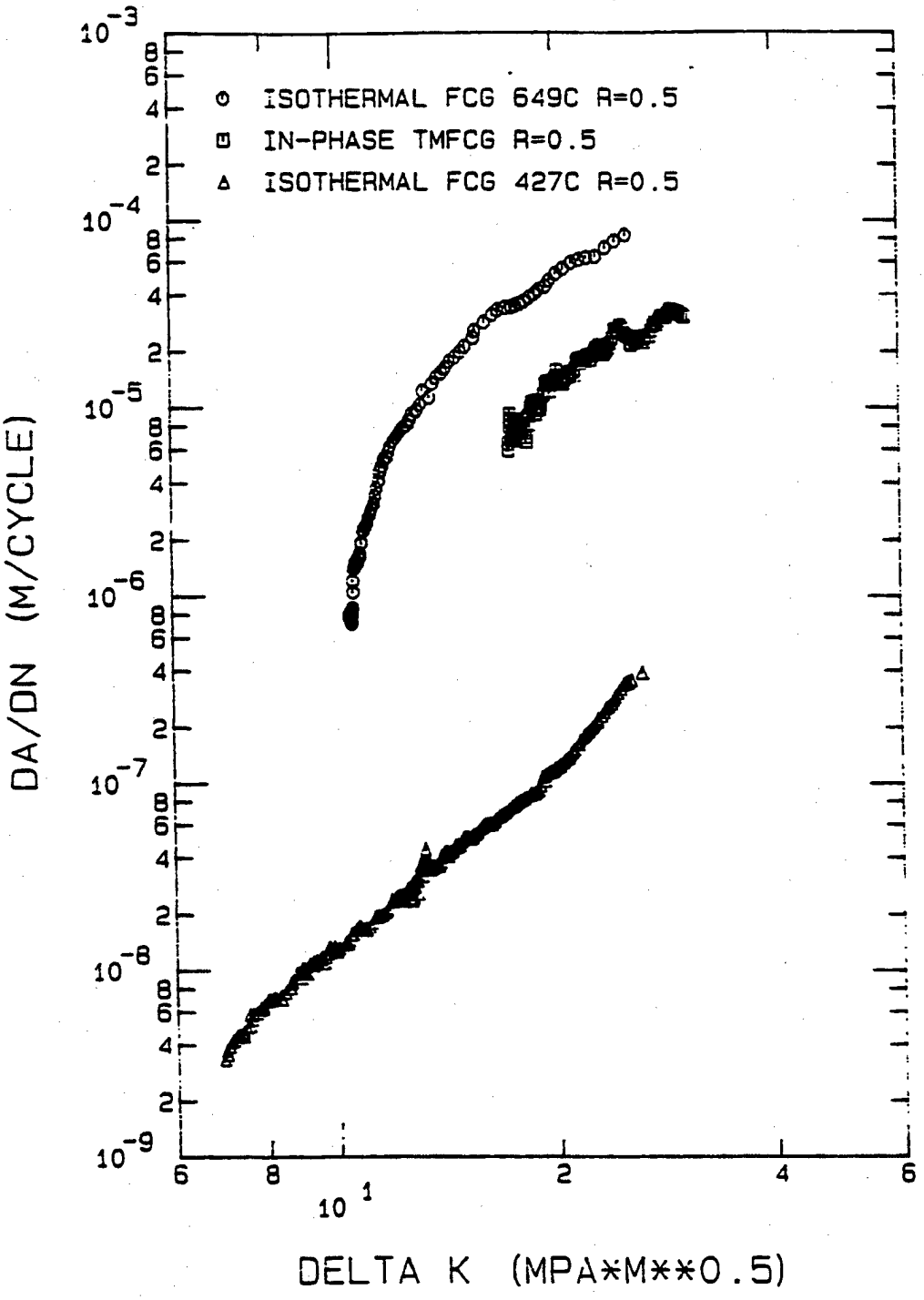

Figure 5.2: In-Phase TMF Crack Growth at R=0.5
Comparison is made with isothermal results at maximum and minimum temperatures for the same load ratio.

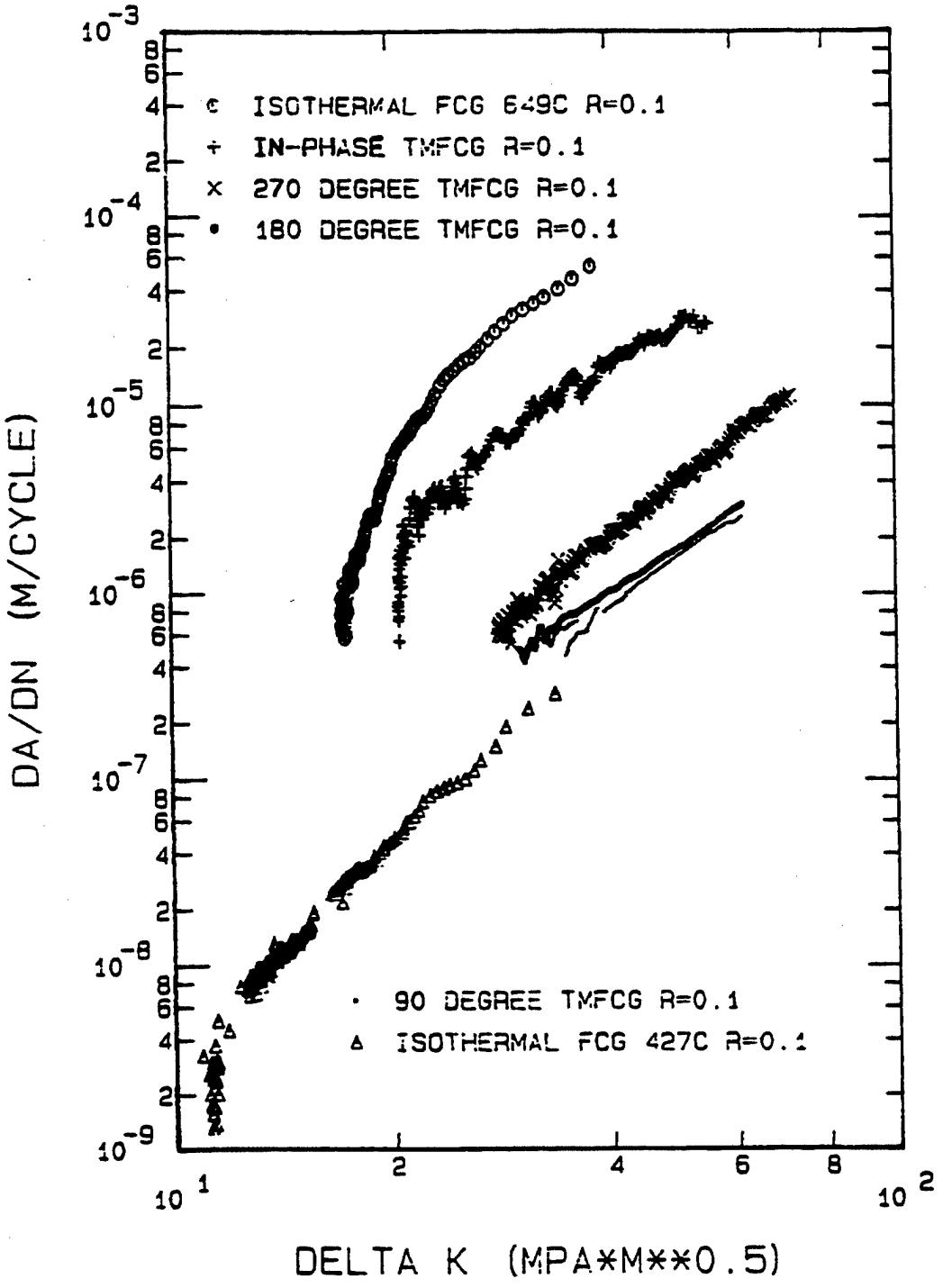

Figure 5.3: 0°, 90°, 180°, and 270° TMF Crack Growth at R=0.1
Comparisons are made with isothermal results at the maximum and minimum temperatures for the same load ratio.

In-phase load and temperature cycling (0°) produces the highest TMF crack growth rates. However, those rates are lower than the isothermal fatigue crack growth rates at the upper temperature limit of the cycle by a factor of approximately four for both R=0.1 and R=0.5. This result agrees qualitatively with the work of Marchand and Pelloux, who found that the in-phase TMF crack growth rates in Inconel X-750 were slightly lower than the isothermal rates at the upper cycle temperature for a load ratio of 0.05 (44). The isothermal fatigue crack growth rates at the upper temperature limit of a TMF cycle appear to be an upper bound for TMF crack growth in Inconel 718. However, other researchers have not found this to be the case in other materials. DeLuca and Cowles found that the in-phase TMF crack growth rates in an advanced cast single crystal alloy were higher than the isothermal growth rates at the upper cycle temperature (40).

The in-phase (0°) TMF crack growth rates were much higher than the 180° out-of-phase rates (see Figure 5.3). This agrees with General Electric's TMF crack growth test results for Inconel 718 (45). However, Rau, Gemma, and Leverant (38) found that out-of-phase TMF cycles produced nearly ten times greater crack growth rates in cast cobalt-and-nickel-base superalloys than in-phase cycles under strain controlled testing. The differences in alloy types, test stress-temperature profiles, and temperature limits (the Rau, et al. temperature limits were 316°C to 1038°C) may account for this apparent inconsistency in test results.

The crack growth rates for 90° and 180° out-of-phase TMF cycles are very close to each other and are over a factor of ten less than the in-phase rates. The crack growth rates for a 270° out-of-phase TMF cycle lie between the 90° out-of-phase and in-phase rates.

The phase diagrams (load versus temperature) for the baseline thermal-mechanical cycles are shown in Figure 5.4. The 90° cycle and 270° cycle have the same diagram but move in opposite directions along the path. Since the 270° cycle produces higher crack growth rates than the 90° cycle, thermal-mechanical fatigue crack growth is dependent upon

the path taken on a phase diagram. In the 90° cycle, the temperature is below 538°C during the loading portion of the cycle. In the 270° cycle, the temperature is above 538°C during the loading portion of the cycle. If the time-dependent crack growth damage occurs only during the loading portion of the cycle, the 270° cycle should produce higher crack growth rates than the 90° cycle. The experimental data results are consistent with this theory.

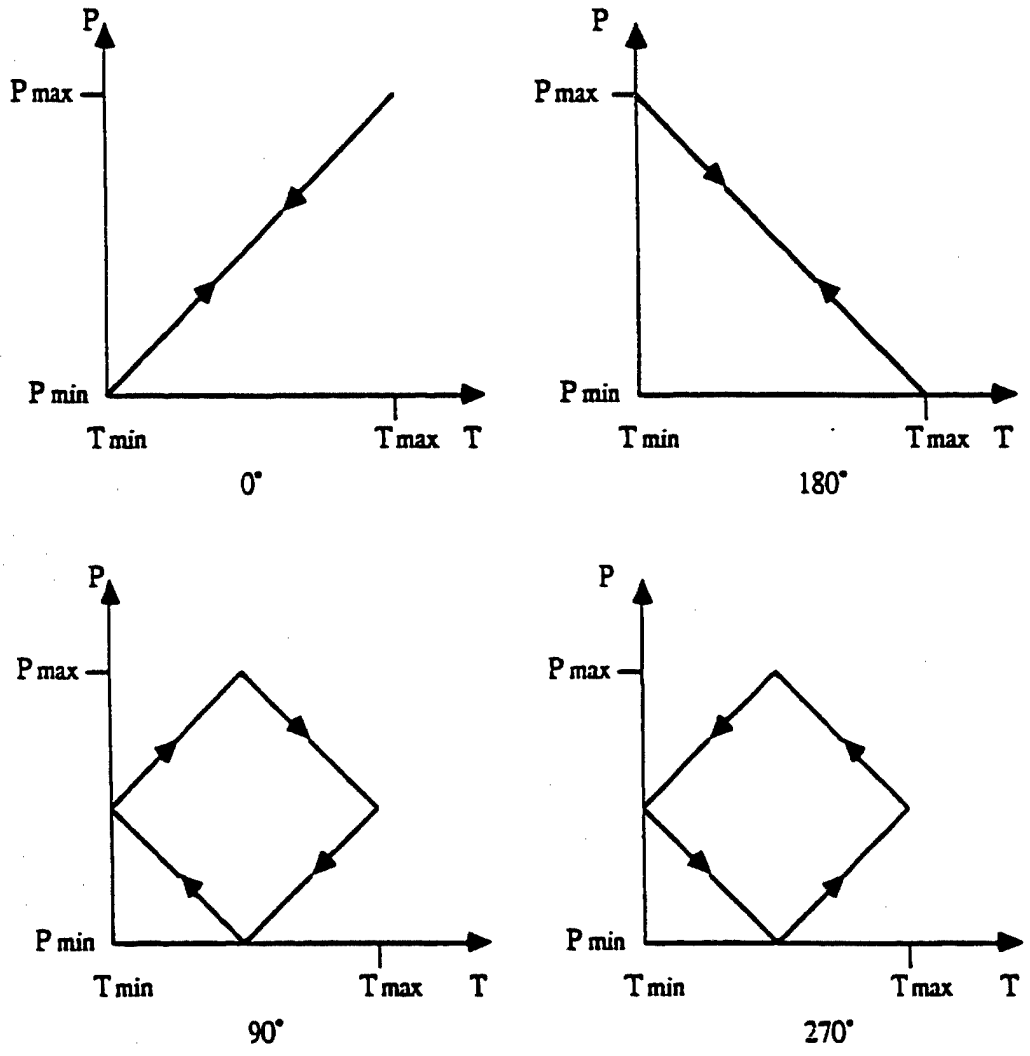

Figure 5.4: Phase Diagram of Baseline TMF Cycles

The linear cumulative-damage model crack growth predictions are compared with experimental results in Figures 5.5 through 5.9. Figure 5.5 compares the in-phase test results for R=0.5 with the model prediction. The time-dependent damage term dominates over the mixed-mode and cycle-dependent damage terms in the linear cumulative-damage model. The model does an excellent job of predicting the test results for this condition.

The in-phase test results for R=0.1 are compared to the linear cumulative-damage model prediction in Figure 5.6. Once again, the prediction is well within a factor of two of the experimental data. The time-dependent term dominates the prediction due to the high sustained-load crack growth rates at the high temperature and load portions of the cycle. The cycle-dependent and mixed-mode damage terms have a negligible effect on the prediction.

Figure 5.7 compares the 90 degree out-of-phase test results for R=0.1 with the model prediction. The model prediction is within a factor of 1.5 of the experimental data. The cycle-dependent damage term dominates the prediction. The time-dependent damage term does not significantly contribute to overall crack growth. This is because the temperature is below 538°C during the loading portion of the cycle. Neglecting the mixed-mode damage term slightly improves the model prediction.

The 180° out-of-phase test results are compared to the model prediction in Figure 5.8. The model predictions are low by a factor of up to 1.8 in the lower stress intensity factor ranges, but converge to the test results at the upper ranges. The cycle-dependent damage term dominates the prediction. The time-dependent damage term contribution is relatively small because temperatures are low at the higher loads in the loading portion of the thermal-mechanical cycle.

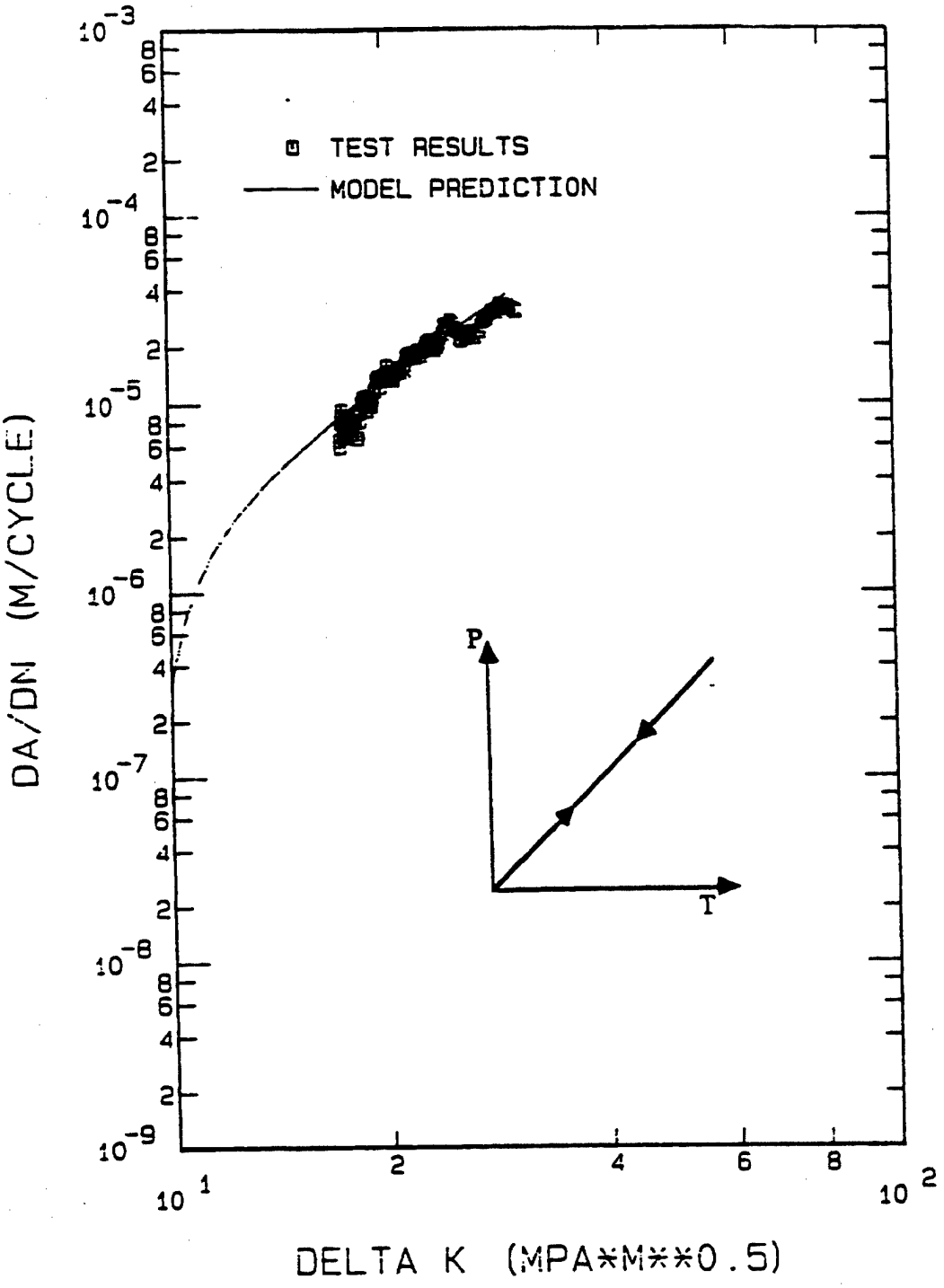

Figure 5.5: Predicted versus Actual TMF Crack Growth
In-Phase R=0.5

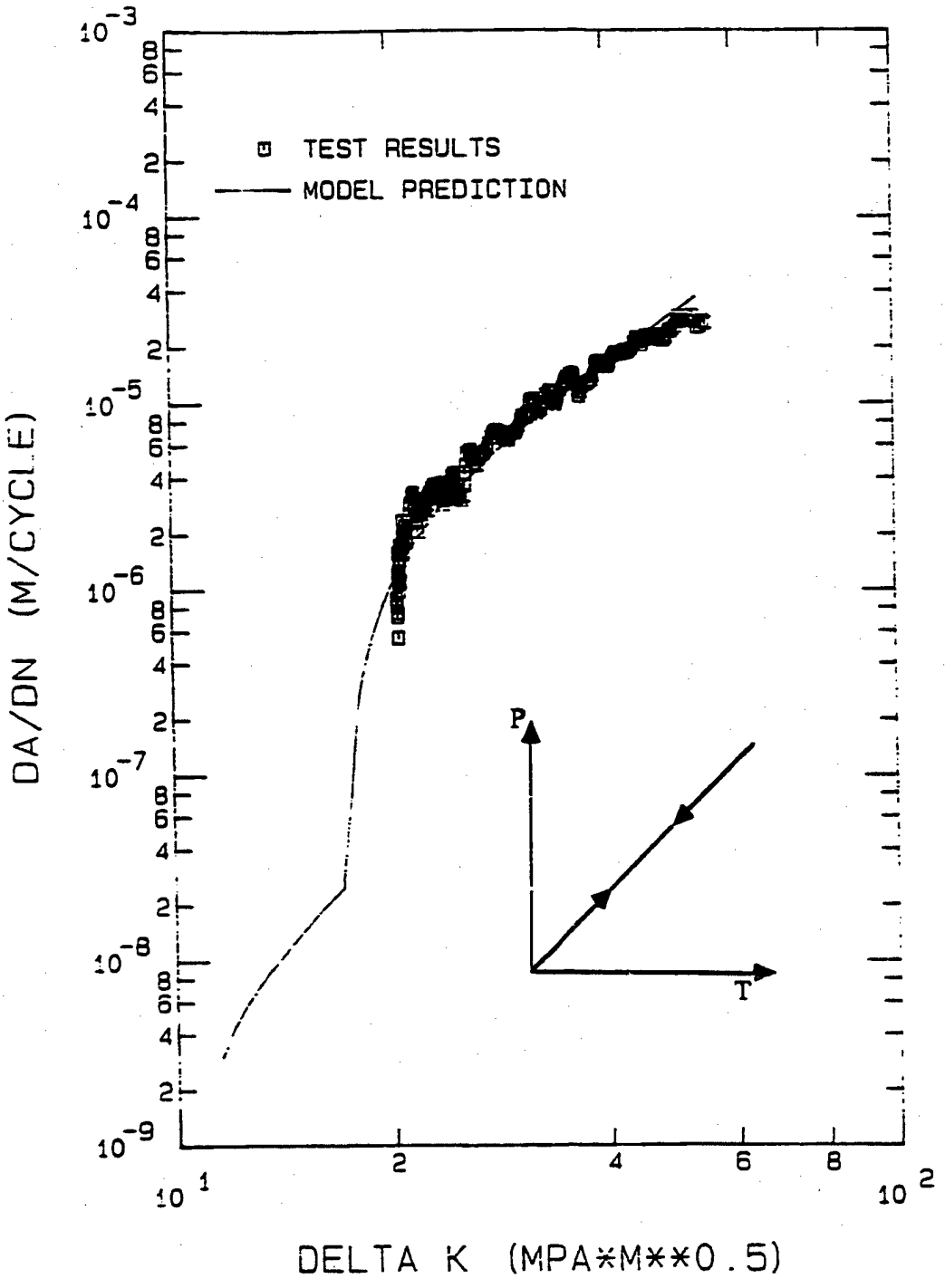

Figure 5.6: Predicted versus Actual TMF Crack Growth
In-Phase, R=0.1

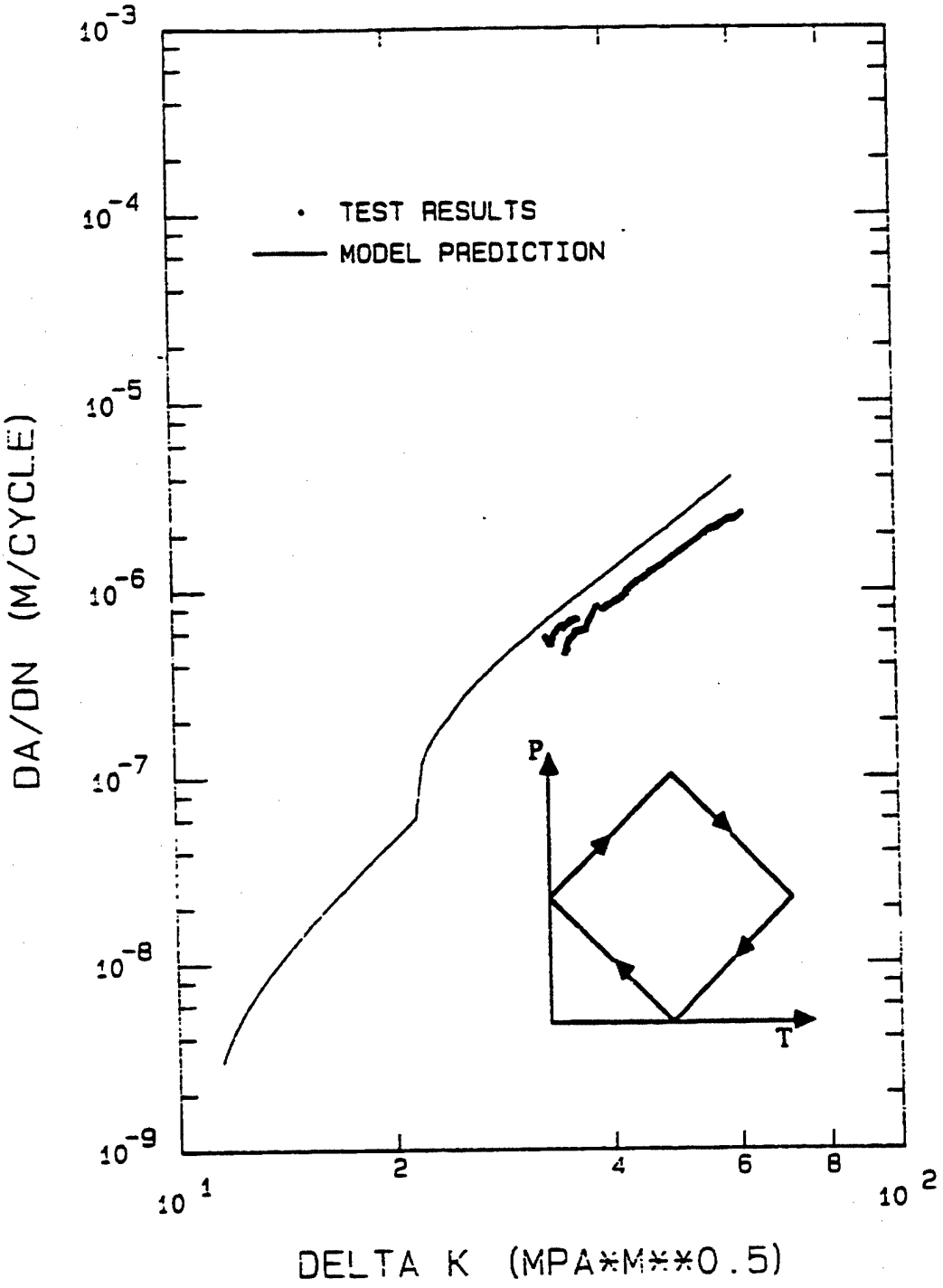

Figure 5.7: Predicted versus Actual TMF Crack Growth
90° Out-of-Phase, R=0.1

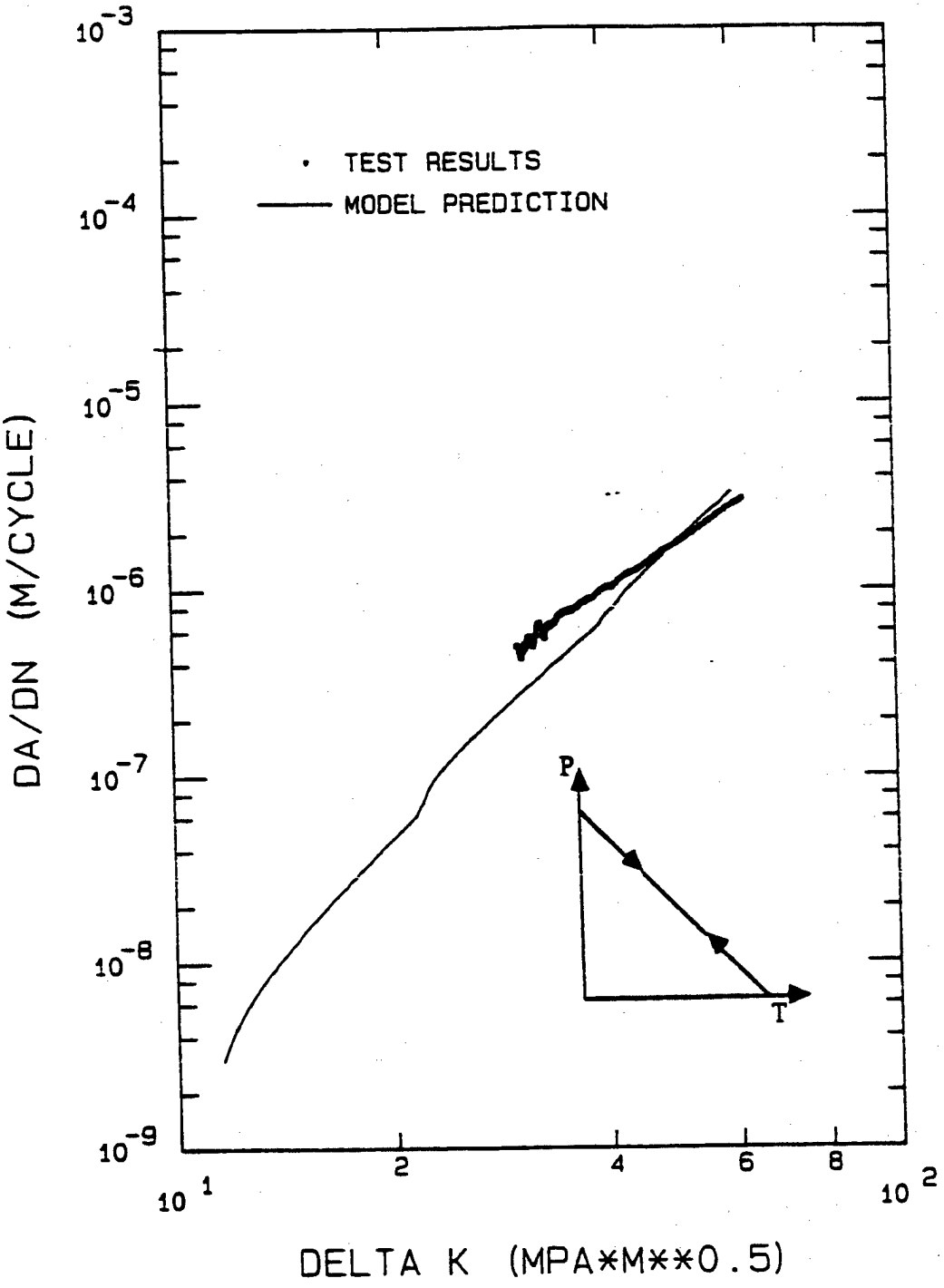

Figure 5.8: Predicted versus Actual TMF Crack Growth
180° Out-of-Phase, R=0.1

The test results and model prediction for a 270° out-of-phase TMF cycle are shown in Figure 5.9. The model prediction is consistently high by a factor of about four. During the loading portion of the cycle, the temperature is always above 538°C. Therefore, the sustained-load crack growth rates are high and the time-dependent damage term dominates the linear cumulative-damage model prediction.

Discussion of Results

The linear cumulative damage model was able to predict the 0°, 90°, and 180° baseline TMF crack growth data reasonably well (within a factor of two). This result was extremely encouraging considering that the model is based entirely on isothermal data and that no load/temperature interaction effects are considered. Interactions between damage mechanisms under conditions of varying load and temperature may retard or enhance crack growth and are not addressed in this linear cumulative damage model. Such interactions were investigated under isothermal conditions by Sadananda and Shahinian (9, 10, 19), Floreen and Kane (13), Pédron and Pineau (14), Weerasooriya (20), Pelloux (29), Nicholas, Weerasooriya, and Ashbaugh (30), and Saxena (33). Allowing temperature to vary during the cycle leads to thermal-mechanical fatigue and additional possible interactions. Such interactions may account for the differences between the linear cumulative damage model predictions and the experimental results.

The major exception to the good predictive capability of the linear cumulative-damage model was the case of the 270° out-of-phase cycle test data, shown in Figure 5.9. Here, the model was consistently higher than the experimental data, the error going from approximately a factor of two to four with increasing stress intensity range. Most of the contribution to the crack growth is from the time-dependent term. This anomolous result led to a reevaluation of the fundamental concepts embodied in the model and development of a modified model as explained below.

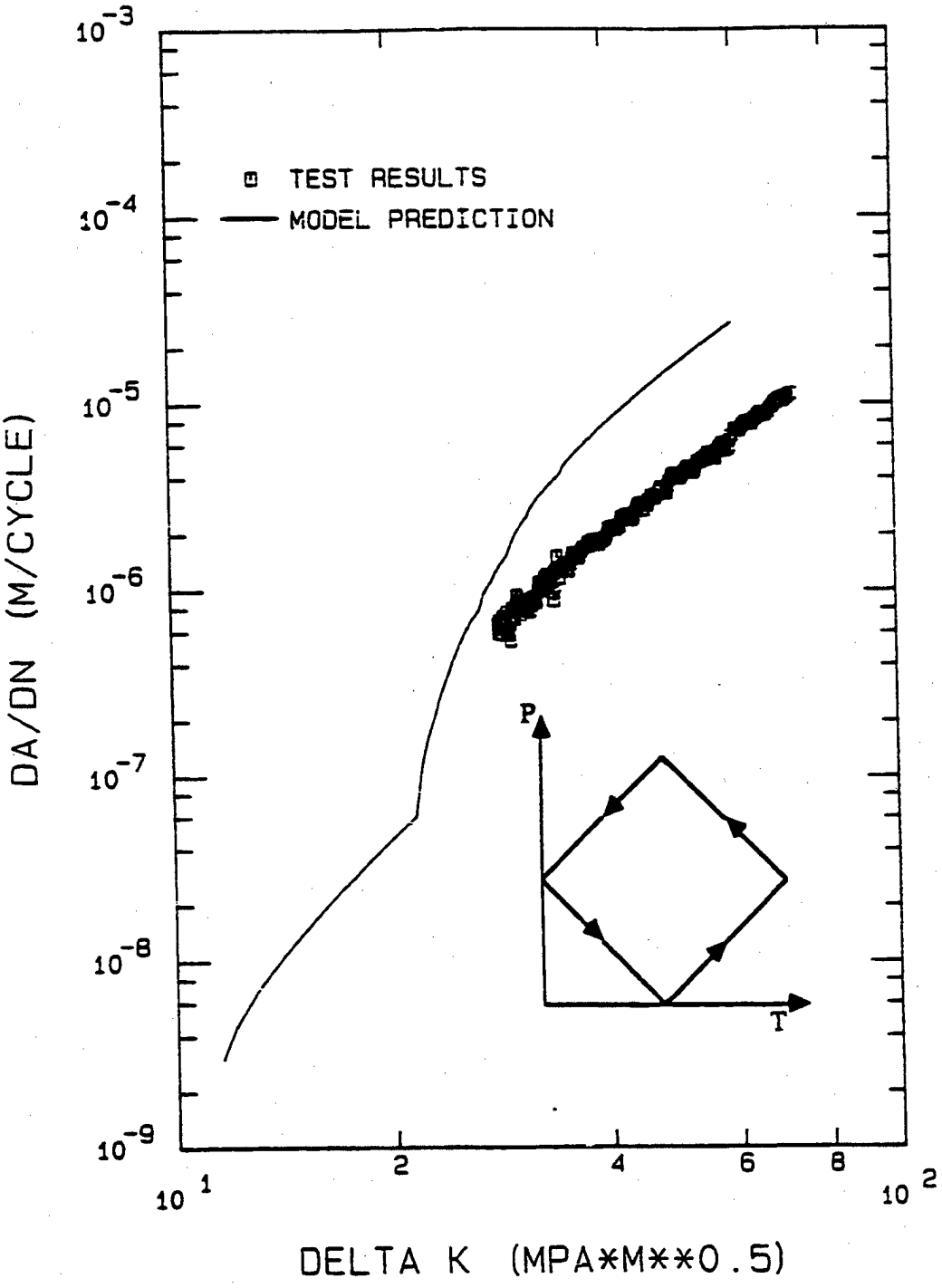

Figure 5.9: Predicted versus Actual TMF Crack Growth
270° Out-of-Phase, R=0.1

Model Modifications

The linear cumulative damage model summed the contributions attributed to cyclic loading and time-dependence. A mixed-mode term was also included, but its contribution to the overall prediction was small and may be neglected. The cyclic term was determined from low temperature data. The time-dependent term was obtained by integrating the sustained load crack growth rate during the loading portion of the cycle only. This concept was based on experimental observations of Nicholas, Weerasooriya, and Ashbaugh (30) and Runkle and Pelloux (34) which demonstrated that crack growth in the time-dependent regime is governed primarily by the duration of the loading portion of a triangular wave form cycle. The duration of the unloading portion of the cycle has little or no effect on the total crack growth rate. It could be deduced, then, that all of the time-dependent damage which contributes to crack growth occurs during the loading portion of a cycle under isothermal conditions. In the work of Nicholas et al. (30), it was demonstrated that crack growth, which was entirely time dependent at the frequencies used, could be accurately predicted by integrating sustained load crack growth during the loading portion of the cycle. It was shown, in fact, that including the contribution of the unloading portion of the cycle gave predicted crack growth rates which were too high. There was no physical explanation proposed for this observation.

If the same logic is used for the non-isothermal case, the 270° out-of-phase results are overpredicted by a large amount. If one examines this TMF cycle (see Fig. 5.1), it is noted that during the rising load portion of the cycle the temperature is first increasing until maximum temperature is reached, and then decreasing while load is still increasing. It was thus postulated that, as in the isothermal case, if the contribution to da/dt starts to decrease at some point in the loading portion of the cycle, there is no further contribution to time-dependent crack growth and the integration should be terminated at that point. In the

isothermal case, the integration was terminated at maximum load. During the unloading portion of the cycle, there is still calculated a value of da/dt from the sustained load data but this value decreases as load decreases and it is not included in the numerical integration. It is thus proposed to use the same logic and terminate the numerical integration of da/dt when the values of da/dt start to decrease. The modified model thus proposed is based on two primary hypotheses:

(1) time-dependent damage contributes to crack growth only when the load is increasing during a TMF cycle, and

(2) time-dependent damage contributes to crack growth only when da/dt as determined from sustained load crack growth data is an increasing function.

The algorithm for the modified model was incorporated in the computer program used to calculate thermal mechanical fatigue crack growth rates. The modified time-dependent damage program is listed as FUNCTION DADNTD in Appendix E.

The modified program predictions are compared to the baseline TMF test results in Figures 5.10 through 5.14. The in-phase predictions at R=0.5 and R=0.1 shown in Figures 5.10 and 5.11 are unchanged from the previous predictions because the sustained load crack growth rate (da/dt) is always increasing during the loading portion of the cycle. This is because increasing temperature and increasing load both tend to increase da/dt. The 90° out-of-phase cycle prediction shown in Figure 5.12 is also unchanged for the same reason.

The sustained load crack growth rate decreases during most of the loading portion of a 180° out-of-phase cycle. This is because the effect of decreasing temperature is greater than the effect of increasing load on da/dt. Therefore, the updated prediction shown in Figure 5.13 is lower than the previous prediction shown in Figure 5.8. However, the effect is very small since time-dependent crack growth plays a minor role in overall crack growth for this cycle.

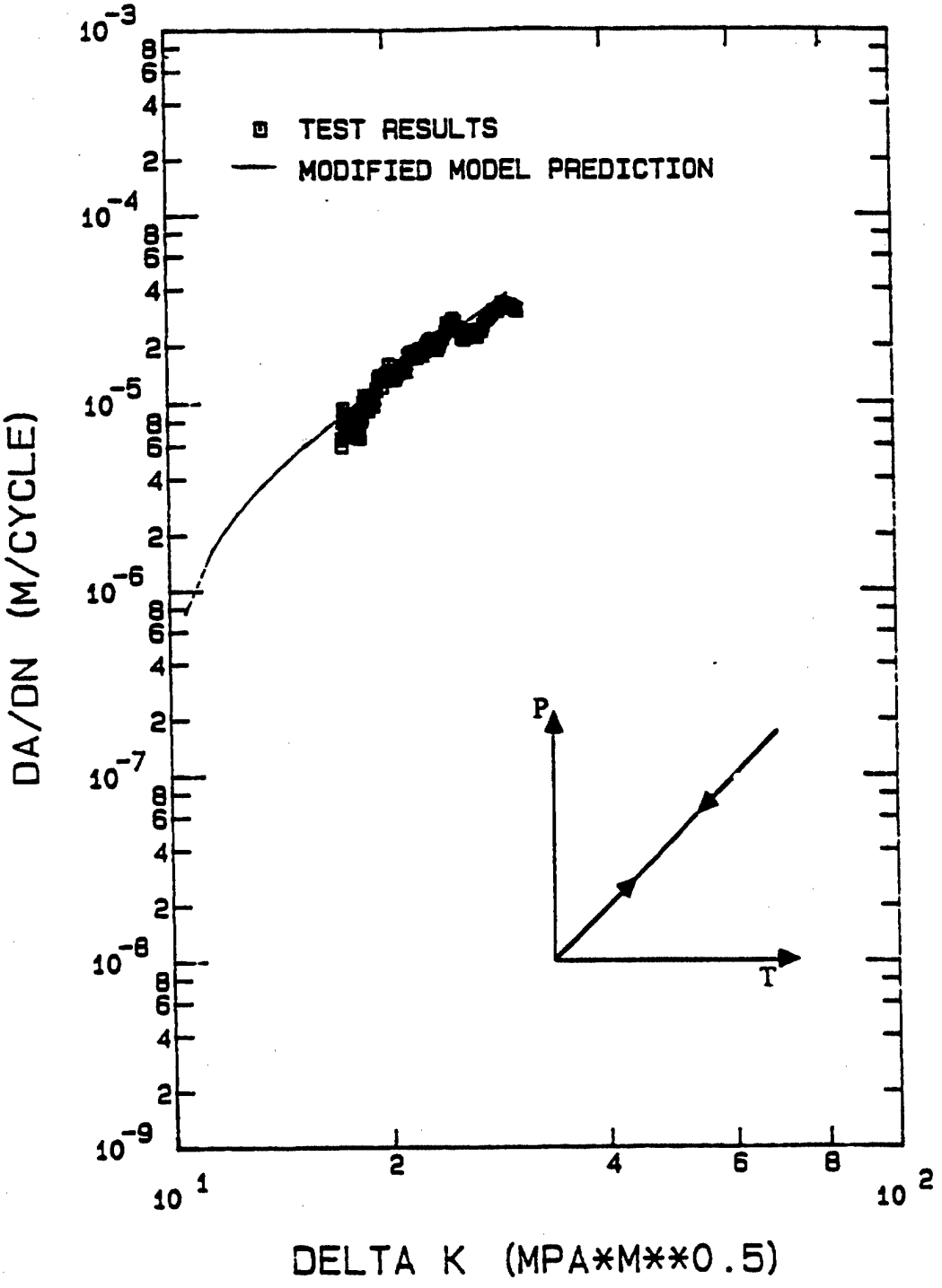

Figure 5.10: Updated TMF Crack Growth Prediction
In-Phase, R=0.5

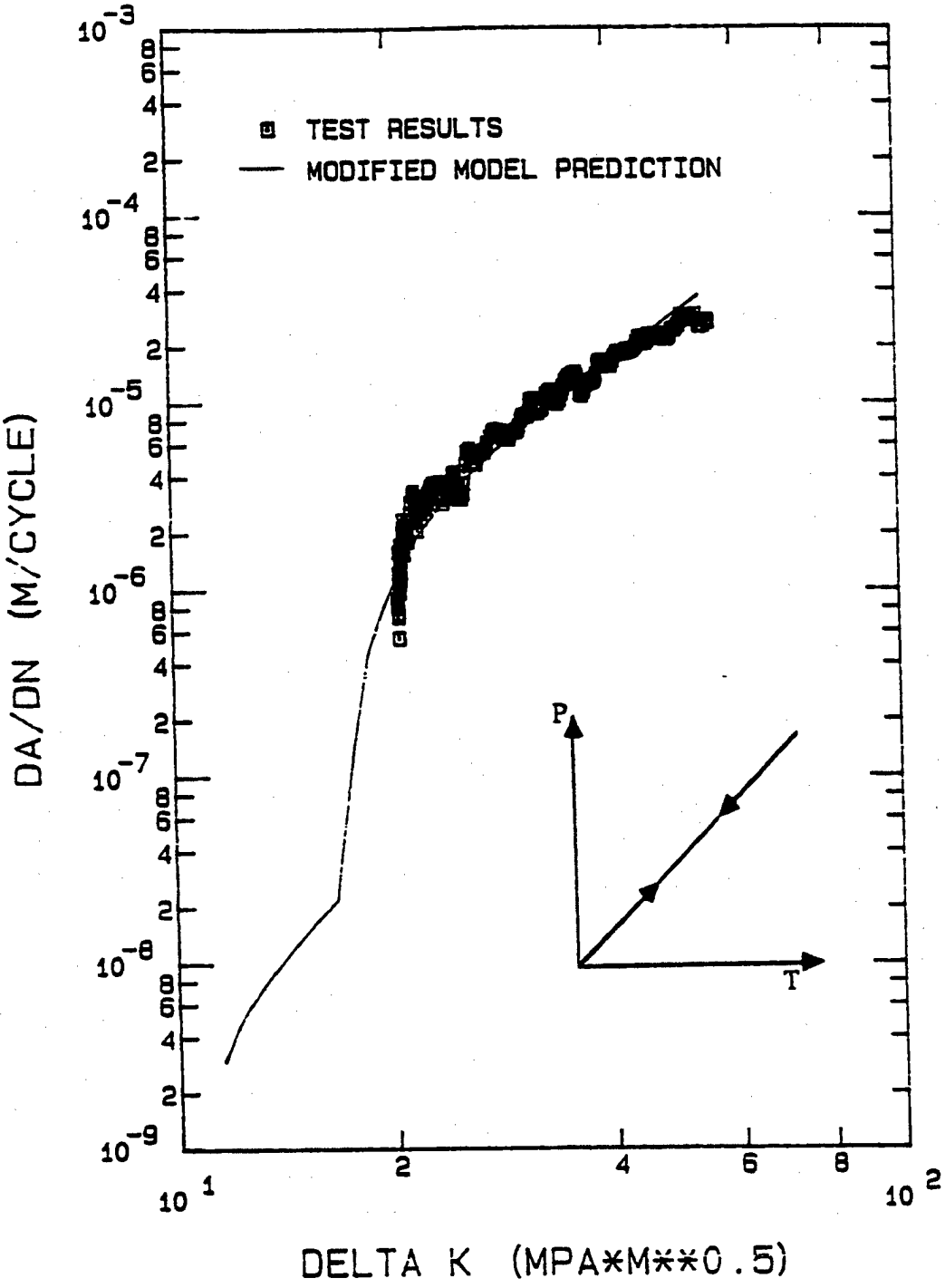

Figure 5.11: Updated TMF Crack Growth Prediction
In-Phase, R=0.1

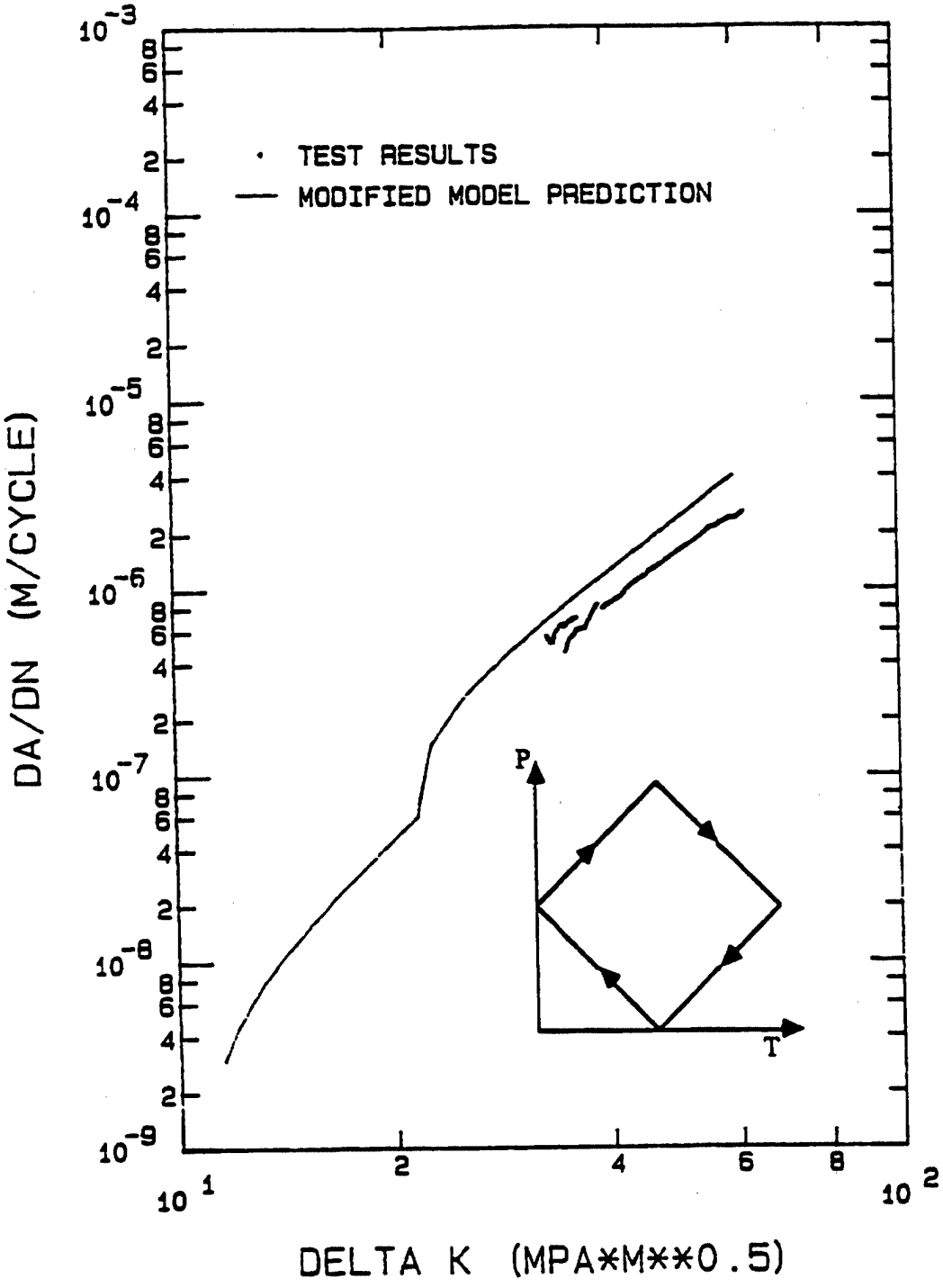

Figure 5.12: Updated TMF Crack Growth Prediction
90° Out-of-Phase, R=0.1

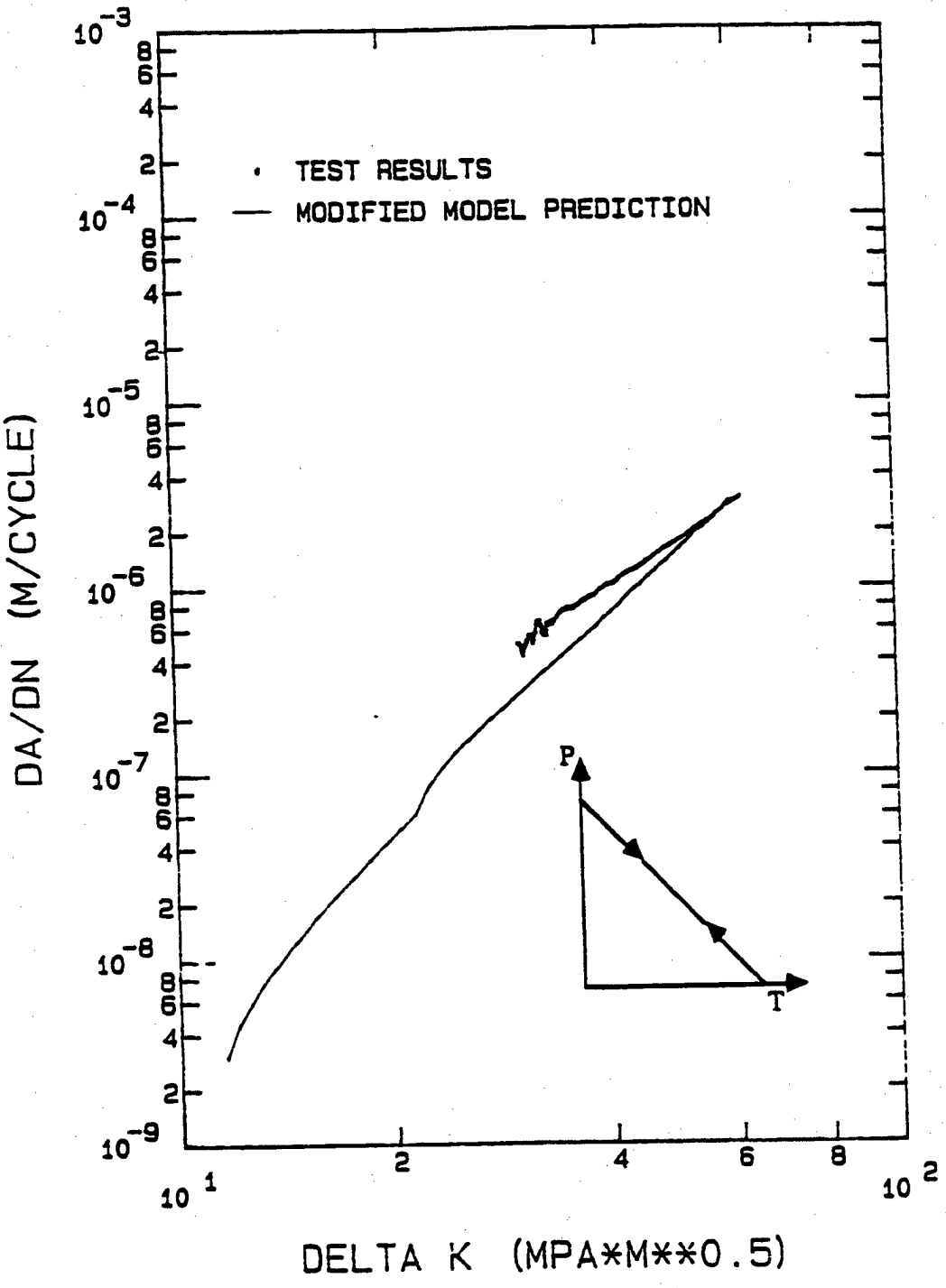

Figure 5.13: Updated TMF Crack Growth Prediction
180° Out-of-Phase, R=0.1

The sustained load crack growth rate decreases during most of the loading portion of a 270° out-of-phase cycle. Therefore, the integration to calculate the time-dependent damage term is over a smaller portion of the cycle and the magnitude of the term decreases. Since time-dependent damage dominates in this cycle, the updated prediction shown in Figure 5.14 is much lower than the previous prediction shown in Figure 5.9 and is significantly closer to the experimental results. The modified prediction exceeds the experimental data at the higher stress intensity factor ranges by a factor of two or less.

The original linear cumulative-damage model integrated the sustained-load crack growth rate over the entire loading portion of the thermal-mechanical cycle to calculate the time-dependent damage term. This resulted in a significant overprediction of TMF crack growth for the 270° out-of-phase cycle. The modified linear cumulative-damage model integrates sustained-load crack growth only when da/dt is an increasing function. This significantly improved the 270° out-of-phase cycle prediction without damaging the other baseline TMF predictions. The modified model predicted all of the baseline TMF test results within a factor of two or less.

TMF Proof Test Selection

Two proof tests were conducted to evaluate the validity of the modified linear cumulative-damage model and compare the original and modified modeling concepts. The two proof test TMF cycles were chosen from the four simple thermal-mechanical cycles shown in Figure 5.15.

The sustained-load crack-growth rate versus time profiles of the four cycles shown in Figure 5.15 were compared to select the two cycles for which the change in modeling concepts has the greatest impact. Time-dependent damage plays a relatively small role in overall crack growth for the 45° and 135° out-of-phase cycles because the temperature is always at or below 593°C during the loading portion of the cycle. Therefore, the modeling

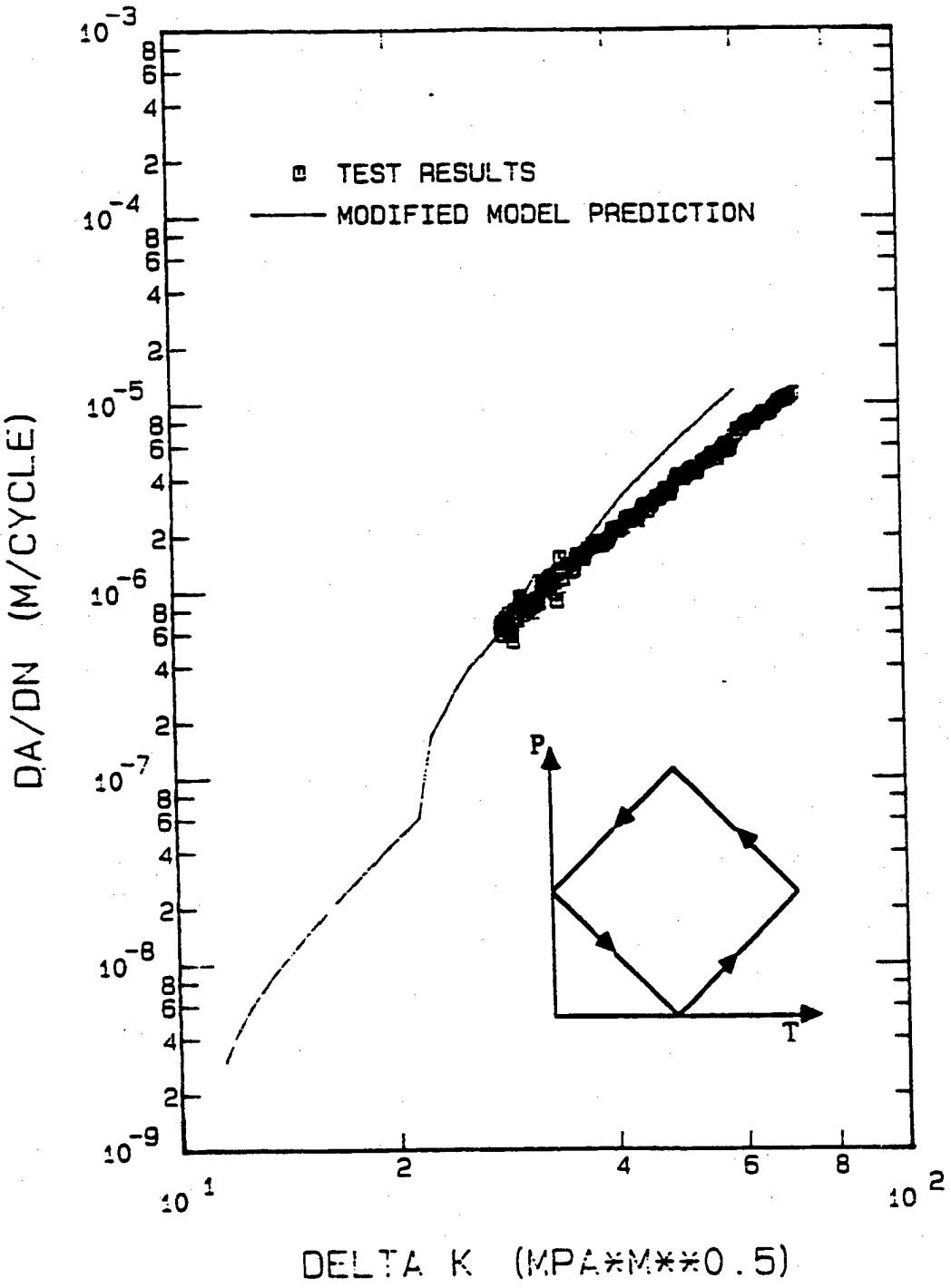

Figure 5.14: Updated TMF Crack Growth Prediction
270° Out-of-Phase, R=0.1

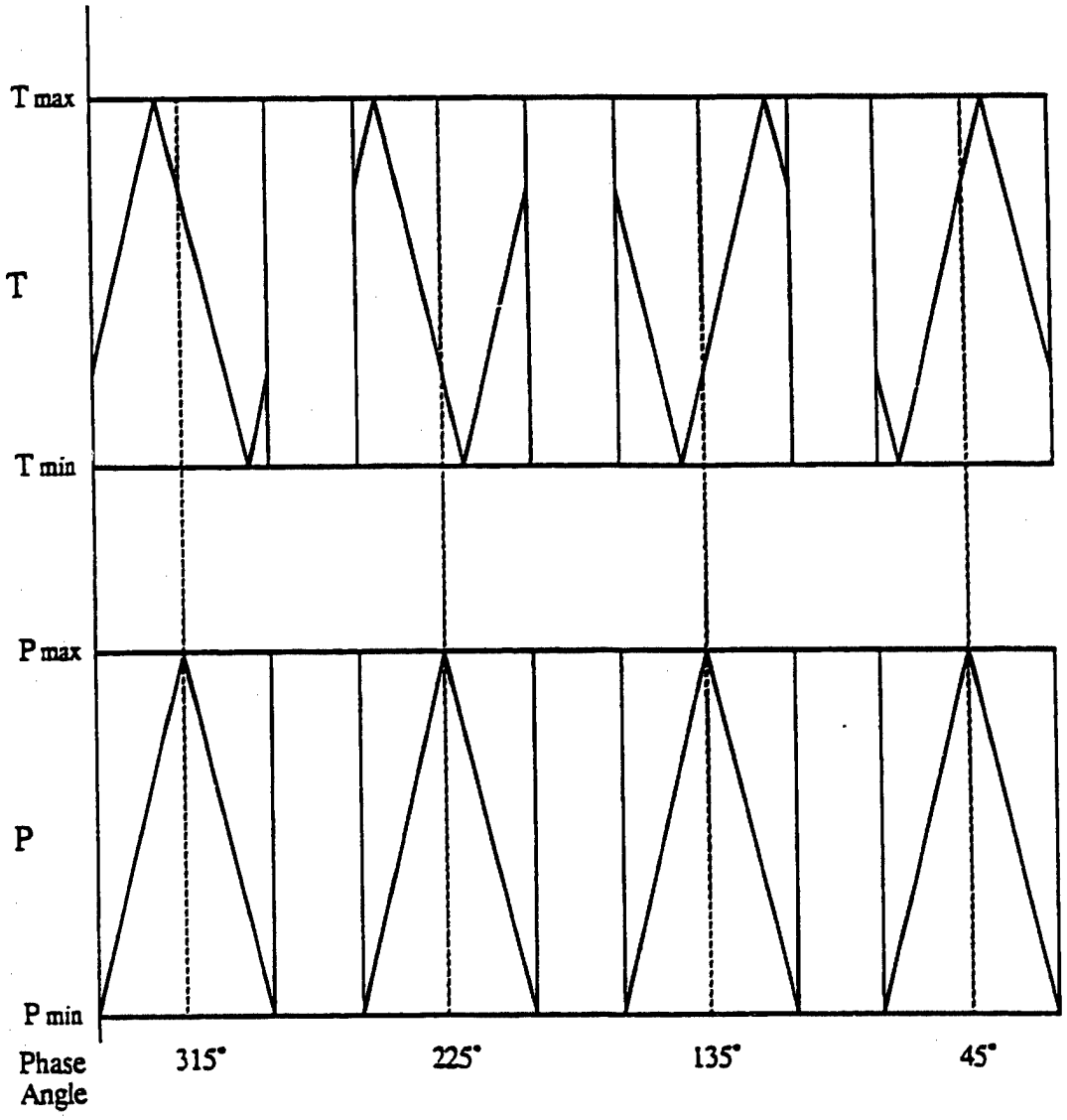

Figure 5.15: Potential TMF Proof Test Cycles

concept change has little effect on the crack growth predictions for those two cycles. The 315° and 225° out-of-phase cycles were chosen for the proof tests.

Time-dependent damage dominates the crack growth prediction for a 315° out-of-phase cycle because the temperature is high at the high load portion of the cycle. Because the temperature begins to drop before the load reaches its peak, the sustained load crack

growth rate will drop and the net contribution to crack growth will be lower in the modified time-dependent damage calculation. Therefore, the modified model will give a lower prediction than the original model.

For the 225° out-of-phase cycle, the temperature is dropping during much of the loading portion of the cycle. Therefore, the sustained load crack growth rate decreases and the modified model will again give a lower crack growth prediction than the original model.

Proof Test Predictions and Results

Thermal-mechanical fatigue crack growth tests were conducted for 315° and 225° out-of-phase cycles to compare the linear cumulative damage modeling concepts. The temperature limits were 427°C to 649°C, the maximum load was held constant during the test, and the cycle period was 96 seconds. The specimens used for the proof tests and test conditions are listed in Table 5.2.

Table 5.2

TMF Proof Test Conditions

Specimen	Phase Angle	Load Ratio	Initial Crack Length (mm)	Maximum Cycle Load (KN)
85-318	315°	0.1	5.202	26.7
85-319	225°	0.1	7.691	31.2

The predicted proof test crack growth rates are compared to the actual observed rates as a function of the applied stress intensity range in Figure 5.16 for the 315° out-of-phase cycle and Figure 5.17 for the 225° cycle. In both proof tests, the modified predictions are closer to the actual crack growth rates than the original predictions. The original model integrates the sustained load crack growth rate over the entire loading portion of the cycle and overpredicts the proof test crack-growth rates. The modified

model integrates the sustained-load crack-growth rate over the loading portion of the cycle only when da/dt is an increasing function. The modified model predictions were within a factor of two of the observed crack growth rates for every TMF test conducted.

The TMF crack growth rates for 0°, 90°, 180°, 225°, 270°, and 315° out-of-phase cycles at a load ratio of 0.1 are compared to the isothermal rates at the cycle temperature extremes (427°C and 649°C) in Figure 5.18. The 315° out-of-phase TMF cycle proof test results lie below the in-phase crack growth rates but well above the 270° out-of-phase rates. The 225° out-of-phase proof test results lie between the 180° and 270° out-of-phase crack-growth rates. The proof test crack growth rate positions relative to the baseline TMF test results are consistent with the linear cumulative damage model predictions. The time-dependent damage term dominates the linear cumulative-damage model predictions for the high crack-growth rate tests (0°, 315°, and 270° phase angles) and the cycle-dependent damage term dominates the predictions for the low growth rate tests (225°, 180°, and 90° phase angles). The mixed-mode damage term contribution to the linear cumulative-damage model is relatively small. It may be neglected without significantly affecting the model crack growth predictions.

Linear cumulative damage modeling may also be applied when the thermal and mechanical cycles have different periods. Hartman and Johnson conducted a TMF crack growth test with a 0.0119 Hz triangular thermal cycle from 427°C to 649°C and a 1.0 Hz triangular load cycle of load ratio of 0.1 (47). The specimen and test equipment used for this test were identical to those described in Chapter III, Experimental Apparatus and Procedure. The reduced data from this test are compared to the linear cumulative-damage model prediction in Figure 5.19. The linear model accurately predicts the crack growth rate for this test condition.

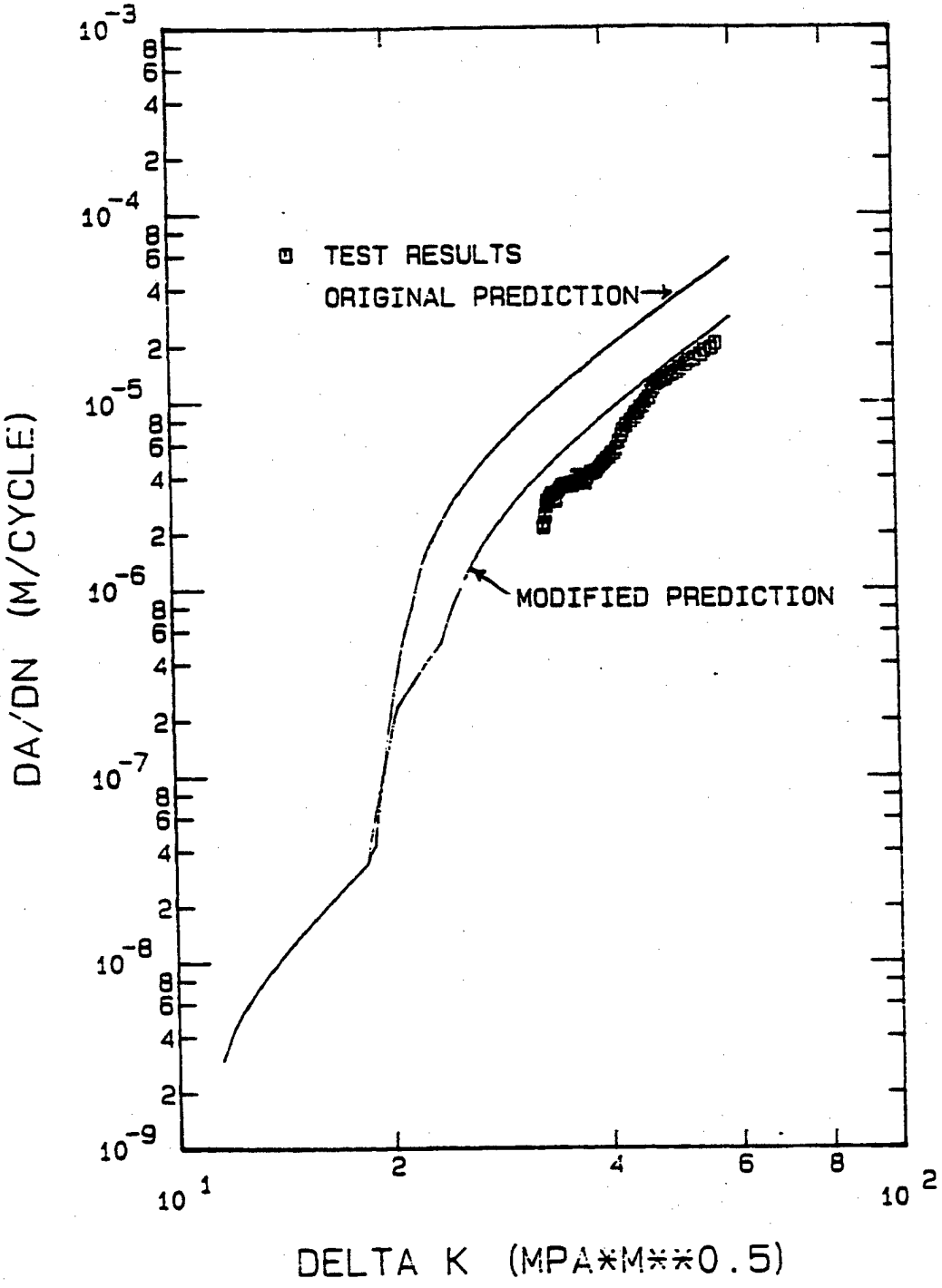

Figure 5.16: Predicted versus Actual TMF Crack Growth
315° Out-of-Phase, R=0.1

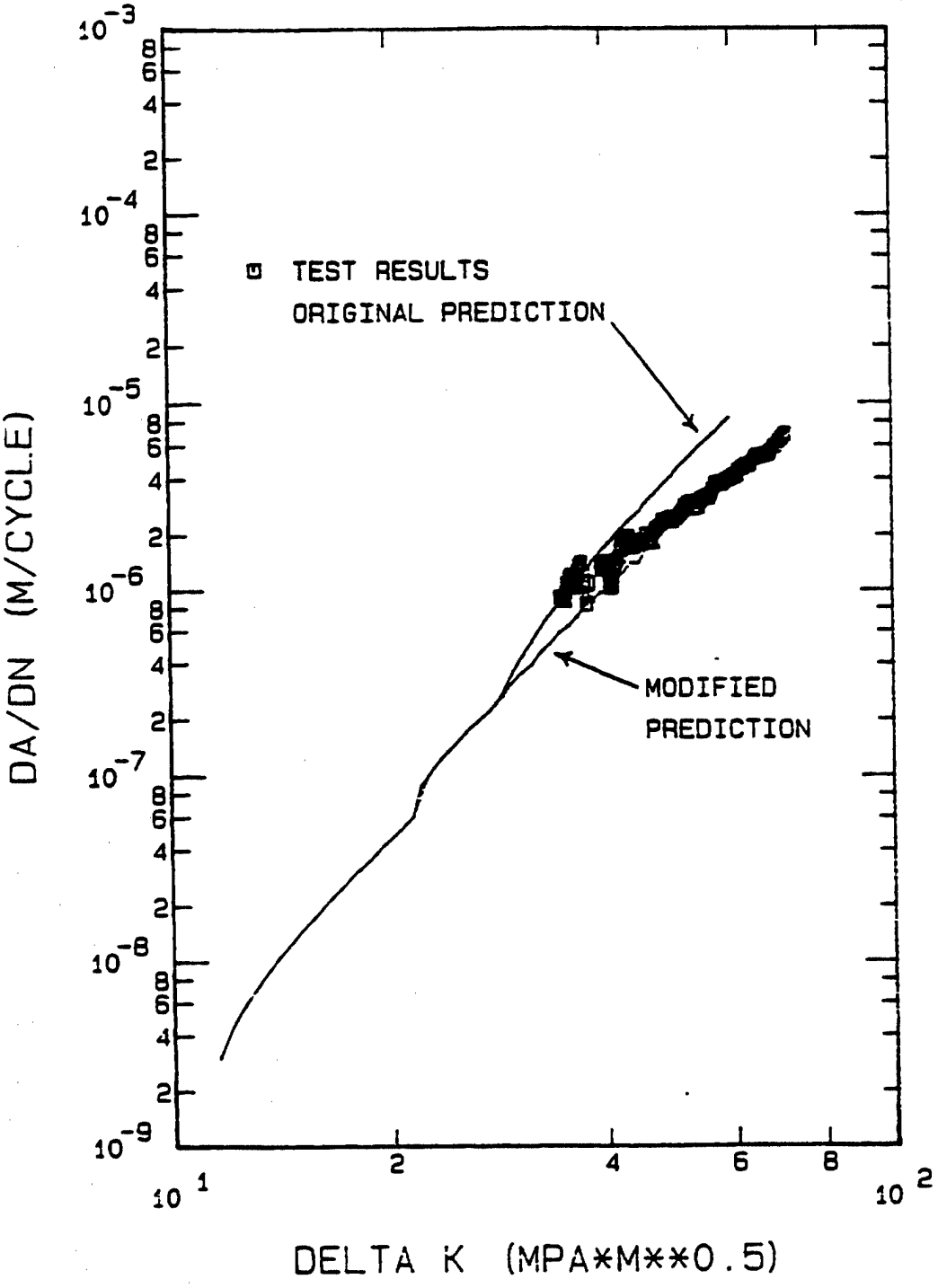

Figure 5.17: Predicted versus Actual TMF Crack Growth
225° Out-of-Phase, R=0.1

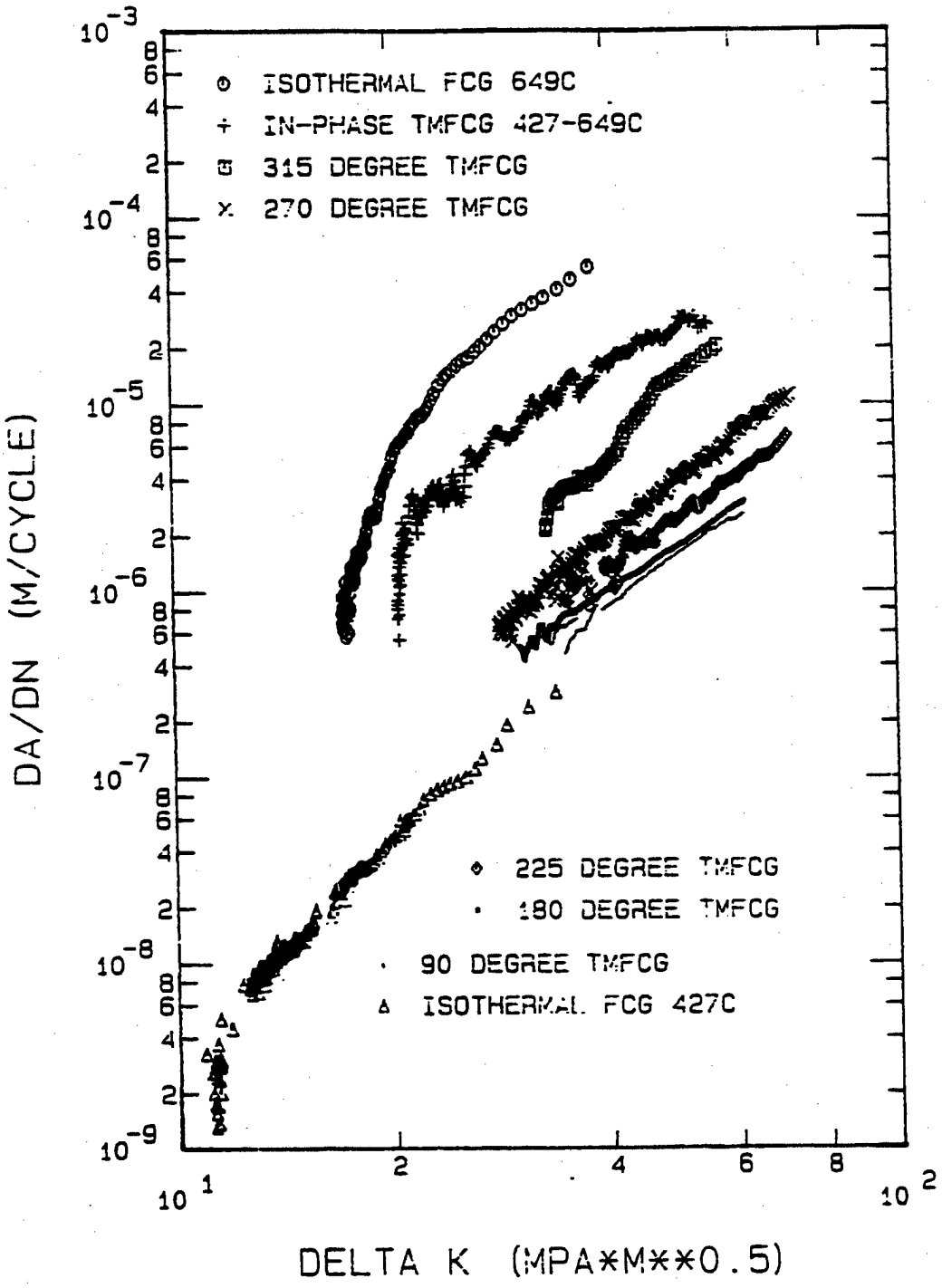

Figure 5.18: TMF Crack Growth at R=0.1

The TMF crack growth rates from this test were very close to the isothermal fatigue crack growth rates obtained at 427°C and R=0.1. This indicates that cycle-dependent damage dominates for this TMF test condition. The linear cumulative damage model prediction verifies this observation. The cycle-dependent damage term dominates the model prediction. The time-dependent damage term is very small because the integration of the sustained load crack growth rate is performed over a short period.

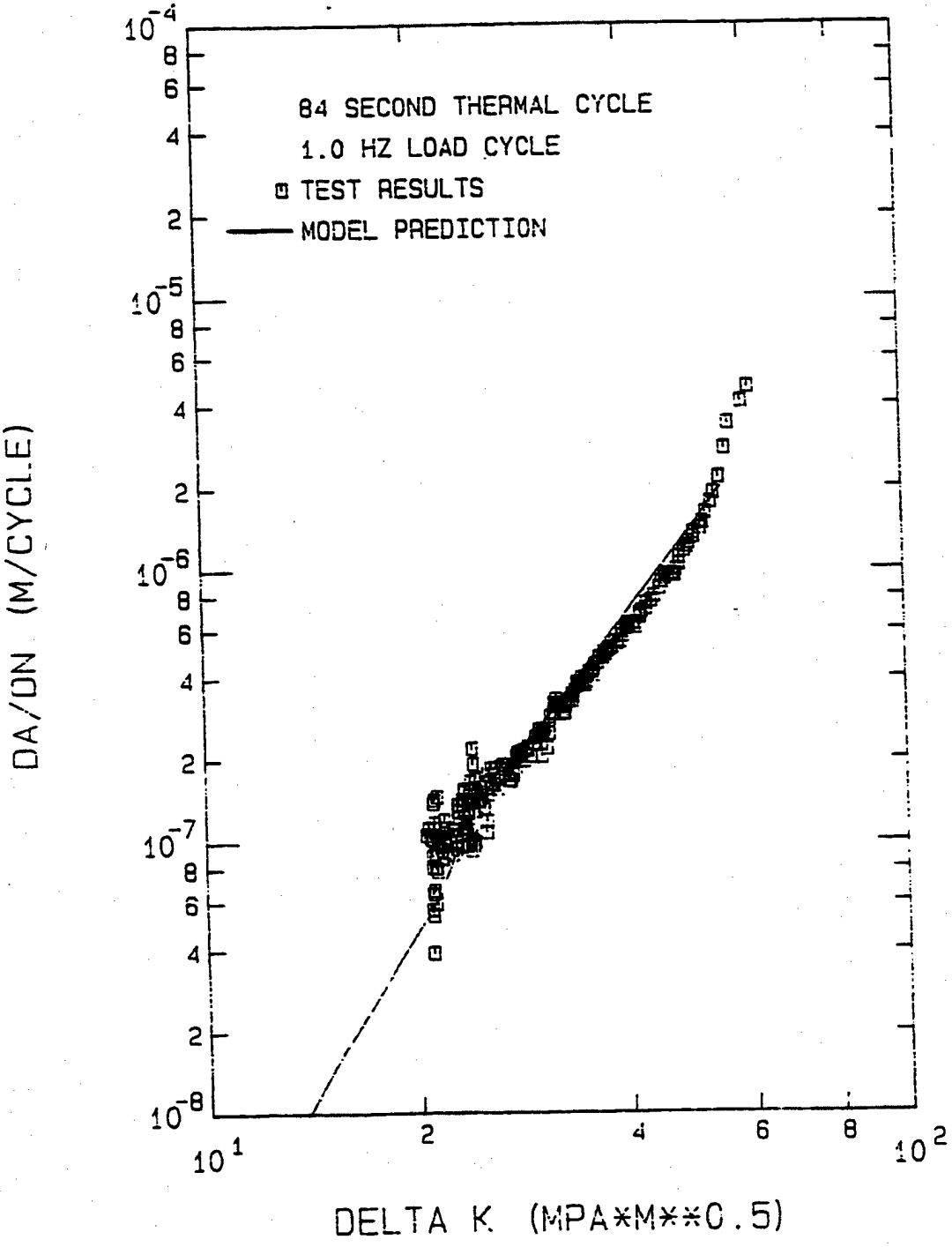

Figure 5.19: Predicted versus Actual TMF Crack Growth

VI. Conclusions and Recommendations

Two linear cumulative damage models were developed in this dissertation to predict crack growth rates in Inconel 718 under thermal-mechanical cycling. The two dominant mechanisms of elevated temperature crack growth in this material provide the basis of the models. Both models sum cycle-dependent, time-dependent, and mixed-mode damages to provide the total crack growth for a given thermal-mechanical cycle. Cycle-dependent damage is due to the first dominant mechanism, mechanical fatigue. The second dominant mechanism, environmental interaction, produces time dependent damage. Mixed-mode damage results from the interaction of the two dominant mechanisms. The models are based entirely on a minimal set of isothermal crack growth data. The cycle-dependent damage term for both models is found from a fatigue crack growth test conducted at a temperature where cycle-dependent damage is known to dominate (427°C). The mixed-mode damage term for both models is found by incrementally summing mixed-mode damage identified from isothermal tests over a thermal-mechanical cycle. The mixed-mode damage term did not significantly contribute to the crack growth rate predictions of either linear cumulative damage model.

The time dependent damage term in the original model was obtained by integrating the sustained-load crack-growth rate over the portion of the thermal-mechanical cycle in which the load is increasing. This calculation is identical to that used by Nicholas, et al. (30), to predict isothermal time-dependent crack growth rates. The original model predicted the TMF crack growth rates for in-phase (maximum temperature at maximum load), 90° out-of-phase (load leading temperature by 90°), and 180° out-of-phase (minimum temperature at maximum load) cycles reasonably well (within a factor of two). However, the model prediction for a 270° out-of-phase cycle was consistently higher than the

experimental data, with the error going from approximately a factor of two to four with increasing stress intensity range. This anomoly led to the development of a modified linear cumulative damage model.

The time-dependent damage term dominates the original model prediction for a 270° cycle because the temperature is high during the loading portion of the cycle. In the modified model, it is postulated that if the sustained load crack growth rate, da/dt, starts to decrease at some point in the loading portion of a cycle, there is no further contribution to time-dependent crack growth. Thus, the time-dependent damage term is calculated by integrating the sustained-load crack growth rate over the loading portion of the thermal-mechanical cycle when da/dt is an increasing function. The sustained load crack growth rate decreases during most of the loading portion of a 270° out-of-phase cycle. Therefore, the modified model prediction for the 270° out-of-phase cycle was significantly lower and closer to the experimental results than the original prediction.

The modified model predictions for the in-phase and 90° out-of-phase cycles were unchanged from the original model predictions because the da/dt always increases during the loading portion of these cycles. The sustained load crack growth rate decreases during most of the loading portion of a 180° out-of-phase cycle leading to a smaller time-dependent damage term in the modified model. However, the cycle-dependent damage term dominates both linear cumulative-damage model predictions for this cycle, so the original and modified predictions differ by very little. The modified model predicted the in-phase, 90° out-of-phase, 180° out-of-phase, and 270° out-of-phase TMF crack growth rates within a factor of two of the experimental results.

Two proof tests were conducted to evaluate the validity of the modified linear cumulative damage model and compare the original and modified modelling concepts. The temperature is high during the loading portion of the cycle for the 315° and 225° out-of-phase cycles, resulting in a significant time-dependent damage term for both models.

However, the sustained load crack growth rate decreases during much of the loading portion of both cycles, leading to a smaller time dependent term prediction for the modified model. In both proof tests, the modified model predictions are closer to the experimental results than the original model predictions.

The modified linear cumulative damage model crack growth rate predictions were within a factor of two of the experimental results for all ΔK values for all of the TMF cycles tested (0°, 90°, 180°, 225°, 270°, and 315° out-of-phase). Less accurate predictions may result for more complex thermal-mechanical cycles because the model does not account for crack closure, overload effects, crack growth retardation, and load/temperature synergism. The isothermal tests used to develop the model were conducted under constant maximum load conditions and no attempt was made to model TMF crack growth in the threshold region.

In-phase load and temperature cycling produced the most rapid TMF crack growth in Inconel 718, with the 315°, 270°, 225°, 180°, and 90° tests following in order. The 0° and 90° crack growth rates were separated by over a factor of ten at all ΔK values tested. The temperature as the cycle approaches its peak load has a major effect on the crack growth rate, with high temperatures causing rapid growth. The upper and lower bounds for TMF crack growth in Inconel 718 appear to be the isothermal fatigue crack growth rates at the maximum and minimum temperatures of the TMF cycle.

Symmetric triangular waveforms were used for all thermal and mechanical cycling during TMF testing. Other thermal-mechanical cycle types should be investigated for their effects upon TMF crack growth and linear cumulative-damage model predictions:

1. Determine the effect of hold times at different loads and temperatures.
2. Investigate different loading and unloading frequencies, as well as different heating and cooling rates.
3. Investigate different temperature limits.

4. Investigate other phase angle differences.

Other possible areas of future research include:

1. Examine the microstructure of the fracture surfaces of the TMF specimens to determine the relative roles of transgranular and intergranular fracture for each TMF cycle type.
2. Perform a decreasing load TMF crack growth test to obtain threshold data.
3. Perform a TMF crack growth test under the thermal-mechanical spectrum of a typical turbine disk location and compare the linear cumulative damage model crack growth prediction to the actual test results.
4. Perform TMF crack growth tests on different materials for which mechanical fatigue and environmental interaction are the dominant crack growth mechanisms to verify the applicability of the linear cumulative damage model developed in this study.

APPENDIX A

HEAT TREATING SCHEDULE AND ALLOY COMPOSITION

Test Specimen Heat Treatment

STEP 1: Anneal at 968°C (1775°F) for 1 hour, then cool to temperature.

STEP 2: Age harden at 718°C (1325°F) for 8 hours, then furnace cool to 621°C (1150°F) at 56°C/hour (100°F/hour).

STEP 3: Age harden at 621°C (1150°F) for 18 hours total aging time (i.e. STEP 2 + STEP 3 = 18 hours total).

STEP 4: Air cool to room temperature.

Composition, weight percent

0.04 C	51.14 Ni	1.00 Ti
0.19 Mn	17.96 Cr	0.52 Al
0.05 Si	3.12 Mo	0.02 Cu
0.005 S	5.19 Cb and Ta	0.003 B
0.005 P	Balance, Fe	0.43 Co

APPENDIX B

MODIFIED SIGMOIDAL EQUATION PROGRAMS

```
C
C       THIS PROGRAM USES THE MODIFIED SIGMOIDAL
C       EQUATION TO MODEL FATIGUE CRACK GROWTH RATE
C       DATA.
C
        PROGRAM FCG
        INTEGER NAME(7),I
        WRITE(5,1)
C
C       INPUT THE MSE PARAMETERS OF THE CURVE FIT.
C       DKSTAR IS THE DELTA-K VALUE OF THE LOWER
C       ASYMPTOTE (THRESHOLD STRESS INTENSITY RANGE).
C
 1      FORMAT(' INPUT DKSTAR IN MPA*M**0.5: ',$)
        READ(5,*)DKSTAR
        WRITE(5,2)
 2      FORMAT(' INPUT LOWER SHAPING COEFFICIENT Q: ',$)
        READ(5,*)Q
        WRITE(5,10)
C
C       DKI IS THE DELTA-K VALUE OF THE CURVE INFLECTION
C       POINT.
C
 10     FORMAT(' INPUT DKI IN MPA*M**0.5: ',$)
        READ(5,*)DKI
        WRITE(5,11)
C
C       DADNI IS THE CRACK GROWTH PER CYCLE AT THE
C       CURVE INFLECTION POINT.
C
 11     FORMAT(' INPUT DADNI IN M/CYCLE: ',$)
        READ(5,*)DADNI
        WRITE(5,12)
C
C       DADNIP IS THE SLOPE OF THE CURVE AT THE
C       INFLECTION POINT IN DECADES PER DECADE.
C
 12     FORMAT(' INPUT DADNIP (NO UNITS): ',$)
        READ(5,*)DADNIP
C
C       MAKE THE CURVE SYMMETRIC BY SETTING D
C       EQUAL TO MINUS Q.
C
        D=-Q
C
C       DKCRIT IS THE DELTA-K VALUE OF THE UPPER
C       ASYMPTOTE.
C
        DKCRIT=(DKI**2)/DKSTAR
        CONST=ALOG(DKI/DKSTAR)
```

```
      CONST1=ALOG(DKCRIT/DKI)
      B=ALOG(DADNI)-Q*ALOG(CONST)-D*ALOG(CONST1)
      P=DADNIP-Q/CONST+D/CONST1
      WRITE(5,3)B,P,Q,D,DKSTAR,DKCRIT
      WRITE(5,4)DKI,DADNI,DADNIP
C
C     SUBROUTINE NEWFIL OPENS A PLOT DATA FILE.
C
      CALL NEWFIL(NAME)
C
C     START CALCULATIONS JUST ABOVE THE LOWER
C     THRESHOLD DELTA-K VALUE.
C
      DK=DKSTAR+.00001
C
C     IF DELTA-K IS ABOVE 70 PER CENT OF THE
C     UPPER ASYMPTOTE, STOP CALCULATIONS.
C
 370  IF(DK.GE.(.7*DKCRIT)) GOTO 380
C
C     CALCULATE THE CRACK GROWTH RATE PER CYCLE
C     WITH FUNCTION SIGM.
C
      DADNFT=SIGM(DK,DKSTAR,DKCRIT,DKI,Q,D,P,B)
      WRITE(2,*)DK,DADNF
      IF(DK.LT.(DKSTAR+1.))THEN
C
C     INCREMENT DELTA-K BY 0.01 IN THE NEAR-
C     THRESHOLD REGION.
C
      DK=DK+.01
      GOTO 370
      ENDIF
C
C     INCREMENT DELTA-K BY 1.0 ELSEWHERE.
C
      DK=DK+1.
      GOTO 370
 380  CONTINUE
C
C     CLOSE THE DATA FILE.
C
      REWIND 2
      CLOSE(2)
C
C     WRITE THE NAME OF THE PLOT DATA FILE TO
C     THE SCREEN.
C
      WRITE(5,390)NAME
 390  FORMAT(/,' YOUR DATA IS UNDER ',7A2)
```

```
 3      FORMAT(//2X,'BPRIME=',F10.4,/2X,'P=',F10.4,/2X,
     *  'Q=',F10.4,/2X,'D=',F10.4,/2X,'DELTA K*=',F10.4,
     *  /2X,' DELTA KCRIT=',F10.4,//)
 4      FORMAT(//2X,'DELTA KI=',F10.4,/2X,'DADNI=',
     *  E15.5,/2X,'DADNIPRIME=',F10.4,//)
        END
C
C
C       SUBROUTINE NEWFIL OPENS A PLOT DATA FILE.
C
C
C
        SUBROUTINE NEWFIL(NAME)
        INTEGER NAME(7)
 500    FORMAT(7A2)
        WRITE(5,600)
 600    FORMAT(' WHAT SHOULD THE OUTPUT FILE BE CALLED?')
        READ(5,500)NAME
        OPEN(UNIT=2,NAME=NAME,TYPE='NEW')
        WRITE(2,700)
 700    FORMAT(' DELTA K, DA/DN [FITTED]')
        RETURN
        END
C
C
C       FUNCTION SIGM CALCULATES THE CRACK GROWTH PER
C       CYCLE USING THE MODIFIED SIGMOIDAL EQUQTION.
C
C
C
        FUNCTION SIGM(DK,DKSTAR,DKCRIT,DKI,Q,D,P,B)
        REAL DK,DKSTAR,DKCRIT,DKI,Q,D,P,B
        SIGM=EXP(B)*((DK/DKI)**P)*((ALOG(DK/DKSTAR))
     *  **Q)*((ALOG(DKCRIT/DK))**D)
        RETURN
        END
```

```
C
C
C       THIS PROGRAM USES THE MODIFIED SIGMOIDAL
C       EQUATION MODEL TO CREATE A SUSTAINED LOAD
C       CRACK GROWTH RATE VERSUS STRESS INTENSITY
C       FACTOR PLOT FILE.
C
C
        PROGRAM SLCG
        INTEGER NAME(7),I
        REAL KI,KSTAR,KCRIT
        WRITE(5,1)
C
C       INPUT THE THRESHOLD STRESS INTENSITY FACTOR,
C       KSTAR.
C
 1      FORMAT(' INPUT KSTAR IN MPA*M**0.5: ',$)
        READ(5,*)KSTAR
        WRITE(5,2)
 2      FORMAT(' INPUT LOWER SHAPING COEFFICIENT Q: ',$)
        READ(5,*)Q
        WRITE(5,10)
C
C       INPUT THE STRESS INTENSITY FACTOR AT THE CURVE
C       INFLECTION POINT, KI.
C
 10     FORMAT(' INPUT KI IN MPA*M**0.5: ',$)
        READ(5,*)KI
        WRITE(5,11)
C
C       INPUT THE CRACK GROWTH RATE AT THE CURVE
C       INFLECTION POINT, DADTI.
C
 11     FORMAT(' INPUT DADTI IN M/SEC: ',$)
        READ(5,*)DADTI
        WRITE(5,12)
C
C       INPUT THE CURVE SLOPE AT THE INFECTION
C       POINT IN DECADES PER DECADE, DADTIP.
C
 12     FORMAT(' INPUT DADTIP (NO UNITS): ',$)
        READ(5,*)DADTIP
C
C       THIS PROGRAM USES A SYMMETRIC MODIFIED
C       SIGMOIDAL CURVE. SET D EQUAL TO MINUS
C       Q TO MAKE THE CURVE SYMMETRIC.
C
        D=-Q
C
C       CALCULATE THE MSE MODEL CONSTANTS.
```

```
C
      KCRIT=(KI**2)/KSTAR
      CONST=ALOG(KI/KSTAR)
      CONST1=ALOG(KCRIT/KI)
      B=ALOG(DADTI)-Q*ALOG(CONST)-D*ALOG(CONST1)
      P=DADTIP-Q/CONST+D/CONST1
C
C     WRITE THE MSE MODEL CONSTANTS TO THE SCREEN.
C
      WRITE(5,3)B,P,Q,D,KSTAR,KCRIT
      WRITE(5,4)KI,DADTI,DADTIP
C
C     NEWFIL CREATES A FILE TO STORE THE
C     CALCULATED DATA.
C
      CALL NEWFIL(NAME)
C
C     START CALCULATIONS JUST ABOVE THE
C     THRESHOLD STRESS INTENSITY FACTOR.
C
      DK=KSTAR+.00001
  100 CONTINUE
C
C     IF THE STRESS INTENSITY FACTOR EXCEDES
C     A MAXIMUM VALUE OF 100, STOP CALCULATIONS.
C
      IF(DK.GE.100.) GOTO 380
C
C     FUNCTION SIGM CALCULATES THE SUSTAINED LOAD
C     CRACK GROWTH RATE USING THE MODIFIED
C     SIGMOIDAL EQUATION.
C
      DADTFT=SIGM(DK,KSTAR,KCRIT,KI,Q,D,P,B)
C
C     WRITE THE STRESS INTENSITY FACTOR AND THE
C     CRACK GROWTH RATE TO A PLOT FILE.
C
      WRITE(2,*)DK,DADTFT
C
C     INCREMENT THE STRESS INTENSITY FACTOR.
C
      DK=DK+.4
      GOTO 100
  380 CONTINUE
      REWIND 2
C
C             CLOSE THE DATA FILE.
C
      CLOSE(2)
C
```

```
C       WRITE THE NAME OF THE PLOT DATA FILE
C       TO THE SCREEN.
C
        WRITE(5,390)NAME
 390    FORMAT(/,' YOUR DATA IS UNDER ',7A2)
 3      FORMAT(//2X,'BPRIME=',F10.4,/2X,'P=',F10.4,/2X,
     *  'Q=',F10.4,/2X,'D=',F10.4,/2X,' K*=',F10.4,
     *  /2X,' KCRIT=',F10.4,//)
 4      FORMAT(//2X,' KI=',F10.4,/2X,'DADTI=',
     *  E15.5,/2X,'DADTIPRIME=',F10.4,//)
        END
C
C
C       SUBROUTINE NEWFIL OPENS A PLOT DATA FILE.
C
C
        SUBROUTINE NEWFIL(NAME)
        INTEGER NAME(7)
 500    FORMAT(7A2)
        WRITE(5,600)
 600    FORMAT(' WHAT SHOULD THE OUTPUT FILE BE CALLED?')
        READ(5,500)NAME
        OPEN(UNIT=2,NAME=NAME,TYPE='NEW')
        WRITE(2,700)
 700    FORMAT(' K, DA/DT [FITTED]')
        RETURN
        END
C
C
C       FUNCTION SIGM USES THE MODIFIED SIGMOIDAL
C       EQUATION TO CALCULATE THE CRACK GROWTH RATE
C       FOR A GIVEN STRESS INTENSITY FACTOR, DK.
C
C
        FUNCTION SIGM(DK,KSTAR,KCRIT,KI,Q,D,P,B)
        REAL DK,KSTAR,KCRIT,KI,Q,D,P,B
        SIGM=EXP(B)*((DK/KI)**P)*((ALOG(DK/KSTAR))
     *  **Q)*((ALOG(KCRIT/DK))**D)
        RETURN
        END
```

```
C
C       THIS PROGRAM CALCULATES THE CYCLE-DEPENDENT,
C       TIME-DEPENDENT, AND MIXED-MODE CRACK GROWTH
C       DAMAGES IN INCONEL 718 FOR A GIVEN TEMPERATURE
C       AND LOAD RATIO. ALL CALCULATIONS ARE BASED ON
C       MODIFIED SIGMOIDAL EQUATION (MSE) FITS OF TEST
C       DATA.
C
        PROGRAM MM
        INTEGER NAME(7)
        REAL K,KI,KSTAR,KCRIT,KMAX
        WRITE(5,1)
C
C       INPUT THE TEST TEMPERATURE T AND LOAD RATIO R.
C
 1      FORMAT(' THIS PROGRAM FINDS THE MIXED-MODE',
     *  ' CONTRIBUTION TO TOTAL CRACK GROWTH PER CYCLE'/
     *  ' FOR A GIVEN TEST TEMPERATURE AND LOAD RATIO.',
     *  ' INPUT THE TEST TEMPERATURE IN'/
     *  ' DEGREES F: ',$)
        READ(5,*)T
        WRITE(5,2)
 2      FORMAT(' INPUT THE TEST LOAD RATIO R: ',$)
        READ(5,*)R
        WRITE(5,3)
C
C       IN A LINEAR CUMULATIVE DAMAGE MODEL, THE TOTAL
C       OBSERVED CRACK GROWTH RATE OF AN ELEVATED
C       TEMPERATURE FATIGUE CRACK GROWTH TEST CONSISTS
C       OF THE SUM OF CYCLE-DEPENDENT, TIME-DEPENDENT,
C       AND MIXED-MODE DAMAGE TERMS.
C
 3      FORMAT(' INPUT THE MSE CURVE FIT PARAMETERS OF',
     *  ' THE OBSERVED TEST DATA.'/
     *  ' USE THE SI SYSTEM OF UNITS.'/
     *  ' INPUT DELTA K* : ',$)
C
C       DKSTRT IS THE THRESHOLD STRESS INTENSITY RANGE
C       VALUE OF THE TOTAL CRACK GROWTH RATE CURVE.
C
        READ(5,*)DKSTRT
        WRITE(5,4)
 4      FORMAT(' INPUT DELTA KI: ',$)
C
C       DKIT IS THE STRESS INTENSITY RANGE VALUE OF THE
C       INFLECTION POINT OF THE TOTAL CRACK GROWTH RATE
C       CURVE.
C
        READ(5,*)DKIT
        WRITE(5,5)
```

```
 5      FORMAT(' INPUT DADNI: ',$)
C
C       DADNIT IS THE CRACK GROWTH RATE VALUE OF THE
C       INFLECTION POINT OF THE TOTAL CRACK GROWTH RATE
C       CURVE.
C
        READ(5,*)DADNIT
        WRITE(5,6)
 6      FORMAT(' INPUT DADNI PRIME: ',$)
C
C       DANIPT IS THE SLOPE OF THE TOTAL CRACK GROWTH
C       RATE CURVE AT THE INFLECTION POINT.
C
        READ(5,*)DANIPT
        WRITE(5,61)
 61     FORMAT(' INPUT THE SHAPING COEFFICIENT Q: ',$)
C
C       QT IS THE SHAPING COEFFICIENT OF THE TOTAL
C       CRACK GROWTH RATE CURVE.
C
        READ(5,*)QT
        WRITE(5,7)
C
C       THE CYCLE-DEPENDENT CRACK GROWTH DAMAGE-TERM
C       COMES FROM A LOW TEMPERATURE HIGH FREQUENCY
C       TEST CONDUCTED AT THE SAME LOAD RATIO AS THE
C       ELEVATED TEMPERATURE TEST. INPUT THE MSE PARAMETERS
C       OF THE LOW TEMPERATURE TEST CURVE FIT.
C
 7      FORMAT(' INPUT THE MSE CURVE FIT PARAMETERS OF',
     *  ' THE CYCLE DEPENDENT TERM TEST DATA.'/
     *  ' INPUT DELTA K* : ',$)
C
C       THE MSE PARAMETERS ASSOCIATED WITH THE CYCLE-
C       DEPENDENT TERM HAVE A 'C' SUFFIX.
C
        READ(5,*)DKSTRC
        WRITE(5,4)
        READ(5,*)DKIC
        WRITE(5,5)
        READ(5,*)DADNIC
        WRITE(5,6)
        READ(5,*)DANIPC
        WRITE(5,61)
        READ(5,*)QC
        WRITE(5,10)
C
C       THE TIME-DEPENDENT DAMAGE TERM IS FOUND BY INTEGRATING
C       THE SUSTAINED LOAD CRACK GROWTH RATE AT THE ELEVATED
        TEST TEMPERATURE OVER THE LOADING PORTION OF A LOAD
```

```
C       CYCLE. THE INTEGRATION IS PERFORMED NUMERICALLY USING
C       SIMPSON'S RULE. THE NUMBER OF INTEGRATION STEPS IS XN.
C
 10     FORMAT(' INPUT THE NUMBER OF TIME INTEGRATION STEPS'/
     *  ' FOR SIMPSONS RULE INTEGRATION: ',$)
        READ(5,*)XN
        CALL NEWFIL(NAME)
C
C       NEWFIL OPENS A FILE FOR PLOT DATA.
C
C
C       START CALCULATIONS AT A DELTA-K (DK) SLIGHTLY
C       LOWER THAN THE ELEVATED TEMPERATURE TEST THRESHOLD.
C
        DK=DKSTRT-4.99
C
C       DADNT IS THE ELEVATED TEMPERATURE TEST TOTAL CRACK
C       GROWTH RATE. DADNC IS THE CYCLE-DEPENDENT TERM
C       CRACK GROWTH RATE. DADN IS A FUNCTION WHICH
C       USES THE MSE MODEL TO CALCULATE THE CRACK
C       GROWTH RATE FOR A GIVEN DELTA-K AND SET OF MSE
C       PARAMETERS.
C
 100    DADNT=DADN(DK,DKSTRT,DKIT,DADNIT,DANIPT,QT)
        DADNC=DADN(DK,DKSTRC,DKIC,DADNIC,DANIPC,QC)
C
C       IF DELTA K EXCEDES THE EXPERIMENTAL DATA MAX
C       VALUE OF SIXTY, STOP CALCULATIONS.
C
        IF(DK.GT.60.)THEN
        GOTO 200
        ENDIF
C
C       DADNTD IS A FUNCTION WHICH CALCULATES THE TIME-
C       DEPENDENT DAMAGE BY INTEGRATING THE SUSTAINED
C       LOAD CRACK GROWTH OVER THE LOADING PORTION OF THE
C       LOAD CYCLE. IF THE TIME DEPENDENT CRACK GROWTH IS
C       EQUAL TO A FLAG VALUE OF TEN, STOP CALCULATIONS
C       AND WRITE THE DELTA-K VALUE ON THE SCREEN.
C
        IF(DADNTD(DK,R,T,XN).EQ.10.)THEN
        WRITE(5,9)DK
        GOTO 200
        ENDIF
C
C       SUM THE CYCLE-DEPENDENT AND TIME-DEPENDENT
C       DAMAGE TERMS.
C
        SUM=DADNC+DADNTD(DK,R,T,XN)
```

```
C
C       FUNCTION DADN USES THE MSE MODEL TO CALCULATE
C       CRACK GROWTH IN METERS PER CYCLE FOR A GIVEN
C       DELTA-K AND SET OF MSE PARAMETERS.
C
C
      FUNCTION DADN(DK,DKSTAR,DKI,DADNI,DADNIP,Q)
C
C       SET D=-Q TO MAKE THE MSE CURVE SYMMETRIC ABOUT
C       ITS INFLECTION POINT.
C
      D=-Q
      DKCRIT=(DKI**2)/DKSTAR
C
C       IF DELTA-K IS LESS THAN THE THRESHOLD VALUE,
C       THERE IS NO CRACK GROWTH.
C
      IF(DK.LE.DKSTAR)THEN
      DADN=0.
      GOTO 100
      ENDIF
C
C       CALCULATE THE REQUIRED CONSTANTS FOR THE
C       MSE MODEL.
C
      CONST=ALOG(DKI/DKSTAR)
      CONST1=ALOG(DKCRIT/DKI)
      B=ALOG(DADNI)-Q*ALOG(CONST)-D*ALOG(CONST1)
      P=DADNIP-Q/CONST+D/CONST1
C
C       APPLY THE MODIFIED SIGMOIDAL EQUATION.
C
      DADN=EXP(B)*((DK/DKI)**P)*((ALOG(DK/DKSTAR))
     *  **Q)*((ALOG(DKCRIT/DK))**D)
  100 RETURN
      END
C
C
C       FUNCTION DADNTD CALCULATES THE TIME-DEPENDENT
C       CRACK GROWTH BY INTEGRATING SUSTAINED LOAD CRACK
C       GROWTH OVER THE LOADING PORTION OF THE LOAD
C       CYCLE. INPUT PARAMETERS ARE DELTA-K (DK), LOAD
C       RATIO (R), TEMPERATURE (T), AND NUMBER OF
C       INCREMENTS FOR SIMPSON'S RULE NUMERICAL
C       INTEGRATION (XN).
C
C
      FUNCTION DADNTD(DK,R,T,XN)
      REAL K,KI,KSTAR,KCRIT,KMAX
C
```

```
C       THE MIXED-MODE DAMAGE TERM IS THE TOTAL CRACK GROWTH
C       MINUS THE TIME-DEPENDENT AND CYCLE-DEPENDENT DAMAGE
C       TERMS.
C
        DADNMM=DADNT-SUM
C
C       WRITE DELTA-K, TOTAL CRACK GROWTH, CYCLE-DEPENDENT
C       CRACK GROWTH, TIME-DEPENDENT CRACK GROWTH, THE SUM
C       OF TIME-DEPENDENT AND CYCLE-DEPENDENT DAMAGES, AND
C       MIXED-MODE CRACK GROWTH TO THE PLOT DATA FILE.
C
        WRITE(2,11)DK,DADNT,DADNC,DADNTD(DK,R,T,XN),SUM,DADNMM
 11     FORMAT(1X,F6.3,5(1X,E12.5))
C
C       INCREMENT DELTA-K.
C
        DK=DK+.25
        GOTO 100
 200    CONTINUE
C
C       CLOSE THE DATA FILE.
C
        REWIND 2
        CLOSE (2)
C
C       WRITE THE NAME OF THE DATA FILE TO THE SCREEN.
C
        WRITE(5,8)NAME
  8     FORMAT(/,' YOUR DATA IS UNDER ',7A2)
  9     FORMAT(' OUTSIDE EXPERIMENTAL DATA RANGE AT',
     *  ' DELTA K = ',F6.2,/,' STOP COMPUTATIONS.'/)
        END
C
C
C       SUBROUTINE NEWFIL OPENS A PLOT DATA FILE.
C
C
        SUBROUTINE NEWFIL(NAME)
        INTEGER NAME(7)
 300    FORMAT(7A2)
        WRITE(5,600)
 600    FORMAT(' WHAT SHOULD THE OUTPUT FILE BE',
     *    ' CALLED?')
        READ(5,300)NAME
        OPEN(UNIT=2,NAME=NAME,TYPE='NEW')
        WRITE(2,700)
 700    FORMAT(' DELTA-K, TOTAL, CD, TD, CD+TD, MM ')
        RETURN
        END
```

```
C       H IS THE TIME STEP SIZE IN SECONDS. SINCE
C       A SYMMETRIC TRIANGULAR 0.01 HZ LOAD CYCLE
C       IS USED, THE LOADING PORTION OF THE CYCLE
C       IS FIFTY SECONDS LONG.
C
        H=50./XN
C
C       ESTABLISH THE MSE PARAMETERS OF THE SUSTAINED
C       LOAD CRACK GROWTH CURVE FOR THE TEST
C       TEMPERATURE (1000F, 1100F, OR 1200F)
C
        Q=0.4
        D=-Q
C
C       KMAX IS THE MAXIMUM STRESS INTENSITY FACTOR
C       REACHED DURING THE LOAD CYCLE.
C
        KMAX=DK/(1.-R)
        IF(T.EQ.1000.)THEN
        KSTAR=24.
        KI=76.
        DADTI=6.5E-8
        DADTIP=1.2
        GOTO 300
        ENDIF
        IF(T.EQ.1100.)THEN
        KSTAR=21.
        KI=73.
        DADTI=8.E-7
        DADTIP=2.
        GOTO 300
        ENDIF
        IF(T.EQ.1200.)THEN
        KSTAR=19.
        KI=60.
        DADTI=1.1E-5
        DADTIP=3.
        GOTO 300
        ENDIF
  200   CONTINUE

C       IF THE MAXIMUM STRESS INTENSITY FACTOR
C       REACHED DURING THE LOAD CYCLE IS LESS
C       THAN THE THRESHOLD STRESS INTENSITY
C       FACTOR FOR SUSTAINED LOAD CRACK GROWTH,
C       NO TIME-DEPENDENT CRACK GROWTH OCCURS.
C
        IF(KMAX.LE.KSTAR)THEN
        DADNTD=0.
        GOTO 310
```

```
      ENDIF
C
C     INITIATE THE SIMPSON'S RULE NUMERICAL
C     INTEGRATION. SO IS THE SUM OF THE FIRST
C     AND LAST INTEGRATION TERMS, S1 IS THE SUM OF
C     ODD INTEGRATION TERMS, AND S2 IS THE SUM OF
C     EVEN INTEGRATION TERMS.
C
 310  I=0
      S0=0.
      S1=0.
      S2=0.
C
C     START AT THE MINIMUM STRESS INTENSITY
C     FACTOR OF THE CYCLE.
C
      K=R*KMAX
C
C     CALCULATE THE APPROPRIATE MSE CONSTANTS.
C
      KCRIT=(KI**2)/KSTAR
      CONST=ALOG(KI/KSTAR)
      CONST1=ALOG(KCRIT/KI)
      B=ALOG(DADTI)-Q*ALOG(CONST)-D*ALOG(CONST1)
      P=DADTIP-Q/CONST+D/CONST1
C
C     IF THE STRESS INTENSITY FACTOR IS GREATER
C     THAN THE EXPERIMENTAL DATA LIMIT OF KI,
C     SET THE TIME-DEPENDENT CRACK GROWTH EQUAL TO
C     A FLAG VALUE OF 10.
C
 315  IF(K.GE.KI)THEN
      DADNTD=10.
      GOTO 340
      ENDIF
C
C     IF THE STRESS INTENSITY FACTOR IS LESS THAN
C     THE THRESHOLD VALUE FOR SUSTAINED LOAD CRACK GROWTH,
C     THERE IS NO SUSTAINED LOAD CRACK GROWTH.
C
      IF(K.LE.KSTAR)DADT=0.
C
C     CALCULATE THE SUSTAINED LOAD CRACK GROWTH RATE DADT
C     USING THE MODIFIED SIGMOIDAL EQUATION.
C
      IF(K.GT.KSTAR)DADT=EXP(B)*((K/KI)**P)*((ALOG(K/KSTAR))
     *  **Q)*((ALOG(KCRIT/K))**D)
C
```

```
C       SUM THE FIRST AND LAST INTEGRATION TERMS TO GIVE S0.
C
        IF(I.EQ.0)THEN
        S0=S0+DADT
        GOTO 320
        ENDIF
        IF(I.EQ.IFIX(XN))THEN
        S0=S0+DADT
C
C       STOP CALCULATIONS IF THE LAST INTEGRATION TERM HAS
C       BEEN REACHED.
C
        GOTO 330
        ENDIF
C
C       SUM EVEN TERMS AS S2 AND ODD TERMS AS S1.
C
        IF(MOD(I,2).EQ.0)THEN
        S2=S2+DADT
        GOTO 320
        ENDIF
        S1=S1+DADT
C
C       INCREMENT TO THE NEXT INTEGRATION TERM.
C
 320    I=I+1
C
C       INCREMENT THE STRESS INTENSITY FACTOR.
C
        K=K+DK/XN
        GOTO 315
C
C       PERFORM THE INTEGRATION OF SUSTAINED LOAD
C       CRACK GROWTH OVER THE LOADING PORTION OF THE
C       CYCLE USING SIMPSON'S RULE.
C
 330    DADNTD=(H/3.)*(S0+4.*S1+2.*S2)
 340    CONTINUE
        RETURN
        END
```

APPENDIX C

LINEAR CUMULATIVE DAMAGE MODEL PROGRAM

```
C
C
C  THIS PROGRAM PREDICTS THE THERMAL-MECHANICAL FATIGUE
C  CRACK GROWTH IN INCONEL 718 USING A LINEAR CUMULATIVE
C  DAMAGE MODEL. THE ELASTIC STRESS INTENSITY FACTOR, K,
C  IS USED AS THE CRACK GROWTH CORRELATION PARAMETER. THE
C  LOAD AND THERMAL WAVEFORMS MUST BE SYMMETRIC, TRIANGULAR,
C  AND OF EQUAL FREQUENCIES. THE MINIMUM TEMPERATURE OF THE
C  CYCLE MAY BE NO LESS THAN 800 DEGREES F AND THE MAXIMUM
C  TEMPERATURE MAY BE NO GREATER THAN 1200 DEGREES F. THE
C  MAXIMUM TEMPERATURE MAY FOLLOW THE MAXIMUM LOAD BY A
C  PHASE ANGLE OF ANY MULTIPLE OF 45 DEGREES.
C
C
      PROGRAM TMFCG
      INTEGER NAME(7)
      REAL KMAX,K
      WRITE(5,1)
    1 FORMAT(' THIS PROGRAM CALCULATES THE',
     *  ' TOTAL CRACK GROWTH OVER A GIVEN TRIANGULAR'/
     *  ' THERMAL-MECHANICAL CYCLE. INPUT THE PHASE',
     *  ' DIFFERENCE IN DEGREES BETWEEN THE'/
     *  ' MAXIMUM LOAD AND MAXIMUM TEMPERATURE',
     *  ' ( MULTIPLE OF 45 ): ',$)
C
C     READ ALL INPUT PARAMETERS FROM THE SCREEN.
C
      READ(5,*)PA
      WRITE(5,2)
    2 FORMAT(' INPUT THE LOAD RATIO R: ',$)
      READ(5,*)RT
C
C     RT IS THE LOAD RATIO OF THE MECHANICAL CYCLE
C     ( MINIMUM LOAD DIVIDED BY THE MAXIMUM LOAD ).
C
      WRITE(5,3)
    3 FORMAT(' INPUT THE TMF CYCLE FREQUENCY IN HZ: ',$)
      READ(5,*)FREQ
      WRITE(5,4)
    4 FORMAT(' INPUT THE MINIMUM TEMPERATURE OF THE',
     *  ' TMF CYCLE IN DEGREES F: ',$)
      READ(5,*)TMIN
      WRITE(5,5)
    5 FORMAT(' INPUT THE MAXIMUM TEMPERATURE OF THE',
     *  ' TMF CYCLE IN DEGREES F: ',$)
      READ(5,*)TMAX
      HALFPD=1./(2.*FREQ)
C
C     HALFPD IS THE PERIOD OF THE UPLOADING PORTION OF
C     THE TMF CYCLE IN SECONDS.
```

```
C
      WRITE(5,6)RT,FREQ,TMIN,TMAX,HALFPD,PA
 6    FORMAT(/' TMF CYCLE PARAMETERS:',/2X,
     *  ' LOAD RATIO = ',F10.4,/2X,' FREQUENCY = ',
     *  F10.4,' HZ',/2X,' MINIMUM CYCLE TEMPERATURE = ',
     *  F10.2,' F',/2X,' MAXIMUM CYCLE TEMPERATURE = ',
     *  F10.2,' F',/2X,' HALF PERIOD OF CYCLE = ',F10.4,
     *  ' SEC.',/2X,' PHASE ANGLE DIFFERENCE BETWEEN',
     *  ' MAX LOAD AND MAX TEMPERATURE = ',F6.2,
     *  ' DEGREES.'/)
      WRITE(5,7)
 7    FORMAT(' INPUT THE NUMBER OF TIME INTEGRATION',
     *  ' STEPS OVER THE CYCLE'/' HALF PERIOD (LOADING',
     *  ' PORTION OF THE CYCLE). SINCE SIMPSONS RULE'/
     *  ' WILL BE USED, THE NUMBER MUST BE EVEN: ',$)
      READ(5,*)XN
C
C     IN A LINEAR CUMULATIVE DAMAGE MODEL, THE TOTAL
C     CRACK GROWTH OVER A THERMAL-MECHANICAL CYCLE
C     CONSISTS OF THE SUM OF CYCLE-DEPENDENT, TIME-
C     DEPENDENT, AND MIXED-MODE DAMAGE TERMS. TO FIND
C     THE TIME-DEPENDENT DAMAGE, THE SUSTAINED LOAD CRACK
C     GROWTH RATE, DA/DT, IS INTEGRATED OVER THE UPLOADING
C     PORTION OF THE THERMAL-MECHANICAL CYCLE. THE NUMBER
C     OF INTEGRATION STEPS USED WITH SIMPSON'S RULE IS XN.
C
      H=HALFPD/XN
C
C     H IS THE TIME STEP SIZE IN SECONDS.
C
      WRITE(5,8)XN,H
 8    FORMAT(' YOU SELECTED ',F8.2,' STEPS GIVING',
     *  ' A TIME STEP SIZE OF ',F10.6,' SECONDS.'/)
      CALL NEWFIL(NAME)
C
C     SUBROUTINE NEWFIL OPENS A DATA FILE.
C
      DKSTRC=10.**(1.041393+1.031217*ALOG10((1.-RT)/.9))
C
C     INITIALIZE DELTA K FOR ALL CALCULATIONS. DKSTRC
C     IS THE THRESHOLD DELTA K FOR THE CYCLE-DEPENDENT
C     DAMAGE TERM USING THE MODIFIED SIGMOIDAL EQUATION
C     ( MSE ) MODEL. START CALCULATIONS AT DKSTRC PLUS
C     0.001.
C
      DK=DKSTRC+.001
100   CONTINUE
C
C     X IS THE CYCLE-DEPENDENT DAMAGE TERM.
C     Y IS THE TIME-DEPENDENT DAMAGE TERM.
```

```
C       Z IS THE MIXED-MODE DAMAGE TERM.
C       FUNCTIONS DADN, DADNTD, AND DADNMM CALCULATE
C       X, Y, AND Z USING THE MSE MODEL. THE FUNCTIONS
C       ARE DESCRIBED AT THE END OF THIS PROGRAM.
C
        X=DADN(DK,RT)
        Y=DADNTD(DK,RT,TMIN,TMAX,PA,FREQ,XN)
        Z=DADNMM(DK,RT,TMIN,TMAX,PA,XN)
C
C       IF THE CYCLE-DEPENDENT OR TIME-DEPENDENT
C       DAMAGE TERMS COME FROM OUTSIDE THE EXPERIMENTAL
C       DATA RANGE AS INDICATED BY A FLAG VALUE OF 10,
C       STOP ALL CALCULATIONS.
C
        IF(X.EQ.10..OR.Y.EQ.10.)THEN
        WRITE(5,9)DK
        GOTO 200
        ENDIF
 9      FORMAT(' OUTSIDE EXPERIMENTAL DATA RANGE AT DELTA K',
     *  ' = ',F6.2/,' STOP CALCULATIONS.'/)
C
C       THE TOTAL CRACK GROWTH IS THE SUM OF THE CYCLE-
C       DEPENDENT, TIME-DEPENDENT, AND MIXED-MODE DAMAGE.
C
        DADNT=X+Y+Z
C
C       STORE THE DATA IN THE DATA FILE.
C
        WRITE(2,*)DK,DADNT,X,Y,Z
C
C       INCREMENT DELTA K.
C
        DK=DK+.5
        GOTO 100
 200    CONTINUE
C
C       CLOSE THE DATA FILE.
C
        REWIND 2
        CLOSE (2)
C
C       WRITE THE NAME OF THE DATA FILE TO THE SCREEN.
C
        WRITE(5,10)NAME
 10     FORMAT(' YOUR DATA IS UNDER ',7A2)
        END
C
C
C       THIS SUBROUTINE OPENS A
C       DATA FILE.
```

```
C
C
      SUBROUTINE NEWFIL(NAME)
      INTEGER NAME(7)
 1    FORMAT(7A2)
 2    FORMAT(' WHAT SHOULD THE OUTPUT FILE BE CALLED?')
 3    FORMAT(' DELTA-K, DADNT, DADNC, DADNTD, DADNMM')
      WRITE(5,2)
      READ(5,1)NAME
      OPEN(UNIT=2,NAME=NAME,TYPE='NEW')
      WRITE(2,3)
      RETURN
      END
C
C
C     FUNCTION DADN CALCULATES THE CYCLE-DEPENDENT DAMAGE
C     TERM FOR A GIVEN DELTA K ( DK ) AND TEST LOAD RATIO
C     ( RT ) USING THE MSE MODEL. THE MSE PARAMETERS WERE
C     BASED ON HIGH FREQUENCY ( 10 HZ ) LOW TEMPERATURE
C     ( 800F ) TESTS.
C
C
      FUNCTION DADN(DK,RT)
C
C     Q, D, DKSTAR, DKI, DADNI, DADNIP, AND DKCRIT ARE
C     THE MSE PARAMETERS. Q IS A SHAPE PARAMETER FOR THE
C     LOWER PORTION OF THE DA/DN VERSUS DELTA K CURVE.
C
      Q=0.4
C
C     FOR A SYMMETRIC MODIFIED SIGMOIDAL EQUATION CURVE,
C     D IS EQUAL TO MINUS Q.
C
      D=-Q
C
C     DKSTAR IS THE LOWER DELTA K ASYMPTOTE OF THE CURVE
C     ( THRESHOLD DELTA K FOR CRACK GROWTH ). THE UNITS
C     ARE MPA*M**0.5 .
C
      DKSTAR=10.**(1.041393+1.031217*ALOG10((1.-RT)/.9))
C
C     DKI IS THE DELTA K VALUE AT THE CURVE INFLECTION
C     POINT ( MPA*M**0.5 ).
C
      DKI=10.**(1.60206+.60681*ALOG10((1.-RT)/.9))
C
C     DADNI IS THE CRACK GROWTH PER CYCLE AT THE CURVE
C     INFLECTION POINT ( M/CYCLE ).
C
      DADNI=10.**(-6.259637+.768961*ALOG10((1.-RT)/.9))
```

```
C
C       DADNIP IS THE SLOPE OF THE CURVE AT THE INFLECTION
C       POINT ( NO UNITS ).
C
        DADNIP=3.5+1.958691*ALOG10((1.-RT)/.9)
C
C       DKCRIT IS THE UPPER ASYMPTOTE OF THE CURVE
C       ( MPA*M**0.5 ).
C
        DKCRIT=(DKI**2)/DKSTAR
C
C       IF DELTA K IS LESS THAN THE THRESHOLD VALUE,
C       THERE IS NO CRACK GROWTH.
C
        IF(DK.LE.DKSTAR)THEN
        DADN=0.
        GOTO 100
        ENDIF
C
C       IF DELTA K EXCEEDS THE EXPERIMENTAL DATA RANGE,
C       SET THE CRACK GROWTH EQUAL TO A FLAG VALUE OF
C       TEN. WHEN THIS VALUE IS DETECTED IN THE MAIN
C       PROGRAM, ALL CALCULATIONS WILL STOP.
C
        IF(DK.GE.60.)THEN
        DADN=10.
        GOTO 100
        ENDIF
C
C       CONST, CONST1, B, AND P ARE CONSTANTS USED IN
C       THE MODIFIED SIGMOIDAL EQUATION MODEL.
C
        CONST=ALOG(DKI/DKSTAR)
        CONST1=ALOG(DKCRIT/DKI)
        B=ALOG(DADNI)-Q*ALOG(CONST)-D*ALOG(CONST1)
        P=DADNIP-Q/CONST+D/CONST1
C
C       DADN IS THE CRACK GROWTH PER CYCLE FOR A GIVEN
C       STRESS RATIO AND DELTA-K.
C
        DADN=EXP(B)*((DK/DKI)**P)*((ALOG(DK/DKSTAR))
     *  **Q)*((ALOG(DKCRIT/DK))**D)
  100   CONTINUE
        RETURN
        END
C
C
C       FUNCTION DADNTD CALCULATES THE TIME-DEPENDENT
C       DAMAGE TERM FOR A GIVEN DELTA-K (DK), TEST LOAD
C       RATIO (RT), MINIMUM CYCLE TEMPERATURE (TMIN),
```

```
C     MAXIMUM CYCLE TEMPERATURE (TMAX), PHASE ANGLE
C     BETWEEN MAXIMUM LOAD AND MAXIMUM TEMPERATURE
C     (PA), TEST FREQUENCY (FREQ), AND NUMBER OF INTEGRATION
C     STEPS (XN). THE FUNCTION INTEGRATES SUSTAINED LOAD
C     CRACK GROWTH (DA/DT) OVER THE LOADING PORTION OF THE
C     THERMAL MECHANICAL CYCLE USING SIMPSON'S RULE.
C
C
      FUNCTION DADNTD(DK,RT,TMIN,TMAX,PA,FREQ,XN)
      REAL K,KI,KSTAR,KCRIT,KMAX
C
C     SUSTAINED LOAD CRACK GROWTH IS A FUNCTION OF
C     TEMPERATURE T AND STRESS INTENSITY FACTOR K.
C     THE MSE MODEL IS USED TO REPRESENT SUSTAINED
C     LOAD CRACK GROWTH. KI IS THE K VALUE AT THE
C     CURVE INFLECTION POINT. KSTAR IS THE LOWER
C     K ASYMPTOTE OF THE CURVE (THRESHOLD K FOR CRACK
C     GROWTH). KCRIT IS THE UPPER ASYMPTOTE OF THE
C     CURVE. KMAX IS THE MAXIMUM STRESS INTENSITY LEVEL
C     REACHED IN A CYCLE OF A GIVEN DELTA-K AND STRESS
C     RATIO.
C
      DT=TMAX-TMIN
C
C     DT IS THE TEMPERATURE RANGE OF THE CYCLE.
C
      HALFPD=1./(2.*FREQ)
C
C     HALFPD IS THE HALF PERIOD OF THE CYCLE IN SECONDS.
C
      H=HALFPD/XN
C
C     H IS THE TIME STEP SIZE IN SECONDS.
C     INITIALIZE THE INTEGRATION STEP COUNTER
C     AT ZERO.
C
      I=0
C
C     INITIALIZE THE SUMNATIONS AT ZERO.
C
      S0=0.
      S1=0.
      S2=0.
      KMAX=DK/(1.-RT)
C
C     THE INITIAL STRESS INTENSITY VALUE IS
C     THE MINIMUM STRESS INTENSITY VALUE.
C
      K=RT*KMAX
C
```

```
C       THE INITIAL TEMPERATURE IS TMIN IF THE CYCLE
C       IS IN PHASE, TMAX IF THE CYCLE IS 180 DEGREES OUT-
C       OF-PHASE, AND HALFWAY BETWEEN TMIN AND TMAX IF
C       THE CYCLE IS 90 OR 270 DEGREES OUT-OF-PHASE.
C
        IF(PA.EQ.0.)T=TMIN
        IF(PA.EQ.45.)T=TMIN+DT/4.
        IF(PA.EQ.90.)T=TMIN+DT/2.
        IF(PA.EQ.135.)T=TMIN+3.*DT/4.
        IF(PA.EQ.180.)T=TMAX
        IF(PA.EQ.225.)T=TMIN+3.*DT/4.
        IF(PA.EQ.270.)T=TMIN+DT/2.
        IF(PA.EQ.315.)T=TMIN+DT/4.
 100    CONTINUE
C
C       FUNCTION DADT CALCULATES THE SUSTAINED LOAD
C       CRACK GROWTH RATE DA/DT AS A FUNCTION OF K AND
C       TEMPERATURE T USING THE MSE MODEL.
C       STOP CALCULATIONS IF THE K VALUE EXCEEDS THE
C       EXPERIMENTAL DATA RANGE AS INDICATED BY A
C       FLAG VALUE OF DADT OF TEN.
C
        IF(DADT(K,T).EQ.10.)THEN
        DADNTD=10.
        GOTO 400
        ENDIF
C
C       PERFORM THE SIMPSON'S RULE SUMNATIONS:
C       S0 FOR THE FIRST AND LAST TERM, S2 FOR
C       EVEN NUMBER TERMS, AND S1 FOR ODD NUMBER
C       TERMS.
C
        IF(I.EQ.0)THEN
        S0=S0+DADT(K,T)
        GOTO 200
        ENDIF
        IF(I.EQ.IFIX(XN))THEN
        S0=S0+DADT(K,T)
        GOTO 300
        ENDIF
        IF(MOD(I,2).EQ.0)THEN
        S2=S2+DADT(K,T)
        GOTO 200
        ENDIF
        S1=S1+DADT(K,T)
 200    CONTINUE
C
C       INCREMENT TO THE NEXT STEP.
C
        I=I+1
```

```
C
C       INCREMENT THE STRESS INTENSITY FACTOR.
C
        K=K+DK/XN
C
C       INCREMENT TEMPERATURE APPROPRIATELY FOR THE
C       PHASE ANGLE RELATIONSHIP BETWEEN TEMPERATURE AND
C       LOAD.
C
        IF(PA.EQ.0.)THEN
        T=T+DT/XN
        GOTO 100
        ENDIF
        IF(PA.EQ.180.)THEN
        T=T-DT/XN
        GOTO 100
        ENDIF
        IF(PA.EQ.90..AND.I.LE.IFIX(XN/2.))THEN
        T=T-DT/XN
        GOTO 100
        ENDIF
        IF(PA.EQ.90..AND.I.GT.IFIX(XN/2.))THEN
        T=T+DT/XN
        GOTO 100
        ENDIF
        IF(PA.EQ.270..AND.I.LE.IFIX(XN/2.))THEN
        T=T+DT/XN
        GOTO 100
        ENDIF
        IF(PA.EQ.270..AND.I.GT.IFIX(XN/2.))THEN
        T=T-DT/XN
        GOTO 100
        ENDIF
        IF(PA.EQ.45..AND.I.LE.IFIX(XN/4.))THEN
        T=T-DT/XN
        GOTO 100
        ENDIF
        IF(PA.EQ.45..AND.I.GT.IFIX(XN/4.))THEN
        T=T+DT/XN
        GOTO 100
        ENDIF
        IF(PA.EQ.135..AND.I.LE.IFIX(3.*XN/4.))THEN
        T=T-DT/XN
        GOTO 100
        ENDIF
        IF(PA.EQ.135..AND.I.GT.IFIX(3.*XN/4.))THEN
        T=T+DT/XN
        GOTO 100
        ENDIF
        IF(PA.EQ.225..AND.I.LE.IFIX(XN/4.))THEN
```

```
      T=T+DT/XN
      GOTO 100
      ENDIF
      IF(PA.EQ.225..AND.I.GT.IFIX(XN/4.))THEN
      T=T-DT/XN
      GOTO 100
      ENDIF
      IF(PA.EQ.315..AND.I.LE.IFIX(3.*XN/4.))THEN
      T=T+DT/XN
      GOTO 100
      ENDIF
      IF(PA.EQ.315..AND.I.GT.IFIX(3.*XN/4.))THEN
      T=T-DT/XN
      GOTO 100
      ENDIF
300   CONTINUE
C
C     CALCULATE THE TOTAL TIME DEPENDENT CRACK
C     GROWTH USING SIMPSON'S RULE.
C
      DADNTD=(H/3.)*(S0+4.*S1+2.*S2)
400   CONTINUE
      RETURN
      END
C
C
C  FUNCTION DADNMM CALCULATES THE MIXED-MODE DAMAGE
C  TERM FOR A GIVEN DELTA-K (DK), TEST LOAD RATIO
C  (RT), MINIMUM CYCLE TEMPERATURE (TMIN), MAXIMUM
C  CYCLE TEMPERATURE (TMAX), PHASE ANGLE BETWEEN MAX
C  LOAD AND MAX TEMPERATURE (PA), AND NUMBER OF INTEGRATION
C  INCREMENTS (XN). THE FUNCTION INTEGRATES A DAMAGE FUNCTION
C  OVER THE LOADING PORTION OF THE THERMAL-MECHANICAL CYCLE
C  USING THE RECTANGULAR RULE.

C
      FUNCTION DADNMM(DK,RT,TMIN,TMAX,PA,XN)
      REAL KMAX
      DT=TMAX-TMIN
C
C     DT IS THE TEMPERATURE RANGE OF THE CYCLE.
C
      I=1
C
C     R1 IS THE LOAD RATIO OF THE LOWER POINT OF
C     THE INTEGRATION INCREMENT. START AT THE OVERALL
C     TEST LOAD RATIO, RT.
C
      R1=RT
C
```

```
C       KMAX IS THE MAXIMUM STRESS INTENSITY FACTOR REACHED
C       DURING THE CYCLE.
C
        KMAX=DK/(1.-RT)
C
C       DK1 IS THE DELTA-K ASSOCIATED WITH R1.
C
        DK1=KMAX*(1.-R1)
C
C       R2 IS THE LOAD RATIO OF THE UPPER POINT OF THE
C       INTEGRATION INCREMENT.
C
        R2=R1+(1.-RT)/XN
C
C       DK2 IS THE DELTA-K ASSOCIATED WITH R2.
C
        DK2=KMAX*(1.-R2)
C
C       THE TEMPERATURE ASSOCIATED WITH THE INCREMENT IS
C       THE TEMPERATURE AT THE MIDPOINT OF THE INCREMENT.
C       FIND THIS TEMPERATURE BASED ON THE PHASE ANGLE
C       BETWEEN THE MAX LOAD AND MAX TEMPERATURE, PA.
C
        IF(PA.EQ.0.)T1=TMIN+DT/(2.*XN)
        IF(PA.EQ.45.)T1=TMIN+DT/4.-DT
     *  /(2.*XN)
        IF(PA.EQ.90.)T1=TMIN+DT/2.-DT
     *  /(2.*XN)
        IF(PA.EQ.135.)T1=TMIN+3.*DT/4.-DT
     *  /(2.*XN)
        IF(PA.EQ.180.)T1=TMAX-DT/(2.*XN)
        IF(PA.EQ.225.)T1=TMIN+3.*DT/4.+DT
     *  /(2.*XN)
        IF(PA.EQ.270.)T1=TMIN+DT/2.+DT
     *  /(2.*XN)
        IF(PA.EQ.315.)T1=TMIN+DT/4.+DT/(2.*XN)
C
C       INITIALIZE THE SUMNATION VARIABLE AT ZERO.
C
        DADNMM=0.
  100   CONTINUE
C
C       THE INTEGRATED DAMAGE FUNCTION FOR THE INCREMENT
C       R1 TO R2 IS THE ISOTHERMAL MIXED-MODE DAMAGE AT T1
C       FOR A CYCLE FROM KMIN=R1*KMAX TO KMAX MINUS THE
C       ISOTHERMAL MIXED-MODE DAMAGE AT T1 FOR A CYCLE FROM
C       KMIN=R2*KMAX TO KMAX. CALCULATE THE ISOTHERMAL MIXED-
C       MODE DAMAGE WITH THE FUNCTION DADNT.
C
        A1=DADNT(R1,T1,DK1)
```

```
      B1=DADNT(R2,T1,DK2)
      DADNMM=DADNMM+A1-B1
 150  CONTINUE
C
C     ADVANCE TO THE NEXT INCREMENT.
C
      R1=R2
      DK1=DK2
      R2=R2+(1.-RT)/XN
      DK2=KMAX*(1.-R2)
C
C     CALCULATE THE TEMPERATURE T1 FOR THE
C     NEXT INCREMENT.
C
      IF(PA.EQ.0.)THEN
      T1=T1+DT/XN
      GOTO 200
      ENDIF
      IF(PA.EQ.180.)THEN
      T1=T1-DT/XN
      GOTO 200
      ENDIF
      IF(PA.EQ.90..AND.I.LT.IFIX(XN/2.))THEN
      T1=T1-DT/XN
      GOTO 200
      ENDIF
      IF(PA.EQ.90..AND.I.GT.IFIX(XN/2.))THEN
      T1=T1+DT/XN
      GOTO 200
      ENDIF
      IF(PA.EQ.270..AND.I.LT.IFIX(XN/2.))THEN
      T1=T1+DT/XN
      GOTO 200
      ENDIF
      IF(PA.EQ.270..AND.I.GT.IFIX(XN/2.))THEN
      T1=T1-DT/XN
      GOTO 200
      ENDIF
      IF(PA.EQ.45..AND.I.LT.IFIX(XN/4.))THEN
      T1=T1-DT/XN
      GOTO 200
      ENDIF
      IF(PA.EQ.45..AND.I.GT.IFIX(XN/4.))THEN
      T1=T1+DT/XN
      GOTO 200
      ENDIF
      IF(PA.EQ.135..AND.I.LT.IFIX(3.*XN/4.))THEN
      T1=T1-DT/XN
      GOTO 200
      ENDIF
```

```
      IF(PA.EQ.135..AND.I.GT.IFIX(3.*XN/4.))THEN
      T1=T1+DT/XN
      GOTO 200
      ENDIF
      IF(PA.EQ.225..AND.I.LT.IFIX(XN/4.))THEN
      T1=T1+DT/XN
      GOTO 200
      ENDIF
      IF(PA.EQ.225..AND.I.GT.IFIX(XN/4.))THEN
      T1=T1-DT/XN
      GOTO 200
      ENDIF
      IF(PA.EQ.315..AND.I.LT.IFIX(3.*XN/4.))THEN
      T1=T1+DT/XN
      GOTO 200
      ENDIF
      IF(PA.EQ.315..AND.I.GT.IFIX(3.*XN/4.))THEN
      T1=T1-DT/XN
      GOTO 200
      ENDIF
 200  CONTINUE
C
C     IF THE UPPER STRESS RATIO OF THE INCREMENT
C     IS TOO HIGH, STOP CALCULATIONS.
C
      IF(R2.GE..9)THEN
      DADNMM=DADNMM+DADNT(R1,T1,DK1)
      GOTO 300
      ENDIF
C
C     SUM THE INCREMENTAL DAMAGES.
C
      I=I+1
      GOTO 100
 300  CONTINUE
C
C     DO NOT ALLOW NEGATIVE MIXED-MODE CONTRIBUTIONS.
C
      IF(DADNMM.LE.0.)DADNMM=0.
      RETURN
      END
C
C
C     FUNCTION DADNT CALCULATES THE ISOTHERMAL MIXED-
C     MODE DAMAGE FOR A GIVEN CYCLE LOAD RATIO (R),
C     TEMPERATURE (T), AND DELTA-K (DK) USING THE MODIFIED
C     SIGMOIDAL EQUATION MODEL.
C
C
      FUNCTION DADNT(R,T,DK)
```

```
C
C       IF R EXCEEDS 0.5, THERE IS NO MIXED MODE DAMAGE.
C
        IF(R.GT..5)THEN
        DADNT=0.
        GOTO 100
        ENDIF
C
C       ESTABLISH THE MIXED-MODE TERM MSE PARAMETERS.
C
        Q=0.3
        DKSTAR=10.**(1.33846+.892641*ALOG10((1.-R)/.9))
        DKI=10.**(1.77677+.684421*ALOG10((1.-R)/.9))
        DADNI=10.**(-5.71942+7.75465*ALOG10((1.-R)/.9))
        DADNIP=2.5
        D=-Q
        DKCRIT=(DKI**2)/DKSTAR
C
C       IF DELTA-K IS LESS THAN THE THRESHOLD VALUE,
C       THERE IS NO MIXED-MODE DAMAGE.
C
        IF(DK.LE.DKSTAR)THEN
        DADNT=0.
        GOTO 100
        ENDIF
        CONST=ALOG(DKI/DKSTAR)
        CONST1=ALOG(DKCRIT/DKI)
        B=ALOG(DADNI)-Q*ALOG(CONST)-D*ALOG(CONST1)
        P=DADNIP-Q/CONST+D/CONST1
        X=EXP(B)*((DK/DKI)**P)*((ALOG(DK/DKSTAR))
     *  **Q)*((ALOG(DKCRIT/DK))**D)
C
C       THE MIXED-MODE DAMAGE IS A PEAK AT 1000F,
C       AND FALLS OFF LINEARLY TO A VALUE OF ZERO
C       AT 800F AND 1200F.
C
        IF(T.LE.1000.)THEN
        DADNT=((T/200.)-4.)*X
        GOTO 100
        ENDIF
        DADNT=(6.-(T/200.))*X
  100   CONTINUE
        RETURN
        END
C
C
C       FUNCTION DADT CALCULATES THE SUSTAINED LOAD
C       CRACK GROWTH RATE AS A FUNCTION OF STRESS
C       INTENSITY FACTOR (K) AND TEMPERATURE (T)
C       USING THE MODIFIED SIGMOIDAL EQUATION MODEL.
```

```
C
C
      FUNCTION DADT(K,T)
      REAL K,KI,KSTAR,KCRIT,KMAX
C
C     CALCULATE THE MSE PARAMETERS FOR THE APPROPRIATE
C     TEMPERATURE RANGE (800F TO 1000F, 1000F TO 1100F,
C     OR 1100F TO 1200F).
C
      Q=0.4
      D=-Q
      IF(T.GE.800..AND.T.LT.1000.)THEN
      KSTAR=10.**(1.69897-1.59379E-3*(T-800.))
      KI=10.**(2.-5.95932E-4*(T-800.))
      DADTI=10.**(-8.55284+6.82878E-3*(T-800.))
      DADTIP=1.2
      GOTO 100
      ENDIF
      IF(T.GE.1000..AND.T.LT.1100.)THEN
      KSTAR=10.**(1.38021-5.79919E-4*(T-1000.))
      KI=10.**(1.88081-1.74907E-4*(T-1000.))
      DADTI=10.**(-7.18709+1.09018E-2*(T-1000.))
      DADTIP=1.2+8.E-3*(T-1000.)
      GOTO 100
      ENDIF
      IF(T.GE.1100..AND.T.LE.1200.)THEN
      KSTAR=10.**(1.32222-4.34657E-4*(T-1100.))
      KI=10.**(1.86332-8.51716E-4*(T-1100.))
      DADTI=10.**(-6.09691+1.1383E-2*(T-1100.))
      DADTIP=2.+1.E-2*(T-1100.)
      GOTO 100
      ENDIF
  100 CONTINUE
      KCRIT=(KI**2)/KSTAR
      CONST=ALOG(KI/KSTAR)
      CONST1=ALOG(KCRIT/KI)
      B=ALOG(DADTI)-Q*ALOG(CONST)-D*ALOG(CONST1)
      P=DADTIP-Q/CONST+D/CONST1
C
C     IF K EXCEEDS THE EXPERIMENTAL DATA RANGE,
C     SET THE CRACK GROWTH RATE DADT EQUAL TO
C     A FLAG VALUE OF TEN.
C
      IF(K.GE.KI)THEN
      DADT=10.
      GOTO 200
      ENDIF
C
C     IF K IS LESS THAN THE THRESHOLD VALUE,
C     THERE IS NO SUSTAINED LOAD CRACK GROWTH.
```

```
C
      IF(K.LE.KSTAR)DADT=0.
C
C     FIND THE SUSTAINED LOAD CRACK GROWTH RATE
C     USING THE MODIFIED SIGMOIDAL EQUATION.
C
      IF(K.GT.KSTAR)DADT=EXP(B)*((K/KI)**P)*
     *  ((ALOG(K/KSTAR))**Q)*((ALOG(KCRIT/K))**D)
  200 CONTINUE
      RETURN
      END
```

APPENDIX D

ALTERNATE MIXED-MODE TERM DERIVATION

Calculating the mixed-mode damage over a thermal-mechanical cycle:

$$\text{Let} \quad \left.\frac{da}{dN}\right)_{\substack{\text{Isothermal} \\ \text{Mixed-mode}}} = \int_{K_{min}}^{K_{max}} f(K)\, dK \qquad \text{(D.1)}$$

Keep K_{min} constant and allow K_{max} to vary. The shaded area in Figure D.1 is expressed in terms of crack growth rates:

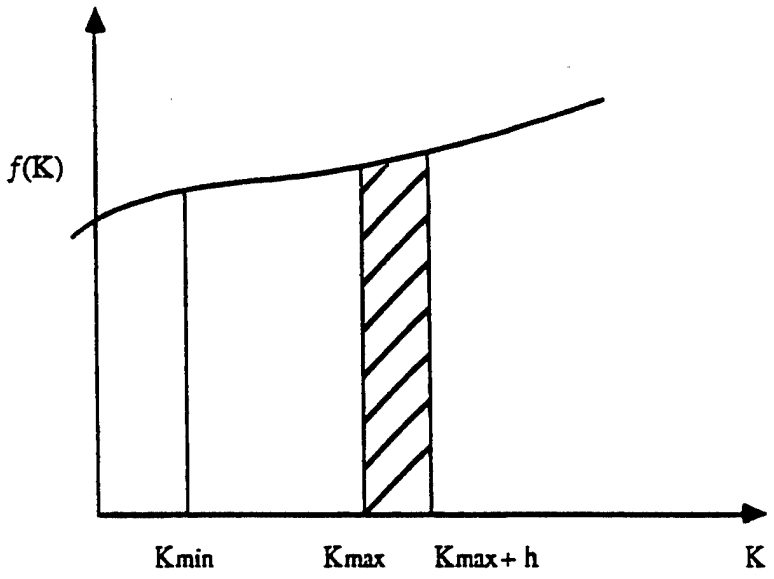

Figure D.1: Integration for an Incremental Variation h in K_{max}

$$\left.\frac{da}{dN}\right)_{K_{max}} = \int_{K_{min}}^{K_{max}} f(K)\, dK \qquad \text{(D.2)}$$

$$\left.\frac{da}{dN}\right)_{K_{max}+h} = \int_{K_{min}}^{K_{max}+h} f(K)\, dK \qquad \text{(D.3)}$$

$$\text{Shaded Area} = \left.\frac{da}{dN}\right)_{K_{max}+h} - \left.\frac{da}{dN}\right)_{K_{max}} = \int_{K_{max}}^{K_{max}+h} f(K)\, dK \qquad (D.4)$$

Apply the mean value theorem:

$$\left.\frac{da}{dN}\right)_{K_{max}+h} - \left.\frac{da}{dN}\right)_{K_{max}} = f(K_{max} + \alpha h)\, h \quad , 0 \le \alpha \le 1 \qquad (D.5)$$

Take the limit as h approaches zero:

$$\lim_{h\to 0} \frac{\left.\frac{da}{dN}\right)_{K_{max}+h} - \left.\frac{da}{dN}\right)_{K_{max}}}{h} = \lim_{h\to 0} \{f(K_{max} + \alpha h)\} \quad , 0 \le \alpha \le 1 \qquad (D.6)$$

$$\frac{\partial(da/dN)}{\partial K_{max}} = f(K) \qquad (D.7)$$

The integration equation to find mixed-mode damage becomes:

$$\left.\frac{da}{dN}\right)_{\text{Mixed-Mode}} = \int_{K_{min}}^{K_{max}} \frac{\partial(da/dn)}{\partial K_{max}}\, dK_{max} \qquad (D.8)$$

The integration and differentiation of equation (D.8) may be performed numerically.

Divide the loading portion of the cycle into N increments as shown in Figure D.2:

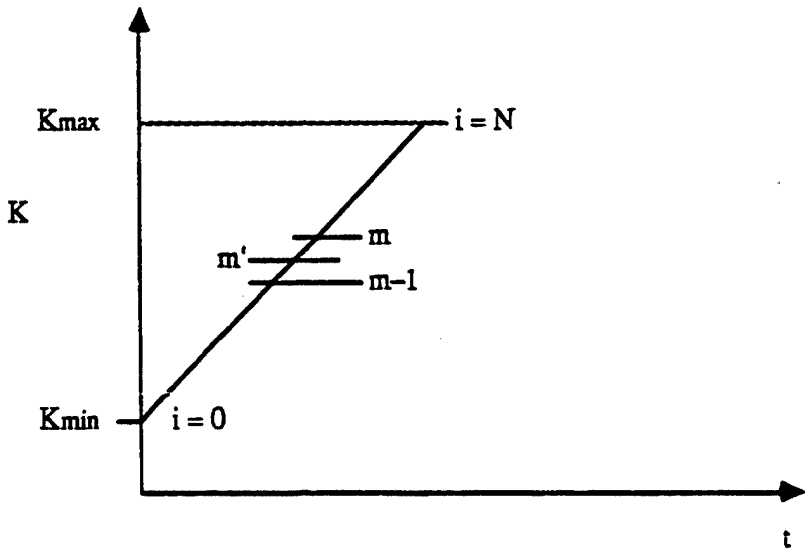

Figure D.2: Load Cycle Increments

The derivative $\partial(da/dN)/\partial K_{max}$ at the midpoint M' between points (M–1) and (M) can be expressed as:

$$\left.\frac{\partial(da/dN)}{\partial K_{max}}\right|_{M'} = \frac{\frac{da}{dN}(K_{max(M)}, T_{M'}) - \frac{da}{dN}(K_{max(M-1)}, T_{M'})}{K_{max(M)} - K_{max(M-1)}} \qquad (D.9)$$

The integration of equation (D.8) is performed numerically using the simple rectangular rule:

$$\left.\frac{da}{dN}\right)_{\substack{TMF \\ Mixed\text{-}Mode}} = \sum_{i=1}^{N} \left[\frac{da}{dN}(K_{max(i)}, T_{i'}) - \frac{da}{dN}(K_{max(i-1)}, T_{i'}) \right] \qquad (D.10)$$

The previously derived expression for mixed-mode crack growth for Chapter IV is:

$$\left.\frac{da}{dN}\right)_{\substack{TMF \\ Mixed\text{-}Mode}} = \sum_{i=1}^{N} \left[\frac{da}{dN}(R_{i-1}, T_{i'}) - \frac{da}{dN}(R_i, T_{i'}) \right] \qquad (4.41) \text{ (repeated)}$$

Equations (D.10) and (4.41) provide ways to approximate mixed-mode damage over a thermal-mechanical cycle using isothermal test results. Both equations provide the exact result for isothermal cycles. However, this does not imply that the calculations are always equivalent when the temperatures are allowed to vary. The two expressions were found to give results differing by a factor of up to two in the case of an in-phase thermal-mechanical cycle. Since the contribution of mixed-mode damage to overall thermal-mechanical fatigue crack growth is relatively small, equation (D.10) may be used in place of equation (4.41) in a linear cumulative damage model without significantly affecting the predictions.

APPENDIX E

MODIFIED TIME-DEPENDENT DAMAGE PROGRAM

```
C
C
C     FUNCTION DADNTD CALCULATES THE TIME-DEPENDENT
C     DAMAGE TERM FOR A GIVEN DELTA-K (DK), TEST LOAD
C     RATIO (RT), MINIMUM CYCLE TEMPERATURE (TMIN),
C     MAXIMUM CYCLE TEMPERATURE (TMAX), PHASE ANGLE
C     BETWEEN MAXIMUM LOAD AND MAXIMUM TEMPERATURE
C     (PA), TEST FREQUENCY (FREQ), AND NUMBER OF INTEGRATION
C     STEPS (XN). THE FUNCTION INTEGRATES SUSTAINED LOAD
C     CRACK GROWTH (DA/DT) OVER THE LOADING PORTION OF THE
C     THERMAL MECHANICAL CYCLE USING SIMPSON'S RULE.
C
C
      FUNCTION DADNTD(DK,RT,TMIN,TMAX,PA,FREQ,XN)
      REAL K,KI,KSTAR,KCRIT,KMAX
C
C     SUSTAINED LOAD CRACK GROWTH IS A FUNCTION OF
C     TEMPERATURE T AND STRESS INTENSITY FACTOR K.
C     THE MSE MODEL IS USED TO REPRESENT SUSTAINED
C     LOAD CRACK GROWTH. KI IS THE K VALUE AT THE
C     CURVE INFLECTION POINT. KSTAR IS THE LOWER
C     K ASYMPTOTE OF THE CURVE (THRESHOLD K FOR CRACK
C     GROWTH). KCRIT IS THE UPPER ASYMPTOTE OF THE
C     CURVE. KMAX IS THE MAXIMUM STRESS INTENSITY LEVEL
C     REACHED IN A CYCLE OF A GIVEN DELTA-K AND STRESS
C     RATIO.
C
      DT=TMAX-TMIN
C
C     DT IS THE TEMPERATURE RANGE OF THE CYCLE.
C
      HALFPD=1./(2.*FREQ)
C
C     HALFPD IS THE HALF PERIOD OF THE CYCLE IN SECONDS.
C
      H=HALFPD/XN
C
C     H IS THE TIME STEP SIZE IN SECONDS.
C     INITIALIZE THE INTEGRATION STEP COUNTER
C     AT ZERO.
C
      I=0
C
C     INITIALIZE THE SUMNATIONS AT ZERO.
C
      S0=0.
      S1=0.
      S2=0.
      KMAX=DK/(1.-RT)
```

```
C
C       THE INITIAL STRESS INTENSITY VALUE IS
C       THE MINIMUM STRESS INTENSITY VALUE.
C
        K=RT*KMAX
C
C       THE INITIAL TEMPERATURE IS TMIN IF THE CYCLE
C       IS IN PHASE, TMAX IF THE CYCLE IS 180 DEGREES OUT-
C       OF-PHASE, AND HALFWAY BETWEEN TMIN AND TMAX IF
C       THE CYCLE IS 90 OR 270 DEGREES OUT-OF-PHASE.
C
        IF(PA.EQ.0.)T=TMIN
        IF(PA.EQ.45.)T=TMIN+DT/4.
        IF(PA.EQ.90.)T=TMIN+DT/2.
        IF(PA.EQ.135.)T=TMIN+3.*DT/4.
        IF(PA.EQ.180.)T=TMAX
        IF(PA.EQ.225.)T=TMIN+3.*DT/4.
        IF(PA.EQ.270.)T=TMIN+DT/2.
        IF(PA.EQ.315.)T=TMIN+DT/4.
        F1=0.
  100   CONTINUE
C
C       FUNCTION DADT CALCULATES THE SUSTAINED LOAD
C       CRACK GROWTH RATE DA/DT AS A FUNCTION OF K AND
C       TEMPERATURE T USING THE MSE MODEL.
C       STOP CALCULATIONS IF THE K VALUE EXCEEDS THE
C       EXPERIMENTAL DATA RANGE AS INDICATED BY A
C       FLAG VALUE OF DADT OF TEN.
C
        IF(DADT(K,T).EQ.10.)THEN
        DADNTD=10.
        GOTO 400
        ENDIF
        F2=DADT(K,T)
        IF(F2.LT.F1)F2=0.
C
C       PERFORM THE SIMPSON'S RULE SUMNATIONS:
C       SO FOR THE FIRST AND LAST TERM, S2 FOR
C       EVEN NUMBER TERMS, AND S1 FOR ODD NUMBER
C       TERMS.
C
        IF(I.EQ.0)THEN
        S0=S0+F2
        GOTO 200
        ENDIF
        IF(I.EQ.IFIX(XN))THEN
```

```
      S0=S0+F2
      GOTO 300
      ENDIF
      IF(MOD(I,2).EQ.0)THEN
      S2=S2+F2
      GOTO 200
      ENDIF
      S1=S1+F2
200   CONTINUE
      F1=DADT(K,T)
C
C     INCREMENT TO THE NEXT STEP.
C
      I=I+1
C
C     INCREMENT THE STRESS INTENSITY FACTOR.
C
      K=K+DK/XN
C
C     INCREMENT TEMPERATURE APPROPRIATELY FOR THE
C     PHASE ANGLE RELATIONSHIP BETWEEN TEMPERATURE AND
C     LOAD.
C
      IF(PA.EQ.0.)THEN
      T=T+DT/XN
      GOTO 100
      ENDIF
      IF(PA.EQ.180.)THEN
      T=T-DT/XN
      GOTO 100
      ENDIF
      IF(PA.EQ.90..AND.I.LE.IFIX(XN/2.))THEN
      T=T-DT/XN
      GOTO 100
      ENDIF
      IF(PA.EQ.90..AND.I.GT.IFIX(XN/2.))THEN
      T=T+DT/XN
      GOTO 100
      ENDIF
      IF(PA.EQ.270..AND.I.LE.IFIX(XN/2.))THEN
      T=T+DT/XN
      GOTO 100
      ENDIF
      IF(PA.EQ.270..AND.I.GT.IFIX(XN/2.))THEN
      T=T-DT/XN
      GOTO 100
      ENDIF
      IF(PA.EQ.45..AND.I.LE.IFIX(XN/4.))THEN
      T=T-DT/XN
      GOTO 100
```

```
      ENDIF
      IF(PA.EQ.45..AND.I.GT.IFIX(XN/4.))THEN
      T=T+DT/XN
      GOTO 100
      ENDIF
      IF(PA.EQ.135..AND.I.LE.IFIX(3.*XN/4.))THEN
      T=T-DT/XN
      GOTO 100
      ENDIF
      IF(PA.EQ.135..AND.I.GT.IFIX(3.*XN/4.))THEN
      T=T+DT/XN
      GOTO 100
      ENDIF
      IF(PA.EQ.225..AND.I.LE.IFIX(XN/4.))THEN
      T=T+DT/XN
      GOTO 100
      ENDIF
      IF(PA.EQ.225..AND.I.GT.IFIX(XN/4.))THEN
      T=T-DT/XN
      GOTO 100
      ENDIF
      IF(PA.EQ.315..AND.I.LE.IFIX(3.*XN/4.))THEN
      T=T+DT/XN
      GOTO 100
      ENDIF
      IF(PA.EQ.315..AND.I.GT.IFIX(3.*XN/4.))THEN
      T=T-DT/XN
      GOTO 100
      ENDIF
 300  CONTINUE
C
C     CALCULATE THE TOTAL TIME DEPENDENT CRACK
C     GROWTH USING SIMPSON'S RULE.
C
      DADNTD=(H/3.)*(S0+4.*S1+2.*S2)
 400  CONTINUE
      RETURN
      END
C
C
C     FUNCTION DADT CALCULATES THE SUSTAINED LOAD
C     CRACK GROWTH RATE AS A FUNCTION OF STRESS
C     INTENSITY FACTOR (K) AND TEMPERATURE (T)
C     USING THE MODIFIED SIGMOIDAL EQUATION MODEL.
C
C
      FUNCTION DADT(K,T)
      REAL K,KI,KSTAR,KCRIT,KMAX
C
C     CALCULATE THE MSC PARAMETERS FOR THE APPROPRIATE
```

```
C       TEMPERATURE RANGE (800F TO 1000F, 1000F TO 1100F,
C       OR 1100F TO 1200F).
C
        Q=0.4
        D=-Q
        IF(T.GE.800..AND.T.LT.1000.)THEN
        KSTAR=10.**(1.69897-1.59379E-3*(T-800.))
        KI=10.**(2.-5.95932E-4*(T-800.))
        DADTI=10.**(-8.55284+6.82878E-3*(T-800.))
        DADTIP=1.2
        GOTO 100
        ENDIF
        IF(T.GE.1000..AND.T.LT.1100.)THEN
        KSTAR=10.**(1.38021-5.79919E-4*(T-1000.))
        KI=10.**(1.88081-1.74907E-4*(T-1000.))
        DADTI=10.**(-7.18709+1.09018E-2*(T-1000.))
        DADTIP=1.2+8.E-3*(T-1000.)
        GOTO 100
        ENDIF
        IF(T.GE.1100..AND.T.LE.1200.)THEN
        KSTAR=10.**(1.32222-4.34657E-4*(T-1100.))
        KI=10.**(1.86332-8.51716E-4*(T-1100.))
        DADTI=10.**(-6.09691+1.1383E-2*(T-1100.))
        DADTIP=2.+1.E-2*(T-1100.)
        GOTO 100
        ENDIF
  100   CONTINUE
        KCRIT=(KI**2)/KSTAR
        CONST=ALOG(KI/KSTAR)
        CONST1=ALOG(KCRIT/KI)
        B=ALOG(DADTI)-Q*ALOG(CONST)-D*ALOG(CONST1)
        P=DADTIP-Q/CONST+D/CONST1
C
C       IF K EXCEEDS THE EXPERIMENTAL DATA RANGE,
C       SET THE CRACK GROWTH RATE DADT EQUAL TO
C       A FLAG VALUE OF TEN.
C
        IF(K.GE.KI)THEN
        DADT=10.
        GOTO 200
        ENDIF
C
C       IF K IS LESS THAN THE THRESHOLD VALUE,
C       THERE IS NO SUSTAINED LOAD CRACK GROWTH.
C
        IF(K.LE.KSTAR)DADT=0.
C
C       FIND THE SUSTAINED LOAD CRACK GROWTH RATE
C       USING THE MODIFIED SIGMOIDAL EQUATION.
```

```
C
      IF(K.GT.KSTAR)DADT=EXP(B)*((K/KI)**P)*
     *  ((ALOG(K/KSTAR))**Q)*((ALOG(KCRIT/K))**U)
 200  CONTINUE
      RETURN
      END
```

Bibliography

1. Larsen, J. M. and T. Nicholas, "Cumulative-Damage Modeling of Fatigue Crack Growth in Turbine Engine Materials," Engineering Fracture Mechanics, Vol 22, No 4, 1985, pp. 713-730.

2. Collins, J. A., Failure of Materials in Mechanical Design Analysis. Prediction. Prevention, New York, John Wiley and Sons, 1981, p. 379.

3. Harris, J. A., D. L. Sims, and C. G. Annis, "Concept Definition: Retirement for Cause of F100 Rotor Components," AFWAL-TR-80-4118, Wright-Patterson AFB, OH, 1980.

4. King, T. T., N. D. Cowie, and W. H. Reimann, "Damage Tolerance Design Concepts for Military Engines," Damage Tolerance Concepts for Critical Engine Components, AGARD Conference Proceedings No. 393, 1985, pp. 3.1-3.5.

5. Larsen, J. M., B. J. Schwartz, and C. G. Annis, "Cumulative Damage Fracture Mechanics Under Engine Spectra," AFML-TR-79-4159, Wright-Patterson AFB OH, 1980.

6. Wallace, R. M., C. G. Annis, and D. L. Sims, "Application of Fracture Mechanics at Elevated Temperatures," AFML-TR-76-176 Part II, Wright-Patterson AFB OH, 1977.

7. Nicholas, T. and J. M. Larsen, "Life Prediction for Turbine Engine Components," Fatigue Environment and Temperature Effects, J. J. Burke and V. Weiss, Eds., Sagamore Army Materials Research Conference (27th: 1980), New York, Plenum Press, 1983, pp. 353-375.

8. Annis, C. G., R. M. Wallace, and D. L. Sims, "An Interpolative Model for Elevated Temperature Fatigue Crack Propagation," AFML-TR-76-176, Part 1, Wright-Patterson AFB OH, 1976.

9. Shahinian, P. and K. Sadananda, "Crack Growth Behavior Under Creep-Fatigue Conditions in Alloy 718," 1976 ASME-MPC Symposium on Creep-Fatigue Interaction, New York, The American Society of Mechanical Engineers, 1976, pp. 365-390.

10. Shahinian, P. and K. Sadananda, "Effects of Stress Ratio and Hold-Time on Fatigue Crack Growth in Alloy 718," Journal of Engineering Materials and Technology, 101, July, 1979, pp. 224-230.

11. Sadananda, K. and P. Shahinian, "Crack Growth Behavior in Alloy 718 at 425°C," Journal of Engineering Materials and Technology, 100, October 1978, pp. 381-387.

12. Floreen, S., and R. H. Kane, "Effects of Environment on High Temperature Fatigue Crack Growth in a Superalloy," Metallurgical Transactions A, 10A, November 1979, pp. 1745-1751.

13. Floreen, S., and R. H. Kane, "An Investigation of the Creep-Fatigue Environment Interaction in a Ni-Base Superalloy," Fatigue of Engineering Materials and Structures, 2, 1980, pp. 401-412.

14. Pédron, J., and A. Pineau, " The Effect of Microstructure and Environment on the Crack Growth Behaviour of Inconel 718 Alloy at 650°C Under Fatigue, Creep, and Combined Loading," Materials Science and Engineering, 56, 1982, pp. 143-156.

15. Sadananda, K., and P. Shahinian, "The Effect of Environment on the Creep Crack Growth Behavior of Several Structural Alloys," Materials Science and Engineering, 43(1), 1980, pp. 159-169.

16. Mills, W. J., and L. A. James, "The Fatigue Crack Propagation Response of Two Nickel-Base Alloys in a Liquid Sodium Environment," Journal of Engineering Materials and Technology, 101, July 1979, pp. 205-213.

17. Ellison, E. G. and M. P. Harper, "Creep Behaviour of Components Containing Cracks — A Critical Review," Journal of Strain Analysis, Vol 13, No 1, 1978, pp. 35-51.

18. Marchand, N. J., Thermal-Mechanical Fatigue Behavior of Nickel-Base Superalloys, Sc.D. Thesis, The Massachusetts Institute of Technology, January, 1986.

19. Sadananda, K., and P. Shahinian, "Creep Crack Growth in Alloy 718," Metallurgical Transactions A, 8A, March 1977, pp. 439-449.

20. Weerasooriya, T., "Effect of Frequency on Fatigue Crack Growth Rate at High Temperatures," AFWAL-TR- ,Wright-Patterson AFB OH, 1986.

21. Broek, D., Elementary Engineering Fracture Mechanics, Third Revised Edition, The Hague, Martinus Nijhoff Publishers, 1984, pp. 250-251.

22. Paris, P. C., M. P. Gomez, and W. E. Anderson, "A Rational Analytic Theory of Fatigue," The Trend in Engineering, 13, January, 1961, pp. 9-14.

23. Sadananda, K. and P. Shahinian, "Review of the Fracture Mechanics Approach to Creep Crack Growth in Structural Alloys," Engineering Fracture Mechanics, Vol 15, No 3-4, 1981, pp. 327-342.

24. Yokobori, T., and H. Sakata, "Studies on Crack Growth Rate Under High Temperature Creep, Fatigue, and Creep Fatigue Interactions 1," Engineering Fracture Mechanics, 13, 1980, pp. 509-522.

25. Landes, J. D. and J. A. Begley, "A Fracture Mechanics Approach to Creep Crack Growth," Mechanics of Crack Growth, ASTM STP 520, American Society for Testing and Materials, 1976, pp. 128-148.

26. Saxena, A., "Evaluation of C^* for the Characterization of Creep Crack Growth Behavior in 304 Stainless Steel," Proceedings of the Twelfth National Symposium on Fracture Mechanics, ASTM STP 700, American Society for Testing and Materials, 1980, pp. 131-151.

27. Myers, G. J., "Fracture Mechanics Criteria for Turbine Engine Hot Section Components Final Report," NASA CR-167896, May 1982.

28. Popp, H. G., and A. Coles, "Subcritical Crack Growth Criteria for Inconel 718 at Elevated Temperatures," AFFDL-TR-70-144, Wright-Patterson AFB OH, 1970, pp. 71-86.

29. Pelloux, R. M.; "Creep-Fatigue Environment Interactions in Superalloys," AFOSR-TR-81-0450, Bolling AFB DC, 1981.

30. Nicholas, T., T. Weerasooriya, and N. E. Ashbaugh, "A Model for Creep/Fatigue Interactions in Alloy 718," Fracture Mechanics: Sixteenth Symposium, ASTM STP 868, M. F. Kanninen and A. T. Hopper, Eds., American Society for Testing and Materials, 1985, pp. 167-180.

31. Weerasooriya, T. and T. Nicholas, "Hold-Time Effects in Elevated Temperature Fatigue Crack Propagation," AFWAL-TR-84-4184, Wright-Patterson AFB OH, 1985.

32. Clavel, M., and A. Pineau, "Frequency and Waveform Effects on the Fatigue Crack Growth Behavior of Alloy 718 at 298K and 823K," Metallurgical Transactions A, 9A, April, 1978, pp. 471-480.

33. Saxena, A., "A Model for Predicting the Effect of Frequency on Fatigue Crack Growth Behavior at Elevated Temperature," Fatigue of Engineering Materials and Structures, 3, 1981, pp. 247-255.

34. Runkle, J. C. and R. M. Pelloux, "Micromechanisms of Low-Cycle Fatigue in Nickel-Base Superalloys at Elevated Temperatures," Proceedings of an ASTM-NBS-NSF Symposium, Kansas City, MO, May 1978, ASTM STP 675, J. T. Fong, Ed., American Society for Testing and Materials, 1979, pp. 501-527.

35. Robinson, E., "Effect of Temperature Variation on the Long-Time Rupture Strength of Steels," Transactions of the ASME, 74, July 1952, pp. 777-781.

36. Miller, J., "Effect of Temperature Cycling on the Rupture Strength of Some High Temperature Alloys," Symposium on Effect of Cyclic Heating and Stressing on Metals at Elevated Temperatures, ASTM STP 165, American Society for Testing and Materials, 1954, pp. 53-66.

37. Haritos, G. K., D. L. Miller, and T. Nicholas, "Sustained-Load Crack-Growth in Inconel 718 Under Nonisothermal Conditions," Journal of Engineering Materials and Technology, 107, April 1985, pp. 172-179.

38. Rau, C. A., A. E. Gemma, and G. R. Leverant, "Thermal-Mechanical Fatigue Crack Propagation in Nickel- and Cobalt-Base Superalloys Under Various Strain-Temperature Cycles," Fatigue at Elevated Temperatures, ASTM STP 520, A. Carden, A. McEvily, and C. Wells, Eds., American Society for Testing and Materials, 1973, pp. 166-178.

39. Gemma, A. E., F. X. Ashland, and R. M. Masci, "The Effects of Stress Dwells and Varying Mean Strain on Crack Growth During Thermal Mechanical Fatigue," Journal of Testing and Evaluation, Vol 19, No. 4, 1981, pp. 209-215.

40. DeLuca, D. P. and B. A. Cowles, "Fatigue and Fracture of Advanced Blade Materials," AFWAL-TR-84-4167, Wright-Patterson AFB OH, 1985.

41. Wright, P. K., H. Jang, and H. G. Popp, "Fatigue and Fracture of Advanced Blade Materials," AFWAL-TR-84-4166, Wright-Patterson AFB OH, 1985.

42. Gemma, A., B. Langer, and G. Leverant, "Thermomechanical Fatigue Crack Propagation in an Anisotropic (Directionally Solidified) Nickel-Base Superalloy," Thermal Fatigue of Materials and Components, ASTM STP 612, American Society for Testing and Materials, 1976, pp. 199-213.

43. Jordan, E. H., and G. J. Meyers, "Fracture Mechanics Applied to Nonisothermal Fatigue Crack Growth," Engineering Fracture Mechanics, Vol 23, No. 2, 1986, pp. 345-358.

44. Marchand, N. and Pelloux, R. M., "Thermal-Mechanical Fatigue Crack Growth in Inconel X-750," Proceedings of the International Conference on Time-Dependent Fracture, K. Karauz and A. Karuz, Eds., Martinus Nijhoff, 1984, pp. 167-178.

45. General Electric, Response to AF RFP F33615-84-R-5032, Unpublished Data.

46. Hartman, G.A., "A Thermal Control System for Thermal Cycling," Journal of Testing and Evaluation, Vol 13, No. 5, September 1985, pp. 363-366.

47. Hartman, G.A. and D.A. Johnson, "DC Electric Potential Method Applied to Thermal-Mechanical Fatigue Crack Growth Testing," to be published in Experimental Mechanics.

48. "Standard Test Method for Constant-Load-Amplitude Fatigue Crack Growth Rates above 10^{-8} m/cycle," ASTM Standard E647-83, 1983 Annual Book of ASTM Standards, Part 10, Metals-Mechanical, Fracture, and Corrosion Testing; Erosion and Wear; Effect of Temperature, American Society for Testing and Materials, 1983, pp. 711-731.

49. Miller, D. L., "Sustained-Load Crack Growth in Inconel 718 Under Non-Isothermal Conditions," M. S. Thesis, Air Force Institute of Technology, Wright-Patterson AFB OH, December 1983.

50. Nicholas, T., G. Haritos, and J. Christoff, "Evaluation of Cumulative Damage Models for Fatigue Crack Growth in an Aircraft Engine Alloy," Journal of Propulsion, Vol 1, No 2, March-April 1985, pp. 131-136.

51. Utah, D. A., "Crack Growth Modeling in an Advanced Powder Metallurgy Alloy," AFWAL-TR-80-4098, Wright-Patterson AFB OH, 1980.

52. Painter, G. O., "Evaluation of Interpolative Modeling Concepts for Fatigue Crack Growth at Elevated Temperature," M. S. Thesis, Air Force Institute of Technology, Wright-Patterson AFB OH, December 1984.

53. Nicholas, T., J. H. Laflen, and R. H. Van Stone, "A Damage Tolerant Design Approach to Turbine Engine Life Prediction," to be published in the proceedings of the Minnowbrook Conference on Life Prediction for High Temperature Gas Turbine Materials, August 27-30, 1985, Minnowbrook Conference Center of Syracuse University, Blue Mountain Lake, N. Y.

54. Ashbaugh, N. E., "Effect of Through-the-Thickness Stress Distribution Upon Crack Growth Behavior in a Nickel-Base Superalloy," Fracture Mechanics: Fourteenth Symposium — Volume II: Testing and Applications, ASTM STP 791, J. C. Lewis, and G. Sines, Eds., American Society for Testing and Materials, 1983, pp. II-517-II-535.

55. Gell, M. and Leverant, G.R., "Mechanisms of High-Temperature Fatigue," Fatigue at Elevated Temperatures, ASTM STP 520, American Society for Testing of Materials, 1973, pp. 37-66.

56. Pineau, A., "Intergranular Creep-Fatigue Crack Growth in Ni-Base Alloys," Flow and Fracture at Elevated Temperatures, R. Raj, Ed., American Society for Metals, 1985, pp. 317-348.

57. Wareing, J., Tomkins, B., and Bretherton, I., "Life Prediction in Austenitic Stainless Steel," Flow and Fracture at Elevated Temperatures, R. Raj, Ed., American Society for Metals, 1985, pp. 251-278.

58. Broek, D., Elementary Engineering Fracture Mechanics, Third Revised Edition, The Hague, Martinus Nijhoff Publishers, 1984, pp. 48-53.

VITA

Major Michael L. Heil was born on 1 June 1953 in Wiesbaden, Germany, in a U.S. military hospital. He graduated from high school in Gambrills, Maryland, in 1971 and attended the United States Air Force Academy. He graduated in June 1975 with a Bachelor of Science in Engineering Science degree and a commission in the USAF. He attended the Institute of Flight Structures at Columbia University on a Guggenheim Fellowship and graduated with a Master of Science in May 1976. He served as a structural engineer in the F-15 System Program Office, Wright-Patterson AFB, Ohio, before returning to the United States Air Force Academy as an Assistant Professor of Engineering Mechanics. In June, 1983, he entered the School of Engineering, Air Force Institute of Technology.

Permanent Address:

1553 Eton Way

Crofton, Maryland 21114